

**Interactions of Phosphorus and Colloidal Iron Oxides in
Model Solutions and Natural Waters**

Timothy David Mayer
B.S., University of Montana, 1981

A dissertation submitted to the faculty of the
Oregon Graduate Institute of Science & Technology
in partial fulfillment of the requirements for the degree
Doctor of Philosophy
in
Environmental Science and Engineering

July 1995

The dissertation "Interactions of Phosphorus and Colloidal Iron Oxides in Model Solutions and Natural Waters" by Timothy David Mayer has been examined and approved by the following examination committee:

Wesley M. Jarrell, Advisor
Professor

John E. Baham
Associate Professor

William Fish
Associate Professor

Carl D. Palmer
Associate Professor

James F. Pankow
Professor

ACKNOWLEDGEMENTS

I wish to gratefully acknowledge Wes Jarrell's support and guidance during this project. Wes's propensity for real world questions and applications truly shaped the finished product and my own world view. Discussions with Jim Pankow concerning science and snow conditions in Utah were always inspiring. I appreciated Bill Fish's ideas and support as well as his cultural tips on the Portland scene. I also wish to thank the other members of my thesis committee, Carl Palmer and John Baham, for their thoughts and critical feedback.

Throughout this project, I was assisted and encouraged by a number of individuals. Claude Errera, Mary Abrams, Chuck Fisher, and the other members of Wes Jarrell's research group are very much appreciated for both their help and their humor. Best of luck to all of them in their endeavors. Jim Tesoriero's friendship throughout our time at OGI really enriched the whole graduate experience for me. Stewart Rounds was a very helpful resource, both at OGI and at the USGS.

Finally, I want to express my deepest thanks to my wife, Susan, for her support and encouragement. At times, the encouragement was understandably stronger than the support but nevertheless she saw me through the completion of this thesis and her love and friendship are greatly appreciated.

TABLE OF CONTENTS

| | |
|---|------|
| ACKNOWLEDGEMENTS | iii |
| TABLE OF CONTENTS | iv |
| LIST OF TABLES | vii |
| LIST OF FIGURES | viii |
| ABSTRACT | xi |
| CHAPTER 1: INTRODUCTION | 1 |
| 1.1 Background | 1 |
| 1.2 Overview | 3 |
| 1.3 References | 3 |
| CHAPTER 2: LITERATURE REVIEW | 5 |
| 2.1 Phosphorus Chemistry in Aquatic Systems | 5 |
| 2.2 Iron Chemistry in Aquatic Systems | 6 |
| 2.2.1 Iron Oxidation States and Kinetics | 6 |
| 2.2.2 Forms of Iron and Oxidation Products | 7 |
| 2.2.3 Surface Chemistry of Iron | 9 |
| 2.3 Iron and Phosphorus Interactions in Laboratory Studies | 12 |
| 2.3.1 Fe(II)- and Fe(III)-Derived Iron Oxides | 12 |
| 2.3.2 Adsorption vs. Coprecipitation Studies | 13 |
| 2.3.3 The Importance of Silica in Iron/Phosphate Interactions | 15 |
| 2.4 Colloid Chemistry of Iron and Phosphorus | 16 |
| 2.4.2 Environmental Implications of Colloidal Iron Phosphate | 17 |
| 2.4.3 Stability of Colloidal Iron Phosphate | 19 |
| 2.4.4 Measurement of Colloidal Iron Phosphate | 22 |

| | |
|--|----|
| CHAPTER 3: COLLOIDAL PHOSPHORUS AND COLLOIDAL IRON IN THE | |
| TUALATIN RIVER BASIN | 29 |
| 3.1 Introduction | 30 |
| 3.2 Materials and Methods | 32 |
| 3.3 Results and Discussion | 35 |
| 3.3.1 Bronson Creek Study - Temporal Variability and Colloidal | |
| Origin | 36 |
| 3.3.2 Tualatin Basin Study | 40 |
| 3.3.3 Phosphorus Forms in each Size Class | 44 |
| 3.3.4 Electron Microscopy Results | 44 |
| 3.4 Conclusions | 46 |
| 3.5 References | 49 |
| CHAPTER 4: FORMATION AND STABILITY OF IRON(II) OXIDATION | |
| PRODUCTS IN THE PRESENCE OF DISSOLVED SILICA | 52 |
| 4.1 Introduction | 53 |
| 4.2 Materials and Methods | 55 |
| 4.3 Results and Discussion | 56 |
| 4.4 Conclusions | 63 |
| 4.5 References | 64 |
| CHAPTER 5: PHOSPHORUS CHEMISTRY DURING IRON(II) OXIDATION | |
| IN THE PRESENCE OF DISSOLVED SILICA | 66 |
| 5.1 Introduction | 67 |
| 5.1.1 Iron/Phosphate Interactions | 67 |
| 5.1.2 Influence of Silicon | 68 |
| 5.1.3 Research Questions | 70 |
| 5.2 Materials and Methods | 71 |
| 5.3 Results and Discussion | 73 |
| 5.3.1 Adsorption vs. Coprecipitation without Silica | 73 |
| 5.3.2 Adsorption vs. Coprecipitation with Silica | 74 |
| 5.3.3 Adsorption Experiments on Pure Fe Oxides and Mixed Fe-Si | |

| | |
|---|-----|
| Solids | 77 |
| 5.3.4 Comparison of Field Data and Laboratory Results | 78 |
| 5.3.5 Experimental Interpretation | 82 |
| 5.4 Conclusions | 84 |
| 5.5 References | 84 |
| CHAPTER 6: SUMMARY AND CONCLUSIONS | 87 |
| APPENDIX A: FILTRATION ARTIFACTS IN DETERMINING SIZE FRACTIONATION | 90 |
| APPENDIX B: ENERGY DISPERSIVE SPECTROSCOPY AS A TOOL FOR ELEMENTAL ANALYSIS OF SUSPENDED SEDIMENTS | 96 |
| APPENDIX C: COMPLETE DATA SETS FOR THE TWO FIELD STUDIES .. | 100 |
| BIOGRAPHY | 112 |

LIST OF TABLES

| | |
|--|----|
| Table 2.1 Theoretical settling times for spherical particles of different diameters . | 19 |
| Table 4.1 Summary of solution chemistry, mineralogy, and settling times for Fe oxide colloids. | 58 |
| Table 4.2 Settling times for a ferrihydrite colloidal suspension in the presence of various calcium concentrations. | 62 |
| Table 5.1 Initial Si and Fe concentrations and final Si sorption densities and soluble Si for adsorption and coprecipitation with dissolved silica | 75 |

LIST OF FIGURES

| | |
|--|----|
| Figure 2.1 Phosphorus and iron transformations in aquatic systems. | 8 |
| Figure 3.1 Location of sampling sites in the Tualatin River watershed: (1) Scoggins Creek, (2) Dairy Creek, (3) Rock Creek, (4) Bronson Creek, (5) Fanno Creek, and (6) the lower Tualatin. The mainstem Tualatin River is grey. | 33 |
| Figure 3.2 Phosphorus (A) and iron (B) concentrations in the colloidal (0.05-1.0 μm) and particulate ($>1.0 \mu\text{m}$) size fractions in the Bronson Creek study. | 37 |
| Figure 3.3 Average colloidal/particulate ratios for P and Fe in the Bronson Creek study. | 38 |
| Figure 3.4 Dissolved O_2 saturation percentages in the Bronson Creek study. | 40 |
| Figure 3.5 Colloidal phosphorus (A) and iron (B) concentrations in the Tualatin River study, for all sites except Scoggins Creek. | 41 |
| Figure 3.6 Average colloidal/particulate ratios for P and Fe in the Tualatin River study, for all sites except Scoggins Creek. | 42 |
| Figure 3.7 Correlation of phosphorus and iron in colloidal form; data from both Bronson Creek and Tualatin River studies. | 43 |
| Figure 3.8 Box plots of the frequency distribution of molar ratios in the colloidal ($<1.0 \mu\text{m}$) and particulate ($>1.0 \mu\text{m}$) size classes. The upper and lower whiskers extend to the 90th and 10th percentile, respectively. | 47 |
| Figure 4.1 Lepidocrocite synthesized from the oxidation of Fe(II) without silicate present. | 58 |
| Figure 4.2 Ferrihydrite synthesized from the oxidation of Fe(II) in the presence | |

| | |
|--|----|
| of silicate. | 58 |
| Figure 4.3 Iron oxides produced from the oxidation of a reduced groundwater sample of the Tualatin River Basin. The larger particles are believed to be clays. | 61 |
| Figure 4.4 Iron oxide colloids retained by a polycarbonate filter from a surface water sample of the Tualatin River Basin. The appearance and composition of these colloids are similar to ferrihydrite synthesized in the presence of silicate. | 61 |
| Figure 5.1 Phosphorus coprecipitation and adsorption experiments without Si (pH=7.0). | 74 |
| Figure 5.2 Phosphorus coprecipitation and adsorption experiments with Si (pH=7.0). | 76 |
| Figure 5.3 Coprecipitation of Fe and P in the presence or absence of Si. This data was previously presented in Figs. 1 and 2. | 76 |
| Figure 5.4 Phosphorus adsorption on pure Fe oxides and mixed Fe-Si oxides (pH=7.0). | 79 |
| Figure 5.5 Calcium adsorption on pure Fe oxides and mixed Fe-Si oxides (pH=7.0). | 79 |
| Figure 5.6 Simultaneous adsorption of P and Si added 24 hours after Fe oxide formation (pH=7.0). | 81 |
| Figure 5.7 Phosphorus adsorption edges on pure Fe oxides and mixed Fe-Si oxides. | 81 |
| Figure 5.8 Sorption densities as a function of soluble P in four coprecipitation experiments and one adsorption experiment, all with Si present, and the natural colloidal material from the Tualatin River waters. (see text for symbol explanation). | 82 |
| Figure A.1 Phosphorus concentrations in river sample filtrates from 0.4 μm and 0.05 μm pore size filters. | 91 |
| Figure A.2 Iron concentrations in river sample filtrates from 0.4 μm and 0.05 μm pore size filters. | 92 |

| | |
|--|----|
| Figure A.3 Scanning electron micrograph of the suspended sediment from a river sample retained by a 1.0 μm filter. | 93 |
| Figure A.4 Scanning electron micrograph of the suspended sediment from a river sample retained on a 0.4 μm filter. | 94 |
| Figure B.1 Example of the energy spectra from a colloid collected in Fanno Creek, July 1993. | 98 |
| Figure B.2 Example of the energy spectra from a colloid collected in Bronson Creek, June 1993. | 99 |

ABSTRACT

Interactions of Phosphorus and Colloidal Iron Oxides in Model Solutions and Natural Waters

Timothy David Mayer

Oregon Graduate Institute of Science and Technology, 1995

Supervising Professor: Wesley M. Jarrell

An important consequence of the oxidation of Fe(II) in aquatic systems is the formation of colloid-sized particles. Colloids are particles with linear dimensions between 0.001 and 1.0 μm . The formation of colloidal Fe oxides is important to surface-reactive species, such as P, that interact with Fe. In general, colloid-associated elements or compounds will behave quite differently from species that are truly dissolved or associated with larger particles.

This research investigated the extent, variability, and formation of colloidal iron phosphate (Fe-P) in surface waters of the Tualatin River Watershed of northwest Oregon. Phosphorus and iron were directly associated in colloid-sized particles but not in larger particles. The extent of colloidal Fe-P varied considerably with location and time of year. Results from a study of a small tributary, Bronson Creek, indicated that colloidal Fe-P was more prevalent during periods of low flow and low dissolved oxygen. This led to the hypothesis that colloidal Fe-P formed as groundwater- or sediment-released Fe(II) and P diffused to oxygen-containing surface waters, causing Fe(II) to oxidize and coprecipitate with P. Silicon and other elements were found with the colloidal Fe-P as well.

Laboratory experiments were conducted to examine the formation and stability of colloidal Fe-P under conditions simulating natural systems. Silicon was found to be important in the formation process. At low concentrations of Si, Fe(II) oxidation resulted

in the formation of unstable colloidal suspensions of lepidocrocite. At background concentrations of Si typical of the Tualatin and other systems, Fe(II) oxidation resulted in the formation of stable ferrihydrite colloids. The Si stabilized the ferrihydrite colloids by (1) increasing the negative surface charge and potential and (2) inhibiting the Ostwald ripening of the solid. The Si also inhibited the release of coprecipitated P from the Fe oxides, resulting in much higher P/Fe solid ratios than in the Fe-P coprecipitates formed in the absence of Si. The synthesized ferrihydrite colloids were very similar in appearance, composition, and structure to natural Fe-, Si-, and P-containing colloids from the surface waters of the Tualatin River.

CHAPTER 1

INTRODUCTION

1.1 Background

The transport and chemistry of solutes in natural waters can be significantly influenced by interactions with suspended particles (O'Melia, 1980; Stumm and Morgan, 1981). One of the most important and least understood classes of suspended particles are colloids, particles with linear dimensions between 0.001 and 1.0 μm (Hiemenz, 1986). For particles of this size, the effects of gravitational forces are small compared to the effects of Brownian motion. Consequently, they settle out of suspension very slowly. In addition, as particle dimensions are reduced, the surface area per unit mass of material increases, which is an important consideration for surface-reactive species.

In general, colloid-associated elements or compounds behave quite differently from species that are truly dissolved or associated with larger particles that settle. Despite this difference, there have been few estimates of the mass of various constituents in the colloidal size class. More information is needed on the extent of colloidal fractions in natural systems.

An important characteristic of naturally-occurring iron (Fe) oxides is their tendency to exist as colloidal-sized particles. Iron oxide colloids have been described in several systems including lakes, rivers, and groundwaters (Laxen and Chandler, 1983; Leppard et al., 1988; Tipping et al., 1989). The characterization and environmental implications of colloidal Fe oxides have only recently been considered (Davison and DeVitre, 1992). Because of the ubiquity and reactivity of Fe, colloidal Fe oxides influence the geochemical behavior of pollutant elements, including phosphorus (P). Questions concerning the mobility, cycling, and bioavailability of Fe oxide-associated

species may remain unresolved until a complete appreciation and understanding of Fe colloid chemistry is developed.

This study has investigated the existence, formation, origin and composition of Fe-containing colloids and their importance to P chemistry in the Tualatin River watershed of northwest Oregon. The 711 square mile watershed is drained by the Tualatin River and a number of tributaries. The upper reaches consist of forested and agricultural lands and the lower reaches are heavily urbanized. Water quality has become a major concern in the river. Phosphorus loadings from sources including wastewater effluent, agricultural and urban runoff, and groundwater, have stimulated primary productivity in the river, resulting in algal blooms and high turbidities. To date, most large point sources have been controlled but nonpoint loading continues to be a problem.

Local soils and groundwaters in the watershed can be high in Fe. Given the relatively recent appreciation of colloidal Fe oxides in natural systems and the strong affinity of P for Fe, it was hypothesized that some of the P in the waters of the Tualatin would be associated with colloidal Fe oxides. The overall objectives of this work were (1) to assess the extent of colloidal P and Fe in the Tualatin waters, (2) to evaluate the origin, formation, and composition of these colloids, and (3) to determine the environmental implications of P and Fe in colloidal form.

Data presented for this research were collected from field studies and from laboratory experiments. The complexity of natural systems required that some of the study objectives be pursued using controlled experimental conditions. Specifically, questions concerning the formation process and stability of the colloidal Fe oxides and the interactions of P, Si, and Fe were investigated in model solutions. However, every effort was made to link field study results with laboratory experimental work. Model solution chemistry, concentrations, and other parameters were carefully based on Tualatin River field data and real world environments. In some cases, actual field samples were studied in the laboratory. The priority given to simulating natural conditions yielded some new and very interesting results concerning P/Fe interactions despite the fact that related systems have been intensively studied for a number of years.

While this research has focused on P chemistry, colloidal Fe oxides can interact

with a variety of pollutants of environmental concern. Consequently, this research should also promote an understanding of the cycling and transport of metals, pesticides, and other chemical pollutants, as well as P, in a variety of environments.

1.2 Overview

A comprehensive literature review is presented in the following chapter. Field and laboratory results are presented in Chapters 3, 4, and 5. These chapters are intended to be articles for publication. The extent of colloidal P and Fe in the Tualatin and the tributaries, the composition of these colloids using electron microscopy analysis, and their relationship to hydrological and biological factors were investigated in Chapter 3. One of the more important findings of this field work was the recognition that Si might be significant in the colloid chemistry of natural systems. The formation and stabilization of colloidal Fe oxides under conditions simulating the natural environment, including background concentrations of Si, was evaluated in Chapter 4. In Chapter 5, the affect of Si on P/Fe interactions was examined. Field data and laboratory data are compared as part of the discussion of the laboratory results. The major conclusions of the thesis are summarized in Chapter 6. In Appendix A, data is presented to help identify the problems and artifacts associated with using filtration for size fractionation of suspended sediments. In Appendix B, the electron microscopy tools used for analysis of suspended sediment are described. Appendix C is a complete compilation of the field data.

1.3 References

- Davison, W., and R. DeVitre. 1992. Iron particles in freshwater. p. 315-356. *In* J. Buffle and H. van Leeuwen (eds.) *Environmental particles*. Lewis Publ., Boca Raton, FL.
- Hiemenz, P. C. 1986. *Principles of colloid and surface chemistry*. Marcel Dekker, Inc., New York, NY.
- Laxen, D. P. H., and I. M. Chandler. 1983. Size distribution of iron and manganese species in freshwaters. *Geochim. Cosmochim. Acta* 47:731-741.
- Leppard, G. G., F. Buffle, R. R. DeVitre, and D. Perret. 1988. The ultrastructure and

physical characteristics of a distinctive colloidal iron particulate isolated from a small eutrophic lake. *Arch. Hydrobiol.* 113:405-424.

O'Melia, C. 1980. Aquasols: The behavior of small particles in aquatic systems. *Environ. Sci. Technol.* 14:1052-1060.

Stumm, W., and J. J. Morgan. 1981. *Aquatic chemistry*. 2nd ed. John Wiley and Sons, New York, NY.

Tipping, E., C. Woof, and D. Cooke. 1989. Iron oxide from a seasonally anoxic lake. *Geochim. Cosmochim. Acta* 45:1411-1419.

CHAPTER 2

LITERATURE REVIEW

2.1 Phosphorus Chemistry in Aquatic Systems

Phosphorus is an essential nutrient for all life forms but much of the phosphorus (P) in the environment is unavailable to organisms. For this reason, it is frequently the element limiting productivity in terrestrial and aquatic systems. In freshwater environments, anthropogenic contributions of P from wastewater or agricultural runoff can stimulate excess productivity and algal growth, a condition known as eutrophication. The importance of P, both as an essential nutrient and a pollutant, has motivated a large body of research directed towards understanding P chemistry (Syers et al., 1973; Syers and Iskandar, 1981; Stevenson, 1986).

In surface waters, P partitions into several major compartments according to a number of chemical, biological and physical processes (Syers et al., 1973). Dissolved P exists mainly as various species of orthophosphate (referred to as phosphate in this text) and is considered immediately bioavailable. At circumneutral pH, the main species of phosphate are H_2PO_4^- and HPO_4^{2-} . Concentrations of phosphate are usually low because of biological utilization of P and reactions of phosphate with inorganic and organic particles. Concentrations in lake waters rarely exceed $1.0 \times 10^{-2} \text{ mM}$ (0.3 mg/L) and are usually considerably less than this (Syers et al., 1973).

In many river systems photosynthesis is limited by light penetration. Phosphate concentrations in these systems are predominately controlled by chemical reactions with suspended materials. The strong interaction between phosphate and the mineral fractions of soils and sediments has been well established (Shukla et al., 1971; Parfitt, 1978; Fox, 1989). Phosphate in the mineral fraction is generally associated with Ca, Fe, or Al

minerals. The particular inorganic P-mineral association is pH-dependent. In neutral to acid pH systems, phosphate is usually associated with Fe and Al hydroxides. When pH is greater than 7.0, calcium phosphates are usually the dominant form (Stevenson, 1986).

2.2 Iron Chemistry in Aquatic Systems

Iron is one of the most abundant elements in the earth's crust and is prevalent in many natural systems. Because of the ubiquity and reactivity of Fe, P concentrations in neutral, oxygenated environments are often believed to be controlled by sorption processes or solid solution reactions involving ferric hydroxides (Syers et al., 1973; Parfitt, 1978; Sigg and Stumm, 1980; Fox, 1989).

This review is concerned with the processes and factors controlling Fe/P interactions in aqueous systems. The exact chemical mechanisms underlying these interactions are still open to interpretation. Adsorption, surface precipitation, solid solution or solid state diffusion have all been postulated (Ryden et al., 1977; van Riemsdijk et al., 1984; Barrow, 1985; Fox, 1989). Therefore, the general term "sorption" will be used to refer to the transfer of aqueous phosphate ion to an Fe oxide solid by any process (Sposito, 1986).

2.2.1 Iron Oxidation States and Kinetics

Interactions between Fe and phosphate depend on Fe chemistry (Fox, 1989; Schwertmann and Taylor, 1989). Aqueous Fe occurs in one of two principal oxidation states, ferrous Fe and ferric Fe. The reduced form, Fe(II), is moderately soluble, but the oxidized form, Fe(III), is extremely insoluble and will hydrolyze and precipitate rapidly at the pH of most natural waters. The ready inter-conversion between the two oxidation states leads to the production and dissolution of Fe oxide particles. Soluble concentrations of phosphate and other species that interact with Fe will be higher under reducing conditions and lower under oxidizing conditions (Fig. 2.1). The association with Fe links P chemistry to redox conditions even though P itself is not redox-active in most environments.

The cycling between Fe(II) and Fe(III) occurs in a number of geochemical

environments: at the sediment-water interface (Fig. 2.1); at the oxic/anoxic boundaries which exist in stratified water columns; in soils subjected to wetting and drying; and at the point where anaerobic groundwaters are exposed to oxygen. Reduction of ferric Fe usually depends on microorganisms and the supply of organic material. Light in natural systems can catalyze Fe(III) reduction by organic matter (Waite and Morel, 1984).

The oxidation of Fe(II) may be biologically mediated at low pH but is thought to occur abiotically within the pH range of 5 to 8 (Davison and DeVitre, 1992). The reaction rate is proportional to $[O_2]$, $[Fe(II)]$, and $[OH^-]^2$ (Stumm and Lee, 1961). Temperature and ionic strength affect the reaction rate as well (Davison and DeVitre, 1992). Since the rate law is second order with respect to $[OH^-]$, the reaction rate strongly depends on pH. Half-lives for Fe(II) in O_2 -saturated waters of pH 8, 7, and 6 at 10°C are approximately 2.34 min, 234 min, and 390 hours, respectively (Davison and DeVitre, 1992).

2.2.2 Forms of Iron and Oxidation Products

Most aquatic systems include regions where dissolved O_2 concentrations are low, and Fe(II) is stable (Fig. 2.1). Such regions frequently occur in the bottom sediments of lakes and streams. Rapid oxidation kinetics ensures that there is a steady supply of new Fe oxide forming in situ at the oxic/anoxic boundary in these systems. This solid phase occurs as homogeneous particles of Fe oxide or as surficial coatings on clays or organic particles. Surface sediments overlain by oxygenated waters are often enriched in Fe oxides. The enriched sediments can appear as crusts, layers, or, in more productive systems, as discrete nodules. In circumneutral surface waters with ample organic matter, Fe in the bottom layers can remain reduced close enough to the sediment-water interface that it will diffuse into the water column before it is oxidized (Davison and DeVitre, 1992). Eddy diffusion can mix and dilute the Fe(II) in the overlying water before significant concentrations develop at the interface. Upon oxidation of the Fe(II), Fe oxide particles are formed in the water column (Davison and DeVitre, 1992).

The main products of Fe(II) oxidation in natural systems are usually poorly-ordered lepidocrocite and ferrihydrite (Schwertmann and Cornell, 1991). At low

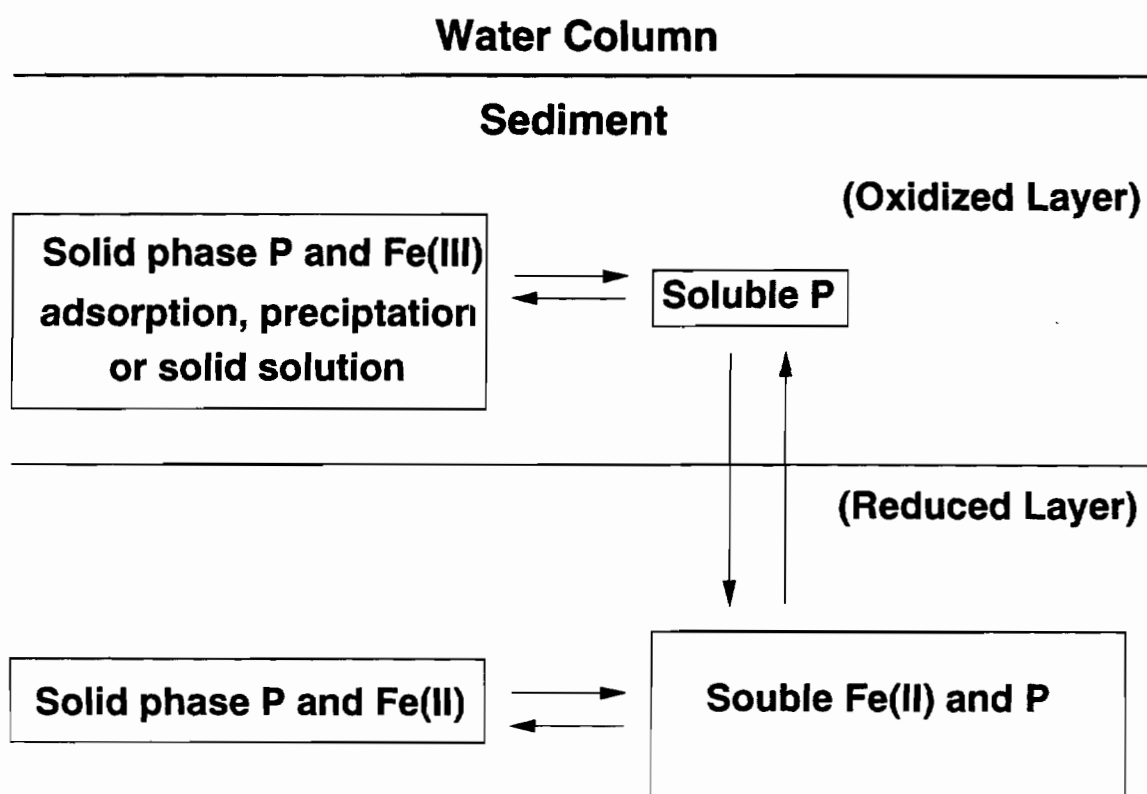


Figure 2.1 Phosphorus and iron transformations in aquatic systems.

concentrations of Si, lepidocrocite, γ -FeOOH, will form (Schwertmann et al., 1984). Lepidocrocite is somewhat crystalline with a characteristic X-ray diffraction pattern and a variety of morphologies including rafts, sheets, needles, and plates. When higher concentrations of Si are present during Fe(II) oxidation, ferrihydrite will form (Schwertmann et al., 1984). The structure of ferrihydrite is not as well characterized. It is thought to be more amorphous and consist of spherical or ellipsoidal particles with very high specific surface areas. These poorly-ordered phases are more soluble than other Fe oxide phases and will convert to crystalline, less soluble forms such as goethite, α -FeOOH (Schwertmann and Cornell, 1991). They form initially because of the lower interfacial free energy of the nuclei. Transformation and recrystallization rates are generally slow and depend greatly on solution conditions (Langmuir and Whittemore, 1971).

2.2.3 Surface Chemistry of Iron

The reaction of phosphate with Fe oxides is affected by the physical and chemical properties of the solid. Two important surface properties are the surface area per unit mass and the net charge of the surface (Dzombak and Morel, 1990). As will be explained below, the two properties affect (a) the capacity and (b) the affinity of the solid for the solute.

Sorption of phosphate onto Fe oxide surfaces depends strongly on the surface area associated with a unit mass of solid. The exposed surface area contains the hydroxyl groups that interact with aqueous phosphate through reversible, ligand exchange reactions. The higher the specific surface area, the greater the number of surface hydroxyls available for reaction with phosphate. In this sense, surface area is thought to affect the capacity of the solid for the solute. Phosphorus sorption capacities of various Fe oxides are approximately equal when normalized on a unit surface area basis (Borggaard, 1983).

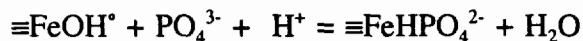
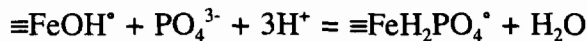
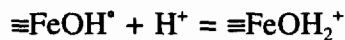
The specific surface areas of naturally-occurring Fe oxides vary over an order of magnitude, from 30-50 m²/g for goethite and hematite (Schwertmann and Taylor, 1989) to 600 m²/g or more for ferrihydrite (Dzombak and Morel, 1990). As expected, specific surface area is inversely correlated with the degree of crystallinity of the solid. The

variation in specific surface areas yields a wide range of maximum sorption densities for different Fe oxides. For example, the average packing density of phosphate sorbed to Fe oxide is $0.6 \text{ nm}^2/\text{PO}_4$ ion (Borggaard, 1983; Goldberg and Sposito, 1984). Using this value, a formula weight of 89 g/mole Fe solid, and the range of specific surface areas, theoretical maximum sorption densities for various Fe oxides can be estimated to be 0.007-0.148 moles P/mole Fe. This compares favorably to experimental values determined in laboratory studies (Ryden et al., 1977; Lijklema, 1980; Anderson et al., 1985). It is important to note that the soluble phosphate concentrations required to sustain these maximum sorption densities may be much higher than the concentrations normally found in aquatic systems.

While high sorption densities are theoretically possible, the extent of coordination on surface sites depends, to a large extent, on the surface charge of the solid. Any charged surface will create a potential gradient through which ions must move. With a positive surface charge and potential, energy will be required to move protons or cations to the surface. The movement of hydroxyls and anions toward the surface will be energetically favorable. Correspondingly, a negative surface charge and potential will repel hydroxyls and anions and attract protons and cations. The net surface charge therefore affects the affinity of the solid for the solute.

Iron oxides generate surface charge through proton transfer reactions and the surface coordination of cations and anions. Specifically sorbed protons and cations will increase the surface charge and surface potential of the solid while specifically sorbed hydroxyls and anions will lower it (Dzombak and Morel, 1990). Reactions with H^+ and phosphate that illustrate this change in surface charge are shown below. The reactions also demonstrate the effect of pH on phosphate sorption. As the H^+ concentration increases, the reactions will be driven toward the right, increasing the surface potential and the sorption of phosphate.

Surface complexation theory states that these reactions can be described using mass law equations and equilibrium constants very similar to those describing analogous coordination reactions in solution. What distinguishes surface reactions from reactions in solution is the electrostatic interaction resulting from the surface charge. Equilibrium



constants for surface reactions account for this interaction through an electrostatic free energy component which is combined with the chemical or "intrinsic" free energy component of the equilibrium constant. This electrostatic term is really a surface activity coefficient (Dzombak and Morel, 1990). The functionality of the electrostatic component is determined through the diffuse layer model or some other model of the oxide/water interface.

The surface functional groups of all Fe oxides are amphoteric in water. The pH at which the surface charge is zero, that is the point at which the concentration of surface hydroxyls equals the concentration of surface protons, is the point of zero net proton charge (PZNPC). The point of zero charge (PZC) is the pH at which the surface charge is zero when there are other specifically sorbed ions present. The PZC will differ from the PZNPC for natural Fe oxides in most environments because of the presence of other specifically sorbed ions. When the pH of the system is less than PZC, the oxides will be positively charged. If the pH of the system is greater than PZC, the oxides will be negatively charged.

Most iron oxides have PZNPC in the pH range 7.0 to 9.0 (Schwertmann and Taylor, 1989). The PZNPC of ferrihydrite is 8.0 as reported by several groups (Dzombak and Morel, 1990). Borggaard (1983) reported a PZNPC for lepidocrocite of 7.1. Reaction with phosphate or other anions will lower the surface charge and the PZC of the oxide. Reactions with cations will raise the surface charge and PZC. Sorption densities of 0.036 and 0.078 (P/Fe) lowered the PZC of ferrihydrite from an initial value of 8.1 to

6.3 and 4.6 respectively (Ryden et al. 1977).

2.3 Iron and Phosphorus Interactions in Laboratory Studies

Much of the information presented to this point is from studies of Fe and P chemistry in model systems. Most laboratory studies of sorption processes and the surface chemistry of Fe oxides have been conducted with pre-formed, pure Fe oxide precipitates that have been aged prior to experimental study. This information has been invaluable in yielding information on the mechanisms of iron phosphate interactions. However, direct application of this research to natural systems may be problematic for several reasons.

(1) In many natural environments, Fe oxides will likely form as a result of Fe(II) oxidation and precipitation in the presence of dissolved ions. The physical and chemical properties of ferrous-derived precipitates differ from those of ferric-derived precipitates.

(2) Sorption of dissolved ions may be different depending on whether they are present during mineral formation or are added later, as is often the case in laboratory studies. Ostwald ripening and particle aggregation can reduce the number of surface sites as oxides age, causing associated ions to be released.

(3) Dissolved ions that are present in natural waters can affect the formation and the surface chemistry of the Fe oxide.

The remainder of this section will be an analysis and review of the research that addresses these issues.

2.3.1 Fe(II)- and Fe(III)-Derived Iron Oxides

In laboratory studies, synthetic Fe oxides are usually derived from the rapid hydrolysis of Fe(III) salts. In natural environments, Fe oxides are usually formed through oxidation and hydrolysis of Fe(II). Ferrous- and ferric-derived oxides are likely to have different surface and sorption characteristics.

Crosby et al. (1983) prepared Fe oxides from Fe(II) and Fe(III) under similar experimental conditions and found significant differences in their mineralogies, surface areas, and porosities. The Fe(III)-derived precipitates were amorphous, spherical

aggregates (probably ferrihydrite) with higher surface areas and porosities than the Fe(II)-derived precipitates. Crystallinity was evident only after 12 days. The Fe(II)-derived precipitates showed early development of a crystalline lepidocrocite phase.

During rapid hydrolysis of Fe(III), a high state of supersaturation is reached. This condition causes an amorphous, metastable solid of higher solubility to form. Precipitate formation from Fe(II) is slower due to its dependence on oxidation as well as hydrolysis rates. This may allow a more crystalline product to form. It also allows nucleation and crystal growth to occur simultaneously which will result in a wider range of particle sizes (Schwertmann and Cornell, 1991). This may explain the different surface and mineralogical properties of the Fe(II)-derived precipitates.

2.3.2 Adsorption vs. Coprecipitation Studies

Dissolved ions in sorption studies can be added to Fe oxide suspensions either prior to mineral formation or after precipitation and aging of the oxide. Typically they have been added a few hours to a few weeks after mineral formation. There are probably several reasons for this.

(1) It allows time for crystal growth, coagulation and stabilization of the oxide structure to occur. This may reduce some of the variability in the structural and surface characteristics of different Fe oxides, facilitate characterization of the solid phase, and allow for comparison between studies.

(2) In many studies of natural systems, soluble concentrations of phosphate, other anions, and trace metals are undersaturated with respect to Fe solids. The assumption has been that adsorption processes control Fe/solute interactions in these cases. The addition of the dissolved ion after mineral formation is viewed as simulating an adsorption process rather than a precipitation process. This may be an appropriate approach to simulating situations where a pollutant or contaminant is added to existing Fe oxides that have stabilized and aged. However, it is probably not appropriate in the numerous systems where Fe is reduced and oxidized cyclically. In these systems the oxide will form in the presence of dissolved ions and experimental procedures should reflect these conditions.

A number of studies have reported higher sorption of cations and anions when

they are present during the formation of Fe oxides rather than when added after precipitation (Anderson and Benjamin, 1985; Laxen, 1985; Fuller et al., 1993). Einsele (1938), in his seminal work on Fe chemistry, showed that the oxidation of 0.18 mM Fe(II) in the presence of 0.18 mM phosphate at pH 6.0-7.0 resulted in stoichiometric precipitation of Fe and P (P/Fe=1.0). Adding Fe(III) and P to a similarly buffered system produced an equivalent precipitation product. However, if either (a) Fe(III) was added to the buffered solution or (b) Fe(II) was allowed to oxidize in the absence of phosphate, and then the phosphate was added, the P/Fe ratio of the solid phase decreased to 0.17.

Tessenow (1974) conducted similar oxidation experiments using more ecologically relevant Fe(II) and phosphate concentrations over a range of pH values. He found that the P/Fe solid molar ratio of the newly-formed Fe oxide depends on the initial P/Fe ratio in solution, but asymptotically approaches a maximum of 0.5-0.58 at higher P/Fe solution ratios. He proposed a chemical formula of $\text{Fe}_2(\text{OH})_3\text{PO}_4$ for the solid.

Neither of these studies considered the effects of Ostwald ripening and particle aggregation. Ostwald ripening is the growth of large particles in a suspension at the expense of smaller ones which redissolve (Schwertmann and Cornell, 1991). The higher interfacial surface energy of smaller particles means that their solubility is increased relative to larger particles of the same composition. Given ample time, the smaller, more soluble particles will be converted to larger, less soluble particles that prescribe a lower solution phase activity. As demonstrated in a few more recent studies (Crosby et al., 1981; Anderson et al., 1985; Fuller et al. 1993), these processes can reduce the number of surface sites as the mineral ages, releasing the initially sorbed phosphate.

Anderson et al. (1985) reported a period of phosphate desorption following uptake onto goethite synthesized from Fe(III), which they attributed to P-induced coagulation of the Fe particles and rejection of some of the previously sorbed P.

Crosby et al. (1981) found that Fe(II)-derived lepidocrocite sorbed phosphate initially but desorbed phosphate with time. This was thought to result from a decrease in surface area accompanying the rapid formation of a more crystalline product through Ostwald ripening. Laboratory Fe oxides derived from oxidative hydrolysis of Fe(II) can crystallize within a few hours (Schwertmann and Cornell, 1991). Phosphate sorption onto

the same Fe(II)-derived precipitates aged 20 hours was negligible. However, phosphate sorption onto Fe(III)-derived precipitates, either freshly prepared or aged, was very strong and no phosphate was desorbed. This may have been due to slower crystallization of the Fe(III)-derived solid. These results caused the authors to question the role of Fe(II)-derived Fe oxides in controlling solution phosphate concentrations in natural systems.

Fuller et al. (1993) reported much greater sorption of arsenate initially on ferrihydrite in coprecipitation experiments compared to adsorption experiments. They described the slow release of coprecipitated arsenate from Fe(III)-derived ferrihydrite over an 800 hour period. Sorption densities of arsenate in the coprecipitation experiments appeared to be converging with analogous adsorption experiments at longer time periods. The sorption chemistry of arsenate, another oxyanion, is expected to be similar to phosphate. The authors did not study the effects of Si, although they did speculate that long-term release of coprecipitated species may be limited by the presence of organic acids and dissolved silica.

2.3.3 The Importance of Silica in Iron/Phosphate Interactions

It is important to recognize that dissolved constituents in natural waters will affect the surface and chemical properties of Fe oxides. A number of dissolved constituents have been shown to inhibit or retard the crystallization of amorphous Fe oxides. These include small quantities of organic anions (Cornell and Schwertmann, 1979), silica and phosphate (Schwertmann and Thalmann, 1976; Anderson and Benjamin, 1985), and arsenate (Waychunas et al., 1993). This section of the review will discuss the effect of silica on the surface and sorption properties of Fe oxides.

Dissolved silica is fairly abundant in surface waters and groundwaters, with concentrations ranging from about 0.1 to 1.0 mM (Stumm and Morgan, 1981). The presence of soluble silica during Fe(II) oxidation favors the formation of ferrihydrite over lepidocrocite or goethite (Schwertmann and Thalmann, 1976). Ferrihydrite has a much higher specific surface area and concentration of surface sorption sites than the other two oxides (Schwertmann and Taylor, 1989). The higher concentration of surface sites implies that phosphate sorption on newly-formed Fe oxides would be enhanced because

of the presence of silica.

However, there are competitive effects of silica, both electrostatic and physical in nature, which will affect phosphate sorption. Reaction of negatively charged silicate anions and Fe oxides will make the surface more negative and lower the PZC of the solid. This will decrease further sorption of anions such as phosphate. Schwertmann and Fechter (1982) reported that the PZC of ferrihydrite dropped from 8.0 to 6.0 as the solid mole ratio ($\text{Si}/[\text{Si}+\text{Fe}]$) increased from 0.0 to 0.30. Anderson and Benjamin (1985) reported that the anionic sorption of selenite decreased with silica content of the Fe oxide, correlating closely with PZC.

In addition, silicate and phosphate may physically compete for anion sorption sites since both anions associate with Fe oxides (Sigg and Stumm, 1980). Values of equilibrium sorption constants suggest that phosphate is sorbed much more strongly than silicate. However, the concentration of silica is usually much greater than phosphate in natural waters.

In summary, the combination of physical and competitive effects suggest that, depending on conditions, silica can either favor or impede the sorption of phosphate on Fe oxides.

2.4 Colloid Chemistry of Iron and Phosphorus

An important consequence of the oxidation of Fe(II) is the formation of a large number of colloid-sized particles. Colloids are particles with linear dimensions between 0.001 to 1.0 μm (Hiemenz, 1986). For particles of this size, the effects of gravitational forces are small compared to the effects of Brownian motion. The characterization and implications of this pool of colloidal Fe have only recently begun to be considered (Davison and DeVitre, 1992). Given the high affinity of phosphate for Fe oxide surfaces, it seems likely that P will be associated with colloidal Fe oxides. Colloidal iron phosphate (Fe-P) may be important in the transport, bioavailability, and management of P.

2.4.1 Field Observations of Colloidal Fe Oxides

The existence of Fe oxide colloids has been reported in several systems including lakes, rivers, and groundwaters. Leppard et al. (1988) isolated Fe oxide colloids at the redox transition boundary of a stratified freshwater lake. The colloids ranged from 0.05 and 0.30 μm in diameter and included P, Ca, and some Si and Al. The P/Fe molar ratio of the particles was 0.25. Tipping and Ohnstad (1984) described a homogeneous population of Fe oxide colloids in a stratified lake with diameters between 0.05 and 0.5 μm . The colloids contained Ca, P, Si, and C and the P/Fe molar ratio was 0.1. Laxen and Chandler (1983) found Fe oxide colloids in three freshwater lakes and a stream with a uniform particle distribution in the 0.05 to 0.4 μm size range. The authors did not measure colloidal concentrations of other elements. Mobile ferrous phosphate colloids of approximately 0.1 μm diameter were detected in a sewage-contaminated groundwater (Gschwend and Reynolds, 1987).

One noteworthy point about these studies is the consistency of the size distribution of the Fe oxide colloids reported for different systems. The diameters of all the Fe colloids are estimated to be between 0.05 and 0.5 μm . Coagulation theory predicts that particles much smaller than this are more likely to aggregate due to their higher diffusion coefficients and collision rates while particles much greater than 1.0 μm in diameter will sediment rapidly (O'Melia, 1980). The most stable population of colloids is expected to be in the 0.1 to 1.0 μm size range. Field observations of colloidal diameters generally agree with theoretical predictions.

2.4.2 Environmental Implications of Colloidal Iron Phosphate

Because of their high specific surface area, high reactivity, and tendency to remain suspended in solution, colloids can greatly affect the transport and cycling of nutrients and contaminants in surface waters and groundwaters (O'Melia, 1980; McCarthy and Zachara, 1989). Elements or compounds associated with colloid-sized particles may be transported much further than expected or predicted because, unlike larger particles, they won't be removed from solution through sedimentation or filtration in a porous medium. This enhanced mobility can be particularly important for organic species that are hydrophobic

or those species that have a high affinity for the solid phase, such as phosphate and metal cations. In addition to facilitating transport, colloids can enhance a pollutant's apparent solubility, and reduce its apparent affinity for the solid phase. The high specific surface areas of colloids mean that, on a mass basis, they can be enriched with surface-reactive species relative to larger particles.

Phosphate associated with Fe oxide colloids may have important implications for bioavailability. The majority of P in land runoff is associated with sediments. There have been several studies evaluating the bioavailability of this suspended sediment P (Logan et al. 1979; Dorich et al. 1985). Kuwabara et al. (1986), using algal assays, showed that phosphate adsorbed on model Ti oxide colloids is utilized by algae.

The approach with natural suspended sediment has been to identify various chemical extractions of soil or sediment P that correlate well with the fraction of P utilized in algal assays. Generally, total P is poorly correlated with bioavailable P. Studies of Ca-bound P or organic P in Lake Michigan sediments indicated that these forms were used minimally by algae (Williams et al., 1980). The best indicator of bioavailable P is the NaOH-extractable fraction of P (Logan et al. 1979). Extraction with NaOH is considered to remove P in iron phosphates, such as strengite, or phosphate bonded by sorption reactions to Fe oxides. This implies that some fraction of the iron phosphate in suspended sediments is bioavailable.

Probably the most important factor in assessing bioavailable P in suspended sediments is the mean residence time of the particle in the photic zone. Colloidal Fe-P will have a longer residence time in the photic zone and will be much more accessible to organisms than P associated with larger particles. Using Stokes equation and assuming a spherical geometry (Hiemenz, 1986), the settling velocities for particles of different diameters are estimated in Table 2.1. Note that as particle diameters are halved, settling velocities decrease by a factor of four due to the second order dependence on particle radius. The third column in Table 2.1 is the theoretical time that a particle of a given diameter would require to settle out of a 1.0 meter photic zone. The smaller the particle diameter, the longer the residence time in the photic zone. A 0.125 μm diameter colloid will not leave the photic zone for 445 days. Obviously, if P in colloidal form is

bioavailable, its longer residence time would benefit organisms. However, colloidal or particulate concentrations that are too high will inhibit light penetration and primary productivity because of the increased light scattering (Cuker, 1987).

Table 2.1: Theoretical settling times for spherical particles of different diameters.

| Particle Diameter | Settling velocity at 20°C | Time to settle one meter |
|-------------------|------------------------------|-----------------------------|
| µm | cm/s | days |
| 2.0 | 6.5×10^{-4} | 1.8 |
| 1.0 | 1.6×10^{-4} | 7.2 |
| 0.5 | 4.1×10^{-5} | 28.2 |
| 0.25 | 1.0×10^{-5} | 113.4 |
| 0.125 | 2.6×10^{-6} | 445.2 |

Management strategies that are designed to control P pollution may need to consider colloidal forms of P that are present. Settling ponds designed to remove particulate material from surface waters may not be effective for colloidal material unless the residence time of the particles is long or coagulation occurs. Constructed wetlands that are designed to remove soluble phosphate from surface waters may not remove colloidal P, since colloidal P will not partition to soil surfaces.

2.4.3 Stability of Colloidal Iron Phosphate

The occurrence and importance of colloids in natural systems depend on the physical characteristics of the system and the solution and surface chemistry. To persist over significant spatial and temporal scales, Fe oxide colloids must be resistant to two processes: (1) Ostwald ripening or recrystallization; and (2) coagulation. Both of these processes lead to the formation of larger particles which are more easily removed from solution through sedimentation or filtration in porous media.

Ostwald ripening is the growth of larger, less soluble particles at the expense of

smaller, more soluble ones. Ostwald ripening is an important process in Fe chemistry where oxidation of Fe(II) often results in the formation of particles that are small, amorphous, and relatively soluble. As mentioned earlier, organic ions, silica, arsenate and phosphate inhibit the recrystallization of Fe oxides, probably by blocking dissolution sites on the solid. Thus, Fe oxide colloids will persist in natural waters where these ions exist in significant concentrations (Liang and Morgan, 1990).

Coagulation can be considered a two-step process involving the physical collision of two particles followed by the attachment and formation of a new, larger particle. With submicron particles, Brownian diffusion is considered to be the main mechanism responsible for collisions (O'Melia, 1980). Van der Waals attraction provides the forces for successful attachment of particles following collision. The stability of colloids, or their resistance to coagulation, depends on electrostatic repulsion and steric effects (O'Melia, 1989). Conditions favorable for successful colloid-colloid attachment result when Van der Waals forces are greater than repulsive forces.

Electrostatic forces result from the interactions of the diffuse layers that surround charged particles in water. Analogous to sorbate/sorbent interactions during surface sorption reactions, colliding particles must negotiate surface potential gradients as they approach each other. Particles with like charges are repelled rather than attracted. This is termed "electrostatic stabilization" of colloidal suspensions. The thicker the double layer or the greater the magnitude of the charge, the more stable the particles. Higher ionic strengths will decrease the thickness of the double layer and reduce the electrostatic stability of the colloid suspension.

Steric stabilization results from adsorption of large polymers such as natural organic material. Adsorbed polymers can have loops or tails extending into solution. When intermolecular interactions between these segments on neighboring particles are energetically unfavorable, the colloids are stabilized sterically.

The two types of stabilization mean that colloidal stability in natural systems is sensitive to surface-reactive species, both small, inorganic solutes and larger macromolecules. O'Melia (1989) states that electrostatic stabilization is expected to be more important at low ionic strengths where calculated double layer thicknesses extend

well past the range of influence of adsorbed polymers. In high ionic strength waters, double layer thicknesses shrink to tenths of nanometers and may be comparable to segments of adsorbed polymers responsible for steric stabilization. Therefore, in oceans or saline waters both types of stabilization may prevail.

Specific sorption of ions can affect the electrostatic stabilization of the particles differently, depending on the concentrations (Liang and Morgan, 1990). Low concentrations of sorbed species can neutralize the surface charge of the particle and cause coagulation. When the net surface charge is reduced to zero, electrostatic stability reaches a minimum. Higher concentrations of sorbed species can reverse the surface charge of the particle and contribute to electrostatic stabilization. Naturally-occurring Fe oxides are almost always negatively charged over the range of pH in waters despite their relatively high PZNPC (Tipping et al., 1981; Loder and Liss, 1985). This has been attributed to specific sorption of organic and inorganic anions which reduce the positive surface charge.

Laboratory measurements have confirmed that natural concentrations of dissolved organic matter or phosphate will reverse the charge of Fe oxides and stabilize the particles (Tipping et al., 1981; Liang and Morgan, 1990). Natural organic matter has often been implicated in the stabilization of Fe oxides in field studies (Tipping et al., 1981). But some evidence questions the role of organic matter in stabilizing Fe oxides. Fox (1984) reported that humic acids and colloidal Fe oxides in several estuaries did not appear to be chemically associated, based on their different rates of settling in estuaries and the failure of humic acids to stabilize laboratory solutions of colloidal Fe. Hiraide et al. (1988) showed that "dissolved" river water Fe ($<1.0 \mu\text{m}$) was predominantly present as negatively charged colloids which may or may not be associated with humic substances.

Because of its strong interaction with Fe oxide, phosphate is a very effective coagulant at low concentrations and a stabilizing agent at higher concentrations. Phosphate stabilization occurs at P/Fe molar ratios above 0.17-0.29 (Cameron and Liss, 1984; Liang and Morgan, 1990). Cameron and Liss (1984) reported that silica was able to stabilize Fe oxides, but only at a concentration of 11.0 mM, which is much higher than concentrations normally found in aquatic environments. However, the results presented

in Chapter 4 indicate that natural background concentrations of silica are very effective at stabilizing colloidal Fe oxide if it is present during the oxidation of Fe(II). As discussed earlier, natural organic material and inorganic anions such as silicate and phosphate will inhibit Ostwald ripening of Fe oxides and contribute to the persistence of stable Fe oxide colloids.

2.4.4 Measurement of Colloidal Iron Phosphate

The preceding discussion has shown that the existence of a significant pool of colloidal P has important implications for the transport, bioavailability, and management of P in natural systems. In general, colloid-associated elements behave quite differently from species of that element that are truly dissolved or associated with larger particles that settle. However, there are very few estimates of the mass of given constituents in colloidal pools (Honeyman and Santschi, 1992). Colloids are usually not considered in sampling schemes or field studies nor are they commonly included in conceptual or mathematical models. One reason for this may be the analytical difficulties in their measurement and identification.

A number of methods have been used for sampling the submicron particle-size spectrum, although no method is perfect. Centrifugation suffers from a lack of size selectivity for particles and particle coagulation and aggregation in the centrifugation tubes is a serious problem for natural samples (Davison and DeVitre, 1992). New techniques such as laser Doppler velocimetry, laser correlation spectrometry, and transmission electron microscopy are emerging as useful tools for well-defined systems but these techniques are expensive and their application to natural systems, with low colloid concentrations and irregular particle size distributions is limited (Honeyman and Santschi, 1992). Filtration is often used for separating solid and dissolved phases and for size fractionation of particles (Laxen and Chandler, 1982). While it offers advantages over other techniques (Buffle et al., 1992), filtration can underestimate or obscure colloidal concentrations in two ways.

First, colloids can be small enough that they pass through the pores of the filter and are included in the "dissolved" phase. The result is that the dissolved phase is

overestimated and the colloidal phase is underestimated.

The inclusion of colloids in filtrates is a problem that has been recognized in other studies (Kennedy et al. 1974; Danielsson, 1982). In water science, it is quite common to use a 0.4 or 0.45 μm pore size filter as the cutoff to distinguish between dissolved and solid phases. But this is larger than colloidal Fe oxide material observed in many field studies. Boyle et al. (1977) found that up to 79% of the "dissolved" Fe in river samples passing through a 0.45 μm filter was subsequently retained by a 0.05 μm filter. Tarapchak et al. (1982) reported that as much as 88% of the phosphate in 0.45 μm filtrates was removed by a 0.1 μm filter. A comparison of Fe and P concentrations in the 0.45 and 0.05 μm filtrates from a number of river samples is presented in Appendix A.

The other way that filtration can obscure colloidal phases results from the fact that filters can retain particles that are much smaller than they were intended to retain. This is due to the coagulation of particles on the filter surface, the high flow rates imposed during filtration, the low porosity of the filters, and clogging of the filters with high filter loads. Since the colloids that are erroneously retained by the filter segregate out with larger particles, the colloidal phase is again underestimated.

This phenomenon is more difficult to evaluate. Buffle et al. (1992) reported that Fe oxides with a size range of 0.05 to 0.3 μm , as established by transmission electron microscopy, were retained on filters with pores much larger than this. In fact, a 3.0 μm pore size membrane filter was capable of retaining approximately 50% of the colloids at higher flow rates. Note that this pore size is 10 times the maximum particle diameter. Particle retention on this filter decreased as a function of flow rate and was negligible at very low flow rates. The authors recommended maximum flow rates of 0.02 $\text{ml}/\text{cm}^2/\text{min}$ for accurate size fractionation through filtration. However, this rate is orders of magnitude below classical syringe filtration rates ($\sim 20 \text{ ml}/\text{cm}^2/\text{min}$) and difficult to attain unless ultrafiltration is used.

Another problem in eliminating surface coagulation during filtration is that particle distributions in natural waters are usually heterogeneous and coagulation with heterodisperse particles is much more efficient than that of a homodispersed system (O'Melia, 1980). The retention of smaller colloids during filtration actually helps

alleviate the first error discussed above. If total separation of particulate and dissolved phases is the objective, high flow rates through a 0.4 or 0.45 μm filter are recommended. It is only when filtration is being used for size fractionation that this phenomenon becomes a problem.

Obviously, colloids are both erroneously included in the "dissolved" phase and retained by larger filters to some extent during filtration of natural samples. Since both types of errors tend to underestimate the concentration of the colloidal phase, it is easy to see why colloids have been overlooked in the past. However, the role of colloids in the partitioning and transport of pollutants is slowly being recognized and appreciated. Colloids should be considered more explicitly in future studies for a complete understanding of many natural systems.

2.5 References

- Anderson, M. A., M. I. Tejedor-Tejedor, and R. R. Stanforth. 1985. Influence of aggregation on the uptake kinetics of phosphate by goethite. *Environ. Sci. Technol.* 19:632-637.
- Anderson, P. R., and M. M. Benjamin. 1985. Effects of silicon on the crystallization and adsorption properties of ferric oxides. *Environ. Sci. Technol.* 19:1048-1053.
- Barrow, N. J. 1985. Reaction of plant nutrients and of pollutants with variable-charge soils. *Adv. Agron.* 38:282-288.
- Borggaard, O. K. 1983. Effect of surface charge and mineralogy of iron oxides on their surface areas and anion-adsorption properties. *Clays Clay Minerals* 31:230-232.
- Boyle, E. A., J. M. Edmond, and E. R. Sholkovitz. 1977. The mechanism for iron removal in estuaries. *Geochim. Cosmochim. Acta* 41:1313-1324.
- Buffle, J., D. Perret, and M. Newman. 1992. The use of filtration and ultrafiltration for size fractionation of aquatic particles, colloids, and macromolecules. p. 171-230. *In* J. Buffle and H. van Leeuwen (eds.) *Environmental particles*. Lewis Publ., Boca Raton, FL.
- Cameron A. J., and P. S. Liss. 1984. The stabilization of "dissolved" iron in freshwaters. *Water Res.* 18:179-185.
- Cornell, R. M., and U. Schwertmann. 1979. Influence of organic anions on the

crystallization of ferrihydrite. *Clays Clay Miner.* 27:402-410.

Crosby, S. E., E. I. Butler, D. R. Turner, M. Whitfield, D. R. Glasson, and G. E. Millward. 1981. Phosphate adsorption onto iron hydroxides at natural concentrations. *Environ. Technol. Lett.* 2:371-378.

Crosby, S. E., D. R. Glasson, A. H. Cuttler, I. Butler, D. R. Turner, M. Whitfield, and G. E. Millward. 1983. Surface areas and porosities of Fe(III)- and Fe(II)-derived oxyhydroxides. *Environ. Sci. Technol.* 17:709-713.

Cuker, B. E. 1987. Field experiment on the influences of suspended clay and on the plankton of a small lake. *Limnol. Oceanogr.* 32:840-847.

Danielsson, L. G. 1982. On the use of filters to distinguish between dissolved and particulate fractions in natural waters. *Water Res.* 16:179-182.

Davison, W. and R. DeVitre. 1992. Iron particles in freshwater. p. 315-356. *In* J. Buffle and H. van Leeuwen (eds.) *Environmental particles*. Lewis Publ., Boca Raton, FL.

Dorich, R. A., D. W. Nelson, and L. E. Sommers. 1985. Estimating algal available phosphorus in suspended sediments by chemical extraction. *J. Environ. Qual.* 13:400-405.

Dzombak, D. A., and F. M. Morel. 1990. *Surface complex modeling: hydrous ferric oxide*. John Wiley and Sons, New York, NY.

Einsele, W. 1938. Über chemische und kolloidchemische Vorgänge in Eisenphosphat-systemen unter limnolchemischen und limnogeologischen Gesichtspunkten. *Arch. Hydrobiol.* 33:361-387.

Fox, L. E. 1984. The relationship between dissolved humic acids and soluble iron in estuaries. *Geochim. Cosmochim. Acta* 48:879-884.

Fox, L. E. 1989. A model for inorganic control of phosphate concentrations in river waters. *Geochim. Cosmochim. Acta* 53:417-428.

Fuller, C. C., J. A. Davis, and G. A. Waychunas. 1993. Surface chemistry of ferrihydrite: Part 2. Kinetics of arsenate adsorption and coprecipitation. *Geochim. Cosmochim. Acta* 57:2271-2282.

Goldberg S. and G. Sposito. 1984. A chemical model of phosphate adsorption by soils II. Noncalcareous soils. *Soil Sci. Soc. Am. J.* 48:779-783.

Gschwend, P. M., and M. D. Reynolds. 1987. Monodisperse ferrous phosphate colloids in an anoxic groundwater plume. *J. Contam. Hydrol.* 1:309-327.

- Hiemenz, P. C. 1986. Principles of colloid and surface chemistry. Marcel Dekker, Inc., New York, NY.
- Hiraide, M., M. Ishi, and A. Mizuike. 1988. Speciation of iron in river water. *Anal. Sci.* 4:605-609.
- Honeyman, B. D., and P. H. Santschi. 1992. The role of particles and colloids in the transport of radionuclides and trace metals in the oceans. p. 379-415. *In* J. Buffle and H. van Leeuwen (eds.) Environmental particles. Lewis Publ., Boca Raton, FL.
- Kennedy, V. C., G. W. Zellweger, and B. F. Jones. 1974. Filter pore size effects on the analysis of Al, Fe, Mn, and Ti in water. *Water Resour. Res.* 10:785-790.
- Kuwabara, J. S., J. A. Davis, and C. C. Y. Chang. 1986. Algal growth response to particle-bound orthophosphate and zinc. *Limnol. Oceanogr.* 31:503-511.
- Langmuir, D. L., and D. Whittemore. 1971. Variations in the stability of precipitated ferric oxyhydroxides. *Am. Chem. Soc., Adv. Chem. Ser.*, 106:209-234.
- Laxen, D. P. H., and I. M. Chandler. 1982. Comparison of filtration techniques for size distribution in freshwaters. *Anal. Chem.* 54:1350-1355.
- Laxen, D. P. H., and I. M. Chandler. 1983. Size distribution of iron and manganese species in freshwaters. *Geochim. Cosmochim. Acta* 47:731-741.
- Laxen, D. P. H. 1985. Trace metal adsorption/coprecipitation on hydrous ferric oxide under realistic conditions. *Water Res.* 19:1229-1236.
- Leppard, G. G., F. Buffle, R. R. DeVitre, and D. Perret. 1988. The ultrastructure and physical characteristics of a distinctive colloidal iron particulate isolated from a small eutrophic lake. *Arch. Hydrobiol.* 113:405-424.
- Liang, L., and J. J. Morgan. 1990. Chemical aspects of iron oxide coagulation in water: Laboratory studies and implications for natural systems. *Aquat. Sci.* 52:32-55.
- Lijklema, L. 1980. Interaction of orthophosphate with iron(III) and aluminum hydroxides. *Environ. Sci. Technol.* 14:537-541.
- Loder, T. C., and P. S. Liss. 1985. Control by organic coatings of the surface charge of estuarine suspended particles. *Limnol. Oceanogr.* 30:418-421.
- Logan, T. J., T. O. Olaya, and S. M. Yaksich. 1979. Phosphate characteristics and bioavailability of suspended sediments from streams draining into Lake Erie. *J. Great. Lakes Res.* 5:112-123.

- McCarthy, J. F., and J. M. Zachara. 1989. Subsurface transport of contaminants. *Environ. Sci. Technol.* 14:537-541.
- O'Melia, C. 1980. Aquasols: The behavior of small particles in aquatic systems. *Environ. Sci. Technol.* 14:1052-1060.
- O'Melia, C. 1989. Particle-particle interactions in aquatic systems. *Colloids Surfaces* 39:255-271.
- Parfitt, R. L. 1978. Anion adsorption by soils and soil materials. *Adv. Agron.* 30:1-50.
- Ryden, J. C., J. R. McLaughlin, J. K. Syers. 1977. Mechanisms of phosphate sorption by soils and hydrous ferric oxide gel. *J. Soil Sci.* 28:72-92.
- Schwertmann, U. and H. Thalmann. 1976. The influence of [Fe(II)], [Si], and pH on the formation of lepidocrocite and ferrihydrite during oxidation of FeCl₂ solutions. *Clay Minerals* 11:189-199.
- Schwertmann, U., and H. Fechter. 1982. The point of zero charge of natural and synthetic ferrihydrites and its relation to adsorbed silicate. *Clay Minerals* 17:471-476.
- Schwertmann, U., L. Carlson, and H. Fechter. 1984. Iron oxide formation in artificial ground waters. *Schweiz. Z. Hydrol.* 46/2:185-191.
- Schwertmann, U., and R. M. Taylor. 1989. Iron oxides. p. 379-438. *In* J.B. Dixon and S.B. Weed (eds.) *Minerals in soil environments*. Soil Sci. Soc. Am., Madison, WI.
- Schwertmann, U., and R. M. Cornell. 1991. *Iron oxides in the laboratory: Preparation and characterization*. VCH, New York, NY.
- Shukla, S. S., J. K. Syers, J. D. H. Williams, D. E. Armstrong and R. F. Harris. 1971. Sorption of inorganic phosphate by lake sediments. *Soil Sci. Soc. Am. Proc.* 35:244-249.
- Sigg, L., and W. Stumm. 1980. The interaction of anions and weak acids with the hydrous goethite (α -FeOOH) surface. *Colloids Surfaces*, 2:101-117.
- Sposito, G. 1986. Distinguishing adsorption from surface precipitation. p. 217-228. *In* J.A. Davis and K.F. Hayes (eds.) *Geochemical processes at mineral surfaces*. ACS Symposium Series 323, Chicago, IL Sept. 8-13, 1985. ACS, Washington, DC.
- Stevenson, F. J. 1986. *Cycles of soil: Carbon, nitrogen, phosphorus, sulfur, micronutrients*. John Wiley and Sons, New York, NY.
- Stumm, W., and G. F. Lee. 1961. Oxygenation of ferrous iron. *Ind. Eng. Chem.* 53:143-146.

- Stumm, W., and J. J. Morgan. 1981. Aquatic chemistry. 2nd ed. John Wiley and Sons, New York, NY.
- Syers, J. F., R. F. Harris, and D. E. Armstrong. 1973. Phosphate chemistry in lake sediments. J. Environ. Qual. 2:1-14.
- Syers, J. K., and I. K. Iskandar. 1981. Soil-phosphorus chemistry. p.571-599. I.K. Iskandar (ed.) *In* Modeling wastewater renovation. John Wiley and Sons, New York, NY.
- Tarapchak, S. J., S. M. Bigelow, and C. Rubitschun. 1982. Soluble reactive phosphorus measurements in Lake Michigan: Filtration artifacts. J. Great Lakes Res. 8:550-557.
- Tessenow, U. 1974. Solution, diffusion, and sorption in the upper layer lake sediments. IV. Reaction mechanisms and equilibria in the system iron-manganese-phosphate with regard to the accumulation of vivianite in Lake Ursee. Arch. Hydrobiol. Suppl. 47:1-79.
- Tipping, E., C. Woof, and D. Cooke. 1981. The adsorption of aquatic humic substances by iron oxides. Geochim. Cosmochim. Acta 45:191-199.
- Tipping, E., and M. Ohnstad. 1984. Colloid stability of iron oxide from a freshwater lake. Nature 308:266-268.
- van Riemsdijk, W. H., L. J. M. Boumans, and F. A. M. de Haan. 1984. Phosphate sorption by soils: I. A diffusion-precipitation model for reaction of phosphate with metal oxides in soil. Soil Sci. Soc. Am. J. 48:537-541.
- Waite, T. D., and F. M. M. Morel. 1984. Photoreductive dissolution of colloidal iron oxides in natural waters. Environ. Sci. Technol. 18:860-868.
- Waychunas, G. A., B. A. Rea, C. C. Fuller, and J. A. Davis. 1993. Surface chemistry of ferrihydrite: Part 1. EXAFS studies of the geometry of coprecipitated and adsorbed arsenate. Geochim. Cosmochim. Acta 57:2251-2269.
- Williams, J. D. H., H. Shear, and R. L. Thomas. 1980. Availability to *Scenedesmus quadricauda* of different forms of phosphorus in sedimentary materials from the Great Lakes. Limnol. Ocean. 25:1-11.

CHAPTER 3

COLLOIDAL PHOSPHORUS AND COLLOIDAL IRON IN THE TUALATIN RIVER BASIN

Although colloids can affect the transport and chemistry of trace constituents in some aquatic systems, there are few estimates of the mass of given constituents in colloidal forms. The existence, variability, and origin of colloidal Fe oxide, and its effect on P chemistry, was evaluated in the Tualatin River Basin of northwestern Oregon. Watershed streams were regularly sampled during 1992 and 1993. The concentrations of P and Fe in the colloidal size class (0.05-1.0 μm) were determined by filtration. Elemental composition of the suspended material was assessed using scanning electron microscopy/energy-dispersive spectroscopy (SEM/EDS). Colloidal P and Fe ranged from 0 to 48% and 2 to 77% of the total P and total Fe, respectively. Since filtration underestimates colloidal concentrations, these are conservative estimates. Concentrations of P and Fe in colloidal form were correlated ($r^2=0.83$; $P<0.001$) but total P, total Fe, and total suspended sediments were not correlated. SEM/EDS analysis showed that, in addition to P and Fe, the colloids contained Si, Al, and Ca. The colloids were enriched with P and Fe relative to Al and Si. Evidence suggests that the colloidal P and Fe particles form as groundwater- or sediment-released Fe(II) is oxidized to Fe(III), which associates with P, either as coatings on the surface of colloidal clays and organics or as homogeneous particles.

3.1 Introduction

The transport and chemistry of trace elements in natural waters are influenced by interactions with suspended particles (Stumm and Morgan, 1981). One of the most important and least understood classes of suspended particles are colloids, particles with linear dimensions between 0.001 and 1.0 μm (Hiemenz, 1986). For particles of this size, the effects of gravity and buoyancy are small compared to the effects of Brownian motion. Consequently, they remain suspended in water in the absence of coagulation. In addition, as particle dimensions are reduced, the surface area per unit mass of material increases. This is an important consideration for surface-reactive species, such as phosphate, trace metals, and organics.

In general, colloid-associated elements or compounds behave quite differently from species that are truly dissolved or associated with larger particles that settle. Colloid-associated material may be transported much further than material associated with larger particles (O'Melia, 1980; McCarthy and Zachara, 1989). Long residence times in the water column and the photic zone affect nutrient bioavailability (Williams et al., 1980). Finally, due to their higher specific surface areas, colloids may be enriched with surface-reactive species relative to larger particles (Sharpley, 1980).

An important characteristic of naturally-occurring Fe oxides is their tendency to exist as colloid-sized particles. Leppard et al. (1988) isolated Fe oxide colloids at the redox transition boundary of a stratified freshwater lake. The colloids ranged from 0.05 to 0.3 μm in diameter and included P, Ca, and some Si and Al. Tipping et al. (1981) described a homogeneous population of Fe oxide colloids in a stratified lake with diameters in the range 0.05 to 0.5 μm . The colloids contained Ca, P, Si, and C as well as Fe. Laxen and Chandler (1983) found Fe oxide colloids with a uniform particle distribution in the 0.05 to 0.4 μm size range in three freshwater lakes and a stream. Mobile ferrous phosphate colloids of approximately 0.1 μm diameter were detected in a sewage-contaminated groundwater (Gschwend and Reynolds, 1987). The size distributions of the Fe oxide colloids in all these studies were similar.

Because of the ubiquity and reactivity of Fe, colloidal Fe oxides influence the geochemical behavior of pollutant elements, including P and many metals. But there are

very few estimates of the relative mass of elements in colloids (Honeyman and Santschi, 1992). Until recently, colloids were usually not considered in field studies nor were they commonly included in conceptual or mathematical models. One reason may be the analytical difficulties in their measurement and identification.

A number of methods have been used for sampling the submicron particle-size spectrum, although no method is perfect. Centrifugation suffers from a lack of size selectivity for particles and particle coagulation and aggregation in the centrifugation tubes is a serious problem for natural samples (Davison and DeVitre, 1992). New techniques such as laser Doppler velocimetry, laser correlation spectrometry, and transmission electron microscopy are emerging as useful tools for well-defined systems but these techniques are expensive and their application to natural systems, with low colloid concentrations and irregular particle size distributions is limited (Honeyman and Santschi, 1992). Filtration is often used for separating solid and dissolved phases and for size fractionation of particles (Laxen and Chandler, 1982). While it offers advantages over other techniques (Buffle et al., 1992), filtration can underestimate or obscure colloidal concentrations in two ways.

First, colloids can be small enough to pass through the pores of the filter (Danielsson, 1982; Tarapchak et al., 1982). Dissolved constituents are commonly defined as those materials that pass through a 0.45 μm filter (APHA, 1989), an operational definition that includes colloidal as well as dissolved phases. Second, colloids can be retained on filters even when they are much smaller than the pores of the filter (Buffle et al., 1992; Horowitz et al., 1992). This is due to the high flow rates imposed during filtration, the low porosity of the filters, and the clogging of filters at higher filter loads.

The advantages of filtration are its low cost and convenience and its widespread use which makes independent data sets comparable. Filtration can be performed in the field, which is important given the dynamic behavior of colloids. The most accurate size fractionation with filtration can be obtained by using sequential filtration, polycarbonate membrane filters, minimal filter loading, and low flow rates (Buffle et al., 1992). Consideration of these factors will improve the accuracy of filtration considerably. In view of the problems inherent with all methods, filtration is a reliable method that

provides a conservative estimate of colloidal concentrations.

The Tualatin River watershed of northwestern Oregon is the site of intensive studies of phosphorus dynamics (e.g., Abrams and Jarrell, 1995). The 1800 km² watershed is drained by the Tualatin River and a number of tributaries. The upper watershed consists of forested and agricultural lands, and the lower watershed is heavily urbanized. Years of high P loadings from point and nonpoint sources, including naturally enriched groundwaters and soils, have stimulated excess productivity and algal growth in this system. Most of the point sources have been controlled, but P loading from subsurface sources and surface runoff continues to be a problem. One of our research goals in the watershed has been to evaluate P forms in the river and its tributaries.

Because local soils and groundwaters are often high in Fe, we hypothesized that P in the waters of the Tualatin are likely associated with colloidal Fe oxides. The objectives of the study were to determine how much colloidal P and Fe existed and whether P and Fe were directly associated in colloidal form.

3.2 Materials and Methods

Northwestern Oregon has a typical maritime climate with moderate, low-intensity rainfall from October to June and an extended dry period from July to September. Parent materials of the Tualatin Basin include weathered sedimentary or igneous bedrock, unconsolidated material deposited by water, or aeolian silts. Natural background levels of P in soils are high, ranging from 660 to 2304 mg P/kg soil (Abrams and Jarrell, 1995).

Two studies of P and Fe were conducted in the Tualatin River Basin. A preliminary study (the "Bronson Creek" study) was conducted on Bronson Creek (Site 4; Fig. 3.1), a small tributary of the Tualatin River. Grab samples were collected every other day for three two-week periods in early August, late September, and mid-November 1992. Two additional samples were collected in February 1993. In April of 1993, the sampling was expanded to sites along several main tributaries, including Site 4 at Bronson Creek, and the mainstem of the Tualatin River (the "Tualatin Basin" study; Fig. 3.1). A total of six sites were sampled once every six weeks from April to November. May to October is the regulated season for P concentrations in the Tualatin Basin.

Filtration was used for size fractionation in this study with efforts made to minimize errors, as discussed above. In the Bronson Creek study, filtration was performed after returning to the lab within ten minutes of sample collection. For the Tualatin Basin study, filtration was performed in the field at all sites. Sequential filtration

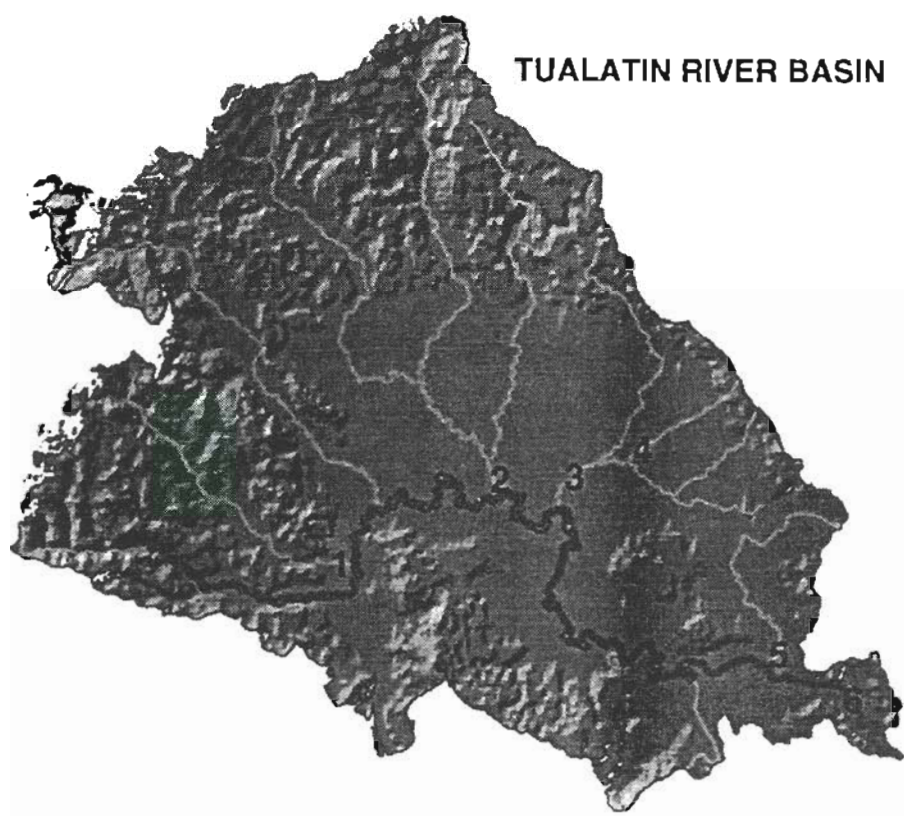


Figure 3.1 Location of sampling sites in the Tualatin River watershed: (1) Scoggins Creek, (2) Dairy Creek, (3) Rock Creek, (4) Bronson Creek, (5) Fanno Creek, and (6) the lower Tualatin. The mainstem Tualatin River is grey.

was performed with Nucleopore (Costar Corp., Cambridge, MA) polycarbonate membrane filters (47 mm diameter) with small sample volumes (2-6 mL/cm²) to minimize clogging. Samples were filtered first through a 1.0 μ m pore size filter and subsequently through a 0.05 μ m pore size filter. While colloid size is a continuum from 0.001 to 1.0 μ m

(Hiemenz, 1986), the lower diameter limit of most Fe oxide colloids described in the literature is 0.05 μm (Tipping et al., 1981; Laxen and Chandler, 1983; Leppard et al., 1988). Therefore, the colloidal fraction in this study was defined by difference as the material that passed through the 1.0 μm filter but not the 0.05 μm filter. Concentrations in the 0.05 μm filtrates were considered to be the dissolved fraction. The particulate fraction was defined as the difference between the concentration in the unfiltered sample and the 1.0 μm filtrate.

Field water quality measurements at each site included pH, temperature, turbidity, flow, and dissolved oxygen. The pH was measured with a glass electrode and a 290A pH meter (Orion Research Inc., Boston, MA) and turbidity with a DRT-15 C turbidimeter (HF Scientific Inc., Fort Myers, FL). Flow was measured with staff plates or a pygmy current meter. Dissolved oxygen was determined using the acidic indigo carmine colorimetric method with CHEMet vials (CHEMetrics Inc., Calverton, VA) and a portable spectrophotometer.

Samples were returned to the lab for chemical analysis of Fe, Si, Al, Ca and P. Total suspended solids (TSS) were also measured in the Tualatin Basin study. All filtrates were acidified with 3.6 M H_2SO_4 immediately after filtration and allowed to stand overnight or longer. Dissolved Fe(II) and total Fe were measured colorimetrically using the phenanthroline method with a detection limit of 0.007 mg/L (Tamura et al., 1973; APHA, 1989). Silicon was measured using the molybdosilicate method (APHA, 1989), Al using catechol violet (Dougan and Wilson, 1974), and Ca determined with atomic absorption spectrometry (APHA, 1989). Total suspended solids were determined from the oven dry weight of the residue retained on a glass fiber filter with a nominal pore size of 0.7 μm (APHA, 1989).

Phosphorus concentrations were measured on an Alpkem autoanalyzer (Perstorp Analytical, Wilsonville, OR) using the ascorbic acid method (APHA, 1989) with a detection limit of 0.005 mg/L. Two P forms were measured: "reactive P," with no preliminary treatment beyond acidification, and "total P," which consisted of a persulfate oxidation in a strong acid digest (APHA, 1989). "Reactive P" is largely a measure of orthophosphate, both dissolved and suspended, although a small amount of organic P will

hydrolyze in the acidic reagents. Phosphorus fractions converted to orthophosphate by the strong oxidant in the acid digest are considered to be organically-bound, so the difference between total P and reactive P is organic P (APHA, 1989). Reactive P and total P were measured in all three size classes: dissolved ($<0.05\ \mu\text{m}$), colloidal ($0.05\text{-}1.0\ \mu\text{m}$), and particulate ($>1.0\ \mu\text{m}$).

Particles retained on the filters from both studies were imaged with a Zeiss DSM-960 scanning electron microscope (SEM) after the filters were desiccated and coated with gold. The purpose of the SEM imaging was to independently evaluate the size distribution of the solids and to examine the efficiency and accuracy of size fractionation by filtration. The image resolution of the SEM approached the lower limit of the size distribution of most Fe oxide colloids ($0.05\ \mu\text{m}$).

Energy-dispersive spectroscopy (EDS) was used for elemental analysis of suspended solids on both the 0.05 and $1.0\ \mu\text{m}$ filters from five representative samples of the Tualatin Basin study. A multi-window X-ray analyzer was used with Link eXL2 software and ZAF-4 quantitative analysis (Williams, 1984). Filters were coated with carbon for elemental analysis since gold interferes with the P signal. Spectra were collected from six to seven colloids on each of five $0.05\ \mu\text{m}$ filters and five to six particles ($> 1.0\ \mu\text{m}$) on each of five $1.0\ \mu\text{m}$ filters. Elemental standards were analyzed and used for quantitative analysis. Synthesized samples were prepared from the oxidation of Fe(II) in the presence of Si, P, and Ca to check the analysis. Spectra from blank polycarbonate filters consisted of C and O only. The SEM/EDS analysis is discussed further in Appendix B.

3.3 Results and Discussion

Sampling in the Bronson Creek study was frequent but localized (one point sampling). This allowed the temporal variability in colloidal P and Fe to be examined and yielded information regarding the formation of colloidal material. The more extensive but less frequent sampling in the Tualatin Basin study (six point transect sampling) permitted examination of the extent of colloidal P and Fe on a watershed scale. The two studies provided different types of information on colloids due to the contrasting

sample methodologies employed. The results from each study will be discussed separately, beginning with the Bronson Creek study. Results for all field and laboratory measurements from both studies are presented in Appendix C.

3.3.1 Bronson Creek Study - Temporal Variability and Colloidal Origin

Concentrations of colloidal P and Fe in Bronson Creek ranged from 0.005 to 0.135 mg/L and 0.095 to 1.625 mg/L, respectively (Fig. 3.2). The colloidal concentrations represented 7 to 49% of the total P and 12 to 98% of the total Fe. Colloidal/particulate ratios ranged from 0.07 to 1.49 and 0.14 to 41.57 for P and Fe, respectively (Fig. 3.3). Phosphorus correlated very strongly with Fe in the colloidal fraction ($r^2=0.89$; $P<0.001$) but not in the particulate fraction ($r^2=0.42$; $P<0.01$), suggesting that P and Fe were more closely associated in colloids. The average P/Fe molar ratio of the colloidal size fraction was 0.16 (S.D. \pm 0.06). Solid phase Fe was present as Fe(III) and dissolved Fe(II) concentrations were low (≤ 0.100 mg/L).

The concentrations and relative fractions of colloidal and particulate P and Fe varied considerably (Fig. 3.2 and 3.3). At least three levels of variability exist. There is a seasonal decrease in the relative fraction of colloidal P and Fe (Fig. 3.3). The average colloidal/particulate ratios for P and Fe in each sampling period decrease through the season. An approximate t-test (Miller and Miller, 1988) showed that the November/February mean ratio is significantly lower than the August mean ratio ($P<0.05$) for both elements. An F test showed that the variance of the mean was significantly higher in August than November/February ($P<0.05$).

Some of the variability within sampling periods appears to be in response to stream hydrologic conditions. Rainfall during the sampling periods occurred on 8/6/92 to 8/7/92 (6.9 mm), 9/23/92 to 9/24/92 (15.5 mm.), and 11/19/92 to 11/22/92 (61.2 mm) (USGS, unpublished data). Stream response to these events was rapid as evidenced by increased dissolved oxygen concentrations (Fig. 3.4), turbidities, and flows. Colloidal fractions of P and Fe decreased and particulate fractions increased after these rain events (Fig. 3.3) especially from 9/23/92 to 9/24/92 and 11/20/92 to 11/25. One reason for this is that higher stream velocities following rainfall events result in erosion and resuspension

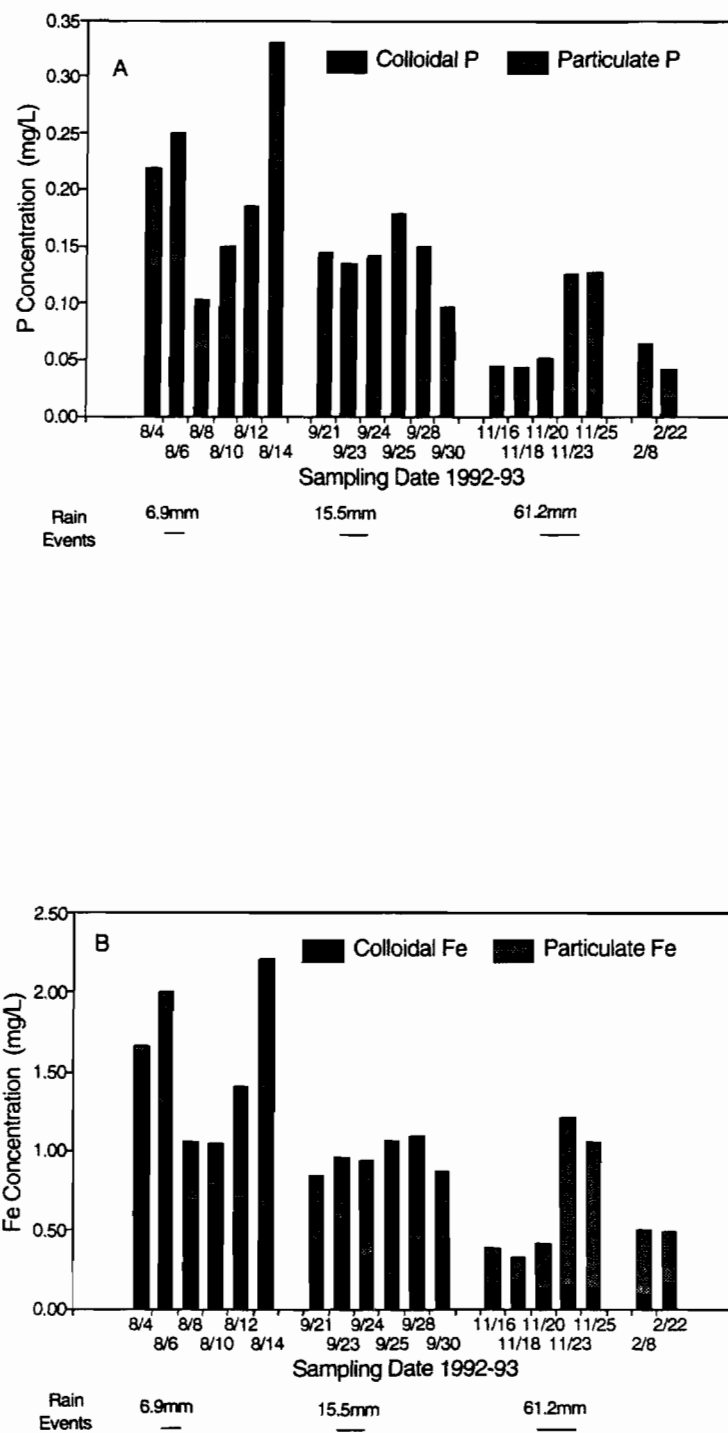


Figure 3.2 Phosphorus (A) and iron (B) concentrations in the colloidal (0.05-1.0 μm) and particulate (>1.0 μm) size fractions in the Bronson Creek study.

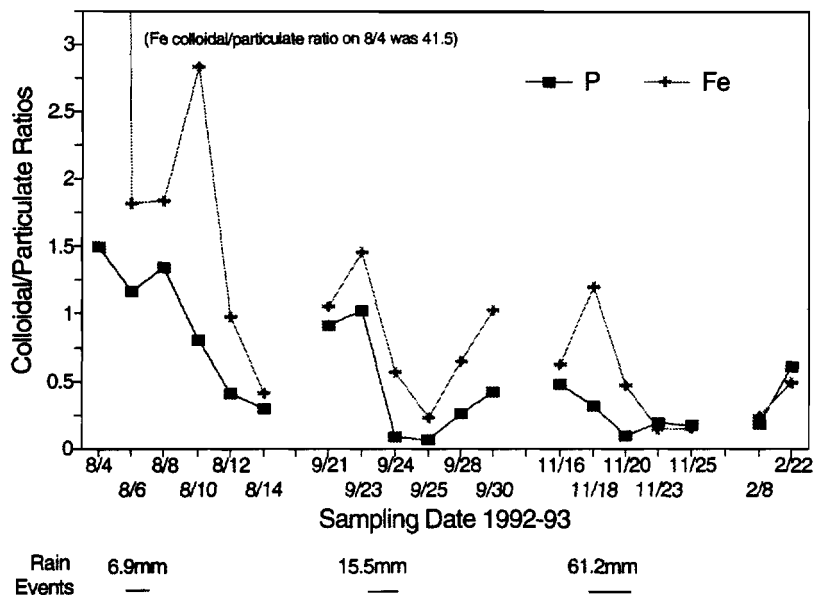


Figure 3.3 Average colloidal/particulate ratios for P and Fe in the Bronson Creek study.

of larger particles and higher particulate fractions. Colloids remain in suspension regardless of flow, but the relative fraction decreases as a result of the increase in particulate concentrations.

Another source of variability in the colloidal and particulate concentrations is related to colloidal stability. Phosphorus and Fe shifted from the colloidal fraction to the particulate fraction between 8/10/92 and 8/14/92 (Fig. 3.3) although there were no hydrologic changes during this period. Observations suggest that coagulation and aggregation of the colloids caused the increases in particulate concentrations. The streambed was covered with a reddish floc on 8/14/92 which was not previously observed. The floc probably formed as colloids aggregated into larger particles which then settled to the bottom during the low-flow conditions. Analysis of settled material revealed a P/Fe molar ratio of 0.34, similar to the P/Fe molar ratio (0.30) of the suspended particulate

fraction on 8/14/92. Colloidal concentrations would be expected to decrease as colloids coagulated to larger particles. However, absolute concentrations of colloidal P and Fe were relatively stable from 8/10/92 to 8/14/92 (Fig. 3.2). A continuous groundwater or sediment source of colloidal Fe-P may have sustained these concentrations despite colloid coagulation.

Many descriptions of natural Fe oxide colloids in the literature involve newly-formed precipitates at the redox interface (Tipping et al., 1981; Leppard et al., 1988; Davison and DeVitre, 1992). Colloidal Fe forms in situ as groundwater- or sediment-released Fe(II) migrates to the sediment/water interface and is oxidized to Fe(III). The Fe(III) precipitates as either homogeneous particles or as surficial coatings on clay and organic colloids. Colloidal flocs formed at the sediment/water interface may subsequently be suspended and dispersed into the water column. Evidence from groundwater chemistry and oxygen concentrations suggests colloidal Fe-P formed in a similar way in Bronson Creek.

Shallow groundwaters in the Tualatin Valley are often reducing and high in P and Fe(II) and may be major sources of P in the watershed, especially during base flow periods (USGS, unpublished data). We did not sample groundwaters adjacent to Bronson Creek, but we did observe groundwater seeps on the banks that were visibly red with Fe that had oxidized upon exposure to atmospheric oxygen. This is evidence that reducing groundwater was entering the stream.

The stream exhibited a high oxygen demand, often exceeding reaeration capacity as indicated by the low percent saturations observed (Fig. 3.4). Given these oxygen deficits, only a thin oxidized layer would have developed in the sediments. Hence, dissolved Fe(II) diffuses to the sediment/water interface or the water column rather than being oxidized deeper in the sediments. The oxidation of Fe(II) results in the formation of colloid-sized Fe oxide particles. A thicker oxidized layer in the sediments prevents the migration of Fe(II) to the sediment/water interface. Therefore, higher dissolved oxygen concentrations in the fall (Fig. 3.4) would be partly responsible for the seasonal decrease in the mass fraction of colloidal P and Fe (Fig. 3.3).

The P/Fe molar ratio of the colloids is high (0.16) compared to laboratory studies

of P adsorption on Fe oxides (Ryden et al., 1977; Lijklema, 1980), especially given the streamwater pH (6.9-7.3) and soluble P concentrations (0.015-0.078 mg/L). Laboratory experiments have demonstrated that such high sorption densities are characteristic of newly-formed or coprecipitated material (Chapter 5).

3.3.2 Tualatin Basin Study

Based on the preliminary findings in Bronson Creek, sampling was expanded to assess colloidal P and Fe throughout the Tualatin Basin in 1993. Colloidal concentrations are shown in Figure 3.5 for five of the six sites, excluding Scoggins Creek (Site 1; Fig. 3.1). Scoggins Creek, near the head of the Tualatin River, had consistently low concentrations of all forms of P and Fe, and colloidal P was nondetectable at this site. For the remaining five sites, colloidal P and Fe concentrations ranged from 0.0 to 0.061 mg L⁻¹ and 0.006 to 0.989 mg L⁻¹, respectively. Actual colloidal concentrations are

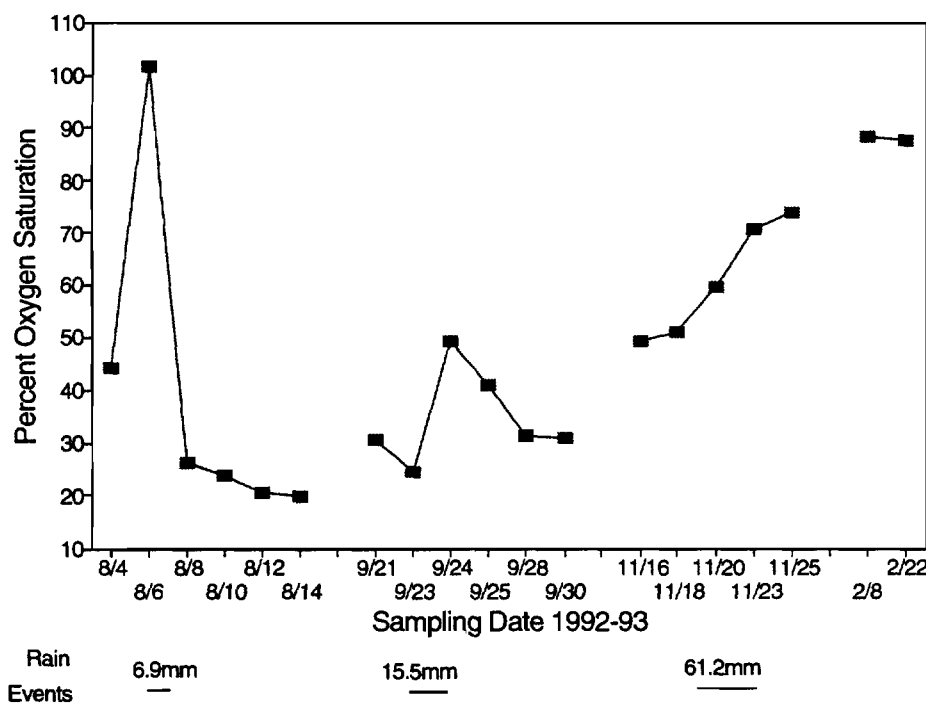


Figure 3.4 Dissolved O₂ saturation percentages in the Bronson Creek study.

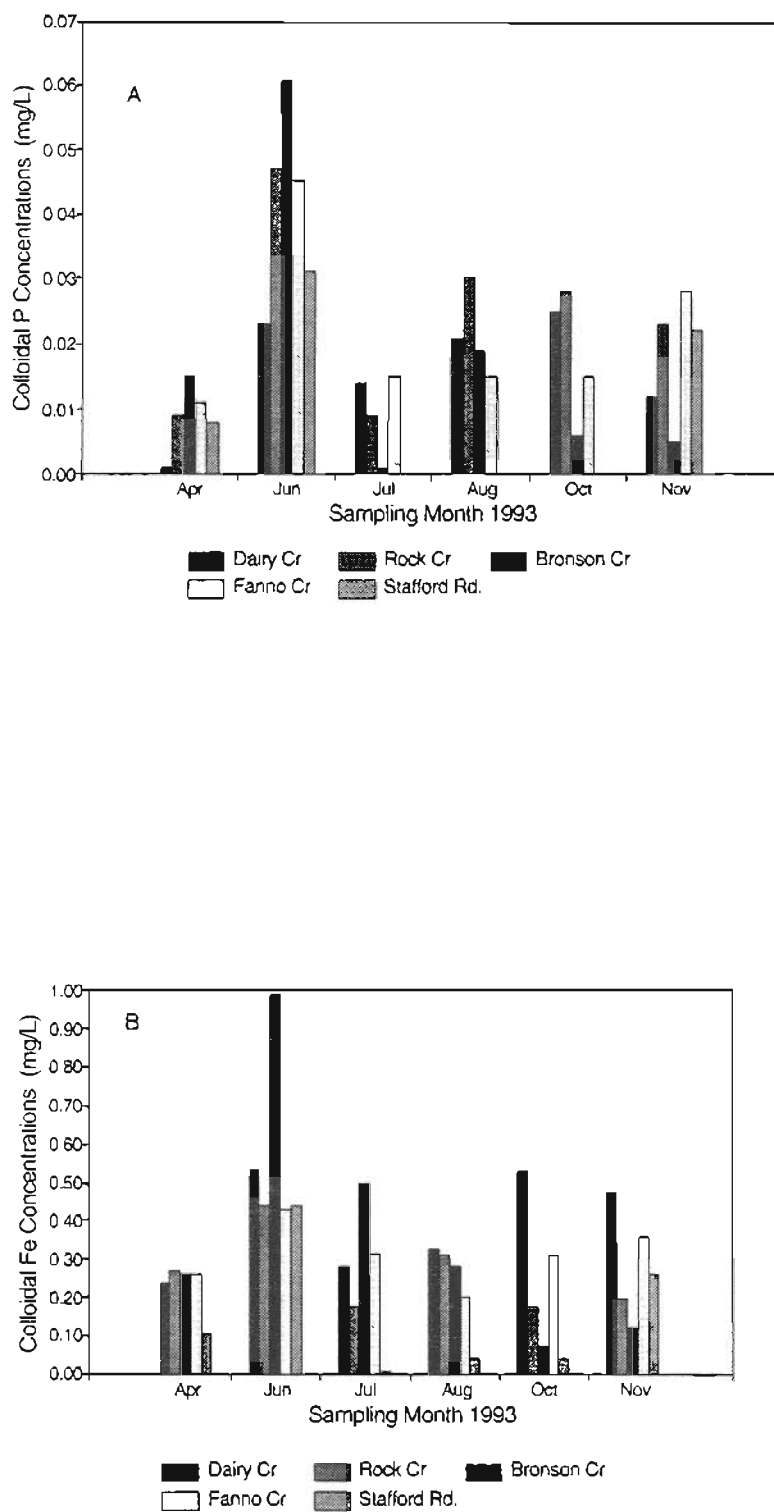


Figure 3.5 Colloidal phosphorus (A) and iron (B) concentrations in the Tualatin River study, for all sites except Scoggins Creek.

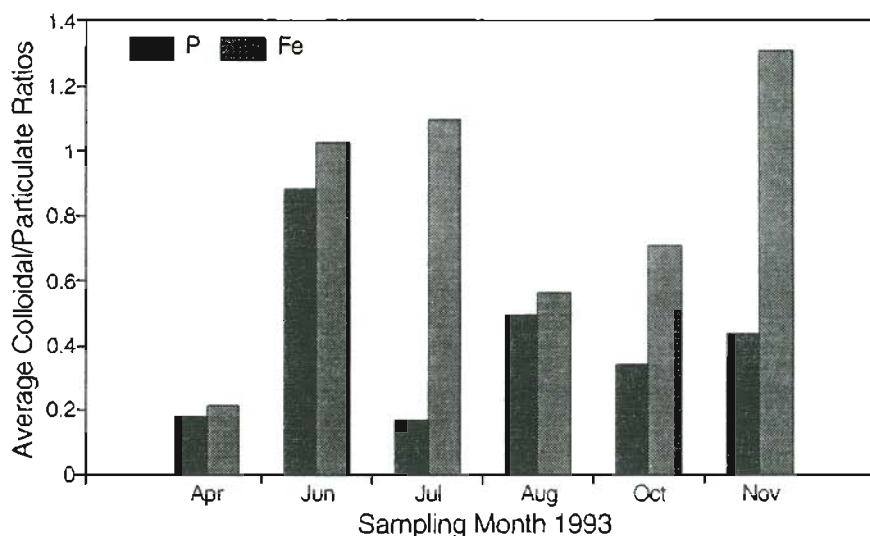


Figure 3.6 Average colloidal/particulate ratios for P and Fe in the Tualatin River study, for all sites except Scoggins Creek.

probably higher, because the colloidal fraction is typically underestimated by filtration (Buffle et al., 1992). Colloidal concentrations represented 0 to 48% of the total P and 2 to 77% of the total Fe. Colloidal/particulate ratios ranged from 0.0 to 1.65 and 0.02 to 3.85 for P and Fe, respectively. Monthly averages of the colloidal/particulate ratios for the five sites are presented (Fig 3.6).

The 1993 colloidal concentrations in the Tualatin Basin study are lower than those observed in the Bronson Creek study, 1992. As discussed above, climatic and hydrologic factors are important in the formation and extent of colloids. The six-month period, April to September, was drier in 1992 than in 1993 (180 versus 272 mm of precipitation) and this may relate to the lower colloidal concentrations in 1993. During wetter periods, groundwater inputs will be relatively less important and larger particles from runoff and resuspension are more prevalent.

Colloidal P was significantly correlated with colloidal Fe in the Tualatin Basin

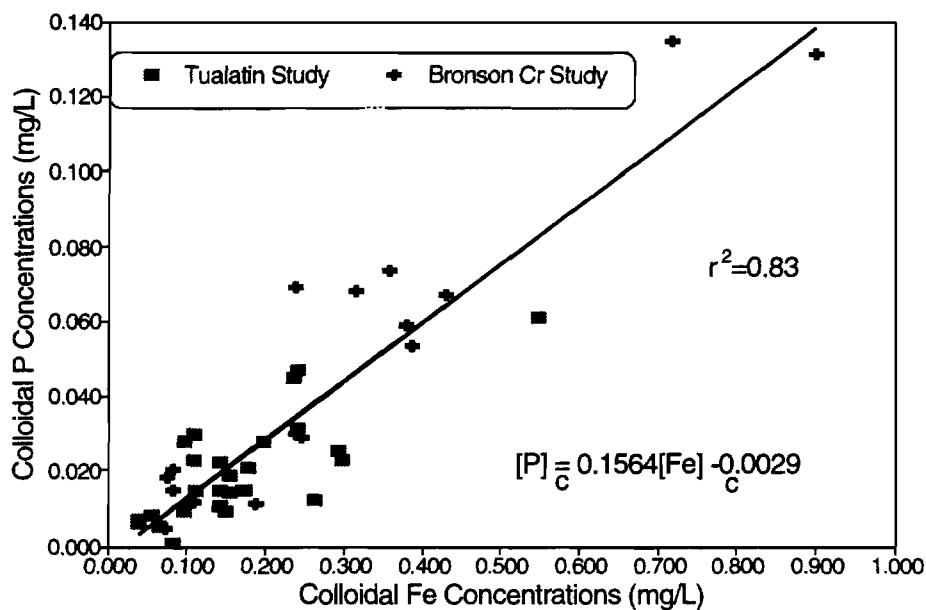


Figure 3.7 Correlation of phosphorus and iron in colloidal form; data from both Bronson Creek and Tualatin River studies.

study ($r^2=0.56$; $P<0.001$). Particulate P and Fe were not correlated in the Tualatin Basin study. The average P/Fe molar ratio of the colloidal size fraction was 0.13 (S.D. \pm 0.06), similar to that in the Bronson Creek study in 1992. Analyzing data from both studies together, the colloidal Fe-P relationship produced an $r^2=0.83$ ($P<0.001$) (Fig. 3.7), with an average P/Fe molar ratio of 0.14 (S.D. \pm 0.07). The significant correlation of colloidal P and Fe across concentration ranges suggests the colloids are similar in composition and origin.

The average colloidal P and Fe concentrations for all five sites was significantly higher in June than all other months except November ($P<0.05$). Two-way analysis of variance was used to estimate the components of variance. Neither the variability with time nor with site were as great as the variability due to unexplained factors.

Colloidal P and Fe concentrations in the mainstem of the Tualatin River at Stafford Road (Site 6; Fig. 3.1) were very low or nondetectable during July, August, and

October (Fig. 3.5). Chlorophyll *a* concentrations at this site increased to 35 mg L⁻¹ or more from July to October, reflecting increased algal activity (Unified Sewerage Agency, Hillsboro, OR; 1993 unpublished data). Chlorophyll *a* concentrations at the other sites were usually much lower (<10 mg L⁻¹). The increased algal activity may have removed colloidal P and Fe through nutrient uptake, dissolution or desorption under the higher pH due to photosynthesis, or settling of attached algal masses (Kuwabara and Chang, 1986).

As colloidal P concentrations in the Tualatin at Stafford Road dropped during the summer, there was a simultaneous increase in total P to the highest value observed (0.322 mg L⁻¹). The increased algal activity resulted in a transfer of P from inorganic to organic forms. While colloidal P decreased during this period, soluble P increased with total P at this site. We feel this was a sampling artifact since filtration can cause soluble P to be released from cells or detritus (Tarapchak et. al, 1982).

3.3.3 Phosphorus Forms in each Size Class

Phosphorus in the colloidal size class was present as inorganic orthophosphate rather than organic P, based on the values of reactive P and total P. As discussed earlier, the total P digestion releases organically bound P so differences between reactive P and total P values represent organic P. A paired t-test of reactive P and total P concentrations in the colloidal size class showed that the mean difference between the two methods was not significant (mean difference=-0.002 mg L⁻¹; P<0.28). Significant differences were found between reactive P and total P in both the dissolved fraction (mean difference=-0.009 mg L⁻¹; P<.001) and the unfiltered fraction (mean difference=-0.16 mg L⁻¹; P<0.001), implying that these fractions contained organic P.

3.3.4 Electron Microscopy Results

Most of the colloids observed with SEM were 0.1 to 0.4 µm in diameter. This is similar to the size of Fe oxide colloids described in other field studies (Tipping et al., 1981; Laxen and Chandler, 1983). Some colloidal material was retained by the 1.0 µm filters although the colloids were smaller than the pores and should have passed through the filters. As discussed in the introduction, high flow rates or high filter loads during

filtration can lead to retention of smaller particles. Retention on the filters results in an underestimate of the material in the colloidal (0.05-1.0 μm) size class and an overestimate of the material in the particulate size class (>1.0 μm). The estimates of colloidal concentrations are low.

Energy-dispersive spectroscopy was used to examine the elemental composition of suspended solids on both the 1.0 μm and the 0.05 μm filters of samples from the five sites, excluding Scoggins Creek. One complication with EDS is that X-ray spatial resolution is not nearly as high as image resolution. This means that filters as well as suspended solids contributed to X-ray spectra. Only atomic ratios from the EDS results were analyzed because atomic percentages are not accurate unless the precise X-ray volume is known. Blank filter spectra consisted of C and O. Carbon and oxygen were undoubtedly associated with the colloids as well but filter contributions prevented quantitative analysis of these elements.

The composition of the colloids was fairly uniform at all sites. In addition to P and Fe, the colloidal particles contained Si, Al, Ca, and occasionally K, Mg, Cl, and S. Silicon was present in all spectra and Al and Ca were present in many of them. The composition of the colloids was similar to the composition of other Fe-containing colloidal material described in the literature (Tipping et al., 1981; Leppard et al., 1988). Silicon, Al, and Ca were detected by macroscopic chemical methods as well, but we had difficulty distinguishing colloidal from soluble forms because of high background concentrations. Filters were not rinsed prior to EDS analysis and there was evidence that the solution chemistry in the river samples affected the elemental results somewhat. The values of Cl, S, Si, and Ca measured on the filters may have been inflated by soluble material retained on the filters. A few of the colloids from Rock Creek and Dairy Creek had significant levels of Ni, Cu, Cr, and Sn associated with the Fe, demonstrating local trace metal sources in these watersheds.

The EDS data showed differences in elemental compositions between colloidal and particulate fractions. The P/Si and Fe/Si molar ratios were higher in the colloids than the larger particles, indicating an enrichment of P and Fe in the colloids relative to Si (Fig. 3.8). A Mann-Whitney U test showed that the difference was significant ($P < 0.001$). A

similar relationship was observed for P/Al and Fe/Al ratios. Some of the P and Fe certainly existed as surface coatings on aluminosilicate solids. As expected, colloidal aluminosilicates accumulate more surficial P and Fe because of their higher specific surface areas.

One difference between the particulate and colloidal fractions was that some of the colloids from each tributary contained Si, Fe, and P with little or no Al. This indicates that some of the colloids consisted of a separate Fe oxide phase with some Si included, rather than Fe oxide coatings on clays. All the larger particles contained Al. Concentrations of dissolved Si were characteristically high in this system, ranging from 2 to 15 mg L⁻¹. The association of Si and Fe oxides has been reported in laboratory and field studies and has important implications for the surface and sorption properties of the oxide (Anderson and Benjamin, 1985). Additionally, our laboratory work has shown that Si can stabilize colloidal Fe oxides very effectively at the concentrations observed in this system (Chapter 4). Silicon may be partially responsible for stabilization of colloids in this system.

3.4 Conclusions

From 0 to 48% of the total P and 2 to 77% of the total Fe occurred in colloidal form in the Tualatin River system, as determined by filtration. This is a low estimate as filtration tends to underestimate the extent of colloidal concentrations. Phosphorus in the colloidal size fraction was inorganic rather than organic. Concentrations of P and Fe were strongly correlated in the colloidal size fraction ($r^2=0.83$; $P<0.001$), but poorly correlated in larger particles.

Colloidal P and Fe concentrations varied with site and season. Results from the Bronson Creek study demonstrated that fractions of colloidal P and Fe were generally greater during low flow and low dissolved oxygen periods, indicating that surface runoff was not the dominant source of colloids. Colloidal P and Fe may have been forming in situ as a result of Fe(II) oxidation and association of P and Fe(III).

Particulate, colloidal, or soluble forms of P were not correlated with TSS concentrations in this study. This does not imply that eroded particulate material contains

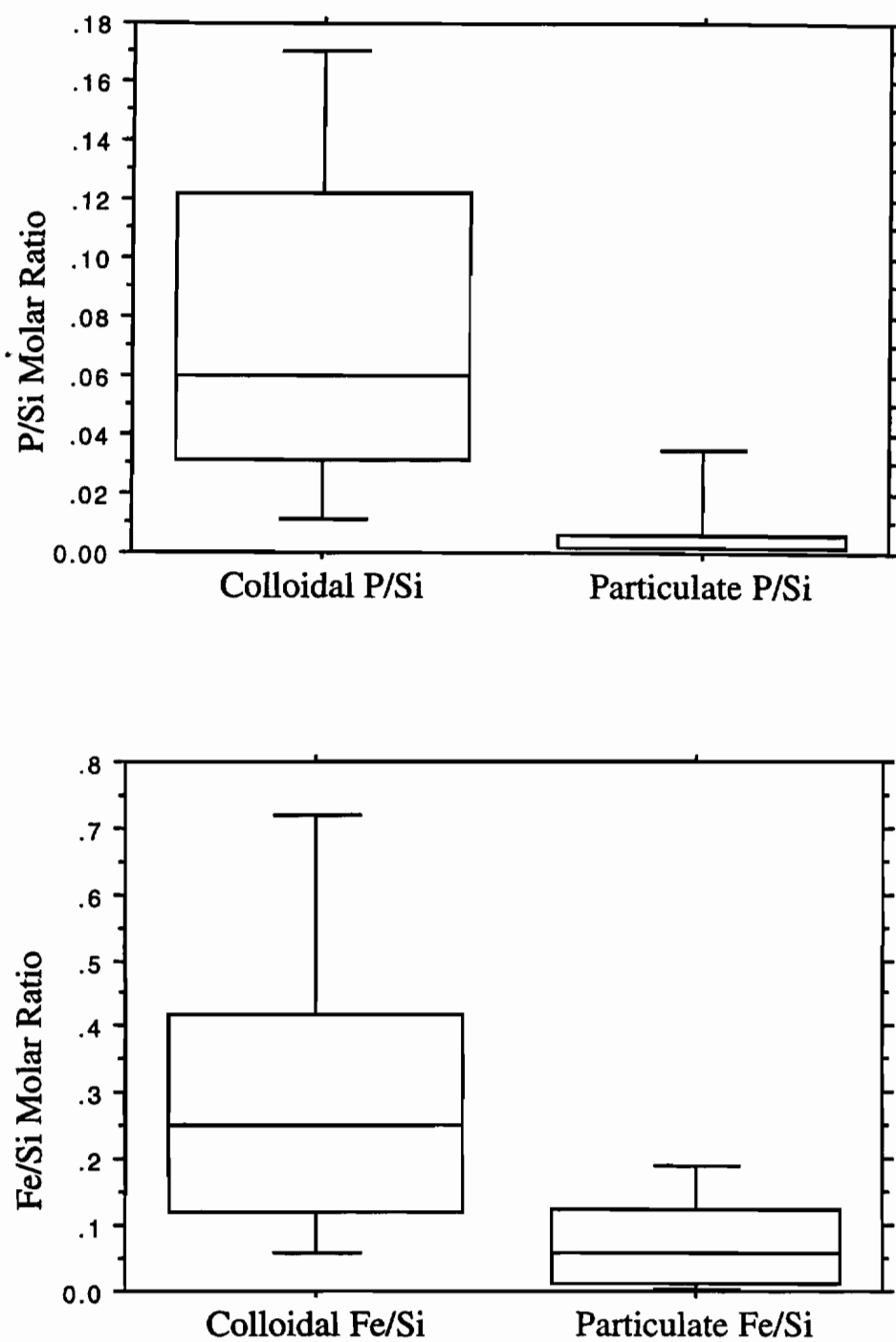


Figure 3.8 Box plots of the frequency distribution of molar ratios in the colloidal (<1.0 μm) and particulate (>1.0 μm) size classes. The upper and lower whiskers extend to the 90th and 10th percentile, respectively.

no P. Rather, this indicates the importance of bottom sediment and subsurface sources of P. Control of P inputs is not just a matter of eliminating surface runoff in this system. Total P and total Fe were not correlated, despite the significant correlation of P with Fe in the colloidal size fraction. Undoubtedly, some P and Fe were associated in the particulate size fraction but it was difficult to distinguish from other forms using macroscopic methods.

Other elements were present in the colloidal material, based on SEM/EDS results. In addition to P and Fe, the colloidal material consisted of Si, Al, and Ca. Compared with the larger particulate size fraction, the colloids were enriched in P and Fe relative to Si and Al.

Colloidal P has important implications for the transport, bioavailability, and management of P in aquatic systems. Colloidal P will be transported along with the dissolved phase, resulting in much greater movement than is expected or predicted for other particulate forms of P. Correspondingly, chemical processes and reactions of colloidal P will differ from dissolved P.

Colloidal forms of P remain in the photic zone of the water column, accessible to algae. Colloidal P associated with Fe oxides has been shown to be bioavailable to algae in several studies (Logan et al., 1979; Dorich et al., 1985; Kuwabara et al., 1986). The decrease in the concentrations of colloidal P and Fe at the Stafford Road site suggests that biological activity affected colloidal forms of P in this study.

Colloids affect several other aspects of aquatic systems. High colloidal concentrations increase turbidity and light scattering, thereby affecting aquatic life (Cuker, 1987). Management strategies to control P are affected by colloidal P. Settling ponds and constructed wetlands intended to remove suspended solids or dissolved constituents may not effectively remove colloids or colloid-associated material. Colloids can complicate water analysis interpretation as well since they may be assigned as either part of the total particulate phase or the dissolved phase, depending on filtering conditions.

3.5 References

- Abrams, M. M., and W. M. Jarrell. 1995. Soil phosphorus as a potential nonpoint source for elevated stream phosphorus levels. *J. Environ. Qual.* 24:132-138.
- American Public Health Association. 1989. Standard methods for the examination of water and wastewater. 17th ed. Amer. Publ. Health Assoc., New York, NY.
- Anderson, P. R., and M. M. Benjamin. 1985. Effects of silicon on the crystallization and adsorption properties of ferric oxides. *Environ. Sci. Technol.* 19:1048-1053.
- Buffle, J., D. Perret, and M. Newman. 1992. The use of filtration and ultrafiltration for size fractionation of aquatic particles, colloids, and macromolecules. p. 171-230. *In: J. Buffle and H. van Leeuwen (eds.) Environmental particles.* Lewis Publ., Boca Raton, FL.
- Cuker, B. E. 1987. Field experiment on the influences of suspended clay and phosphorus on the plankton of a small lake. *Limnol. Oceanogr.* 32:840-847.
- Danielsson, L. G. 1982. On the use of filters for distinguishing between dissolved and particulate fractions in natural waters. *Water Res.* 16:179-182.
- Davison, W., and R. DeVitre. 1992. Iron particles in freshwater. p. 315-355. *In: J. Buffle and H. van Leeuwen (eds.) Environmental particles.* Lewis Publ., Boca Raton, FL.
- Dorich, R. A., D. W. Nelson, and L. E. Sommers. 1985. Estimating algal available phosphorus in suspended sediments by chemical extraction. *J. Environ. Qual.* 13:400-405.
- Dougan, W. K., and A. L. Wilson. 1974. The adsorptiometric determination of aluminum in water. A comparison of some chromogenic reagents and the development of an improved method. *Analyst* 99:413-430.
- Gschwend, P. M., and M. D. Reynolds. 1987. Monodisperse ferrous phosphate colloids in an anoxic groundwater plume. *J. Contam. Hydrol.* 1:309-327.
- Hiemenz, P. C. 1986. Principles of colloid and surface chemistry. Marcel Dekker, Inc., New York, NY.
- Honeyman, B. D., and P. H. Santschi. 1992. The role of particles and colloids in the transport of radionuclides and trace metals in the oceans. p. 379-415. *In: J. Buffle and H. van Leeuwen (eds.) Environmental particles.* Lewis Publ., Boca Raton, FL.
- Horowitz, A. J., K. A. Elrick, and M. R. Colberg. 1992. The effect of membrane filtration on dissolved trace element concentrations. *Water Res.* 26:753-763.

- Kuwabara, J. S., J. A. Davis, and C. C. Y. Chang. 1986. Algal growth response to particle-bound orthophosphate and zinc. *Limnol. Oceanogr.* 31:503-511.
- Laxen, D. P. H., and I. M. Chandler. 1982. Comparison of filtration techniques for size distribution in freshwaters. *Anal. Chem.* 54:1350-1355.
- Laxen, D. P. H., and I. M. Chandler. 1983. Size distribution of iron and manganese species in freshwaters. *Geochim. Cosmochim. Acta* 47:731-741.
- Leppard, G. G., F. Buffle, R. R. DeVitre, and D. Perret. 1988. The ultrastructure and physical characteristics of a distinctive colloidal iron particulate isolated from a small eutrophic lake. *Arch. Hydrobiol.* 113:405-424.
- Lijklema, L. 1980. Interaction of orthophosphate with iron(III) and aluminum hydroxides. *Environ. Sci. Technol.* 14:537-541.
- Logan, T. J., T. O. Olaya, and S. M. Yaksich. 1979. Phosphate characteristics and bioavailability of suspended sediments from streams draining into Lake Erie. *J. Great Lakes Res.* 5:112-123.
- McCarthy, J. F., and J. M. Zachara. 1989. Subsurface transport of contaminants. *Environ. Sci. Technol.* 14:537-541.
- Miller, J. C., and J. N. Miller. 1988. *Statistics for analytical chemistry*. 2nd ed. John Wiley and Sons, New York, NY.
- O'Melia, C. 1980. Aquasols: The behavior of small particles in aquatic systems. *Environ. Sci. Technol.* 14:1052-1060.
- Ryden, J. C., J. R. McLaughlin, and J. K. Syers. 1977. Mechanisms of phosphate sorption by soils and hydrous ferric oxide gel. *J. Soil Sci.* 28:72-92.
- Sharpley, A. N. 1980. The enrichment of soil phosphorus in runoff sediments. *J. Environ. Qual.* 9:520-521.
- Stumm, W., and J. J. Morgan. 1981. *Aquatic Chemistry*. 2nd ed. John Wiley and Sons, New York, NY.
- Tamura, H., K. GoTo, T. Yotsuyanagi, and M. Nagayama. 1973. Spectrophotometric determination of iron (II) with 1,10-phenanthroline in the presence of large amounts of iron (III). *Talanta* 21:314-318.
- Tarapchak, S. J., S. M. Bigelow, and C. Rubitschum. 1982. Soluble reactive phosphorus measurements in Lake Michigan: Filtration artifacts. *J. Great Lakes Res.* 8:550-557.

Tipping, E., C. Woof, and D. Cooke. 1981. Iron oxide from a seasonally anoxic lake. *Geochim. Cosmochim. Acta* 45:1411-1419.

Williams, D. B. 1984. Practical analytical microscopy in material science. VCH, New York, NY.

Williams, J. D. H., H. Shear, and R. L. Thomas. 1980. Availability to *Scenedesmus quadricauda* of different forms of phosphorus in sedimentary materials from the Great Lakes. *Limnol. Ocean.* 25:1-11.

CHAPTER 4
FORMATION AND STABILITY OF IRON(II) OXIDATION PRODUCTS
IN THE PRESENCE OF DISSOLVED SILICA

Model solutions were used to evaluate the effect of dissolved silica on the mineralogy and stability of Fe(II) oxidation products. Mineralogy was evaluated with scanning electron microscopy (SEM) and X-ray diffraction. Stability was determined by measuring the decrease in turbidity of colloidal suspensions with time. At total Si/Fe molar ratios of 0.1 or less, oxidation of Fe(II) produced lepidocrocite, a moderately crystalline oxide that rapidly settled out of solution. At total Si/Fe molar ratios of 0.36 or higher, ferrihydrite formed from the oxidation of Fe(II). The ferrihydrite consisted of 0.1 μm spherical particles which were poorly crystalline and increasingly stable with higher Si/Fe molar ratios. The ferrihydrite was very similar in structure and composition to Fe oxide colloids isolated from two natural samples: (1) a reduced groundwater sample that was allowed to oxidize in the laboratory and (2) the colloidal particles in the <1.0 μm size class of surface water samples from the Tualatin River watershed of northwest Oregon.

4.1 Introduction

The cycling of Fe(II) and Fe(III) occurs in a number of geochemical environments. An important consequence of the oxidation of Fe(II) is the formation of colloid-sized particles. Colloids are particles with linear dimensions between 0.001 and 1.0 μm (Hiemenz, 1986). Particles of this size are unique because of their high specific surface areas, high surface free energies, and very slow settling characteristics (O'Melia, 1980; McCarthy and Zachara, 1989). The chemistry and transport of trace constituents in some natural systems will be strongly influenced by interactions with colloidal Fe oxides (Tipping et al., 1989).

To persist over significant temporal scales, Fe oxide colloids must be stable or resistant to two processes: (1) Ostwald ripening or recrystallization, and (2) coagulation. Ostwald ripening is the growth of larger particles in a suspension at the expense of smaller particles (Schwertmann and Cornell, 1991). The high interfacial surface energy of small particles means they are more soluble than larger particles. Ions released from the smaller particles reprecipitate as larger, less soluble particles that prescribe a lower solution phase activity. Coagulation is the process of particle collision, attachment, and aggregate formation (O'Melia, 1980). Colloids resistant to both Ostwald ripening and coagulation are referred to as "stable."

The stability of Fe oxide colloids depends on the solution chemistry and the surface chemistry. Dissolved organic matter and inorganic anions such as phosphate, silicate, and arsenate inhibit the Ostwald ripening of Fe oxides (Liang and Morgan, 1990; Schwertmann and Cornell, 1991; Waychunas et al., 1993). High surface concentrations of adsorbed species stabilize colloidal Fe oxide with respect to coagulation. The adsorption of natural organic matter is believed to be particularly important in stabilizing Fe oxide colloids (Boyle et al., 1977; Sholkovitz et al., 1978; Cornell and Schwertmann, 1979). The net negative surface charge of most naturally-occurring Fe oxide colloids has been ascribed to associated organic matter (Cameron and Liss, 1984; Tipping and Ohnstad, 1984). But some evidence questions the role of organic matter in stabilizing Fe oxides. Fox (1984) reported that humic acids and colloidal Fe oxides in several estuaries did not appear to be chemically associated, based on their different rates of settling in

estuaries and the failure of humic acids to stabilize laboratory solutions of colloidal Fe. Hiraide et al. (1988) showed that "dissolved" river water Fe ($<1.0 \mu\text{m}$) was predominantly present as negatively charged colloids which may or may not be associated with humic substances. In addition to organic matter, high surface concentrations of anionic inorganic species such as phosphate and silicate will also cause Fe oxides to become negatively charged and may be important in stabilizing colloids (Sigg and Stumm, 1980; Liang and Morgan, 1990).

Dissolved silica is particularly interesting since it occurs in most natural waters, sometimes reaching millimolar concentrations (Stumm and Morgan, 1981). Adsorption of silicate anion results in electrostatic stabilization of colloidal Fe oxides (Cameron and Liss, 1984), although the concentrations required are reported to be much higher than background concentrations of Si in natural waters. In addition, adsorbed Si can inhibit the Ostwald ripening of amorphous Fe oxides, stabilizing the colloids with respect to this process (Schwertmann and Thalmann, 1976; Anderson and Benjamin, 1985). Therefore, the presence of Si could potentially stabilize Fe oxide colloids in natural waters.

In a field study of colloidal Fe in the Tualatin River Basin of northwestern Oregon, Si was a significant constituent in both the aqueous phase and in colloidal Fe oxide particles (Chapter 3). It was hypothesized that Si was stabilizing colloids in this system. The purpose of this research was to examine the ability of dissolved silica to stabilize colloidal Fe oxide in laboratory solutions.

In the Tualatin Basin, and in many environments, Fe oxides form as a result of Fe(II) oxidation and precipitation in the presence of naturally-occurring ions, including silicate. This natural process differs from the method of Fe oxide synthesis employed in many laboratory studies, which have used Fe(III)-derived precipitates aged prior to experimental study. While these laboratory studies have yielded valuable information concerning Fe oxides, direct application of this research to natural systems may be problematic. The physical and chemical properties of Fe(II)- and Fe(III)-derived precipitates are different (Crosby et al., 1983). The presence of dissolved ions during mineral formation can affect the surface and colloidal characteristics of the precipitate as well. For example, at near neutral pH, the presence of moderate concentrations of soluble

Si during Fe(II) oxidation favors the formation of ferrihydrite over lepidocrocite or goethite (Schwertmann and Thalmann, 1976; Tipping et al., 1989). Ferrihydrite differs significantly from these other Fe oxides in terms of crystallinity, specific surface area, and other surface characteristics. To explain the persistence of Fe oxide colloids in the Tualatin Basin, this study investigated the formation of Fe oxides under laboratory conditions that simulate the natural formation process in the environment.

4.2 Materials and Methods

Experiments were designed to examine the mineralogy and stability of Fe oxides derived from the oxidation of Fe(II) with a range of Si concentrations. Solutions of 5.0 mM NaHCO₃ and 0.0 to 2.5 mM Na₂SiO₃ were buffered at pH 7.0 with a CO₂/air mixture. The P_{CO_2} was between 1.3 and 1.6 and the concentration of total dissolved carbon was estimated to be 6.0 mM, which is near the measured values observed in the Tualatin Basin (0.6 to 3.5 mM). A pH of 7.0 was chosen because many natural waters, including those in the Tualatin Basin, are near neutral pH. Iron(II) was added to the solutions, in the form of FeCl₂, at initial concentrations of 0.1 or 0.5 mM. This concentration is slightly higher than most background concentrations of Fe but it may represent concentrations in some highly reducing environments. The Si/Fe molar ratios of the solutions ranged from 0.0 to 4.5. Air was the source of O₂ for Fe(II) oxidation. The solution pH dropped slightly (0.5-0.8 pH unit) upon addition of FeCl₂ but returned to pH 7.0 within 30 to 60 minutes.

The oxidation of Fe(II) was followed by measuring Fe(II) spectrophotometrically using 1,10 phenanthroline and NH₄F as a masking agent for Fe(III) (Tamura et al., 1973). The oxidation was essentially complete in about 2 hours, consistent with the published rate law (Stumm and Lee, 1961). At the highest concentration of Si (2.5 mM), the oxidation was slightly slower. The concentration of Si was measured using the molybdo-silicate method (APHA et al., 1989) in both filtered (<0.05 µm) and unfiltered samples. Because Fe is photoreactive (Waite and Morel, 1984), light was excluded from all solutions with an aluminum foil wrap. Silicon contamination from glass reaction vessels

was evaluated but was not significant relative to the concentrations added, probably because high pH, high temperature solutions were not used (Dzombak and Morel, 1990).

Samples were filtered with polycarbonate membrane filters to determine the size distribution of the Fe oxide. The solid material was imaged with a Zeiss DSM-960 scanning electron microscope (SEM). Image analysis yielded additional information on the size distribution of the solids as well as crystallographic and morphologic features. The mineralogy of the Fe oxides was determined using X-ray diffraction.

The stability of the Fe oxides was evaluated by monitoring the turbidity of quiescent samples over time with an HF Scientific turbidimeter (Model DRT-15C). Samples were collected 24 hours after the oxidation was complete. It was assumed that the stability of the colloids could be assessed from the changes in the light scattering properties of the solution. Unstable colloidal suspensions would form larger particles that would settle, resulting in a decrease in turbidity, whereas the turbidity of stable colloidal suspensions would vary little over time. The colloids were considered to have settled when the turbidity decreased to 10% of the initial value. For comparison, settling times of all samples were also measured in the presence of 0.1 M NaCl. The effect of a range of CaCl_2 concentrations on settling was examined for one sample.

A reduced groundwater sample was collected from the Tualatin River Basin and oxidized in the laboratory at pH 7.0 under a CO_2 /air mixture as described above. This sample had 0.26 mM Fe(II), 1.0 mM Si, and an alkalinity of 5.4 mM. The mineralogy, particle size distribution and settling rate of the oxidation product were compared with those of the synthetic Fe oxides.

4.3 Results and Discussion

At total Si/Fe molar ratios of 0.0 to 0.1, the oxidation of Fe(II) resulted in the formation of lepidocrocite, a moderately crystalline oxide (Table 4.1). The lepidocrocite had an orange color, a characteristic X-ray diffraction pattern, and a folded, crumpled structure as observed with the SEM (Fig. 4.1).

At total Si/Fe molar ratios of 0.36 and higher, the Fe oxidation product was ferrihydrite, a poorly crystalline oxide. This Si/Fe molar ratio is similar to the value

reported by Schwertmann et al. (1984), who found that a Si/Fe molar ratio of 0.39 was required for conversion of lepidocrocite to ferrihydrite from Fe(II) oxidation. The ferrihydrite in our study was dark reddish-brown and had a characteristic X-ray diffraction pattern with two broad maxima at 2.54 and 1.5 Å. At the highest initial Si/Fe molar ratio (4.5), the Si/Fe ratio in the solid phase was 28%. Scanning electron microscopy indicated that the ferrihydrite consisted of spherical particles on the order of 0.1 µm in diameter (Fig. 4.2). Size fractionation through filtration of the samples gave a similar estimate; essentially all of the ferrihydrite passed through a 0.4 µm filter but was retained by a 0.05 µm filter.

Settling times are presented in Table 4.1 for the various oxidation products. Solutions of lepidocrocite settled within 18 to 24 hours, with or without NaCl. The fact that there was no difference in settling time with 0.1 M NaCl suggests that Ostwald ripening rather than coagulation was the dominant process in destabilizing the colloids.

Settling times in the absence of NaCl increased as the Si/Fe molar ratio increased and the oxidation product was dominantly ferrihydrite (Table 4.1), although most solids settled rapidly with the addition of 0.1 M NaCl. The Si had to be present during the oxidation to affect stability; addition of Si 24 hours after lepidocrocite had formed had no effect on settling times in these solutions. At the highest Si/Fe molar ratio (Si/Fe=4.5), the ferrihydrite was very stable, remaining in solution for more than 1000 hours. The settling in this solution was not affected by NaCl. This solution was 2.5 mM Si, a high concentration compared with natural background concentrations. For this reason, a less concentrated solution of the same ratio (0.45 mM Si, 0.1 mM Fe, Si/Fe=4.5), very realistic concentrations for many natural waters including the Tualatin River system, was also examined. This solution was also very stable (settling time > 1000 hours) although settling was quite rapid in the presence of NaCl, in contrast to the more concentrated solution of the same Si/Fe ratio.

The concentration of Si required for stabilization is much lower than the value reported by Cameron and Liss (1984), who found that 11.0 mM Si was needed to stabilize 0.02 mM Fe (Si/Fe=550). In contrast to our conclusions, the authors felt that Si would

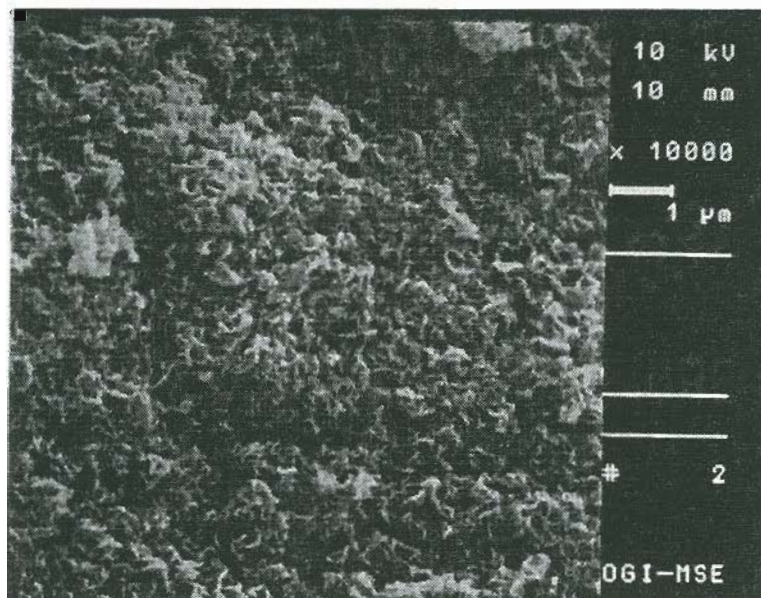


Figure 4.1 Lepidocrocite synthesized from the oxidation of Fe(II) without silicate present.

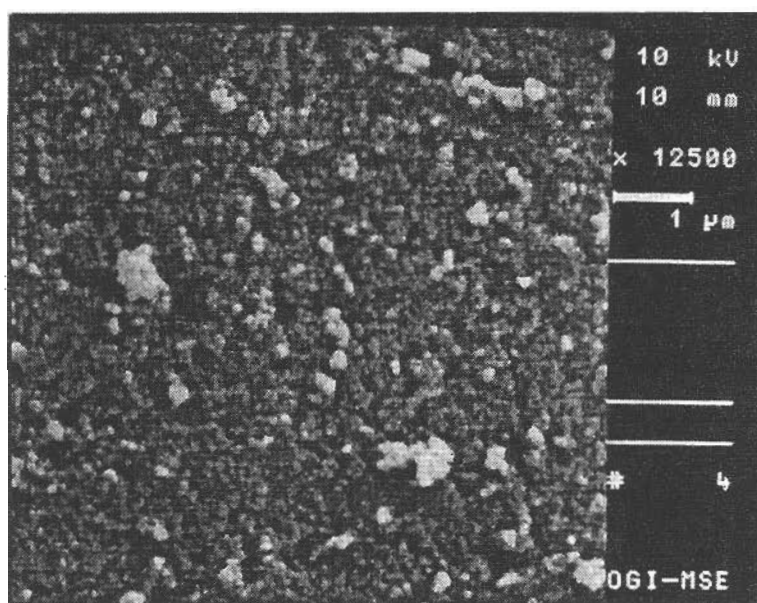


Figure 4.2 Ferrihydrite synthesized from the oxidation of Fe(II) in the presence of silicate.

Table 4.1: Summary of solution chemistry, mineralogy, and settling times for Fe oxide colloids.

| Type of Oxidation Product | Total [Fe] | Total [Si] | Total Si/Fe ratio | Settling time | |
|---------------------------------|---------------|---------------|-------------------------|------------------|----------------------|
| | | | | no NaCl | 0.1 <i>M</i> NaCl |
| | <i>mM</i> | <i>mM</i> | | hours | hours |
| Synthetic Lepidocrocite | 0.5 | 0.0 | 0.00 | 18 | 18 |
| Synthetic Lepidocrocite | 0.5 | 0.05 | 0.10 | 24 | 24 |
| Synthetic Ferrihydrite | 0.5 | 0.18 | 0.36 | 34 | 22 |
| Synthetic Ferrihydrite | 0.5 | 0.5 | 1.0 | 162 | 18 |
| Synthetic Ferrihydrite | 0.1 | 0.45 | 4.5 | >1000 | 36 |
| Natural Ferrihydrite | 0.26 | 1.0 | 3.8 | 30 | 21 |

not be responsible for Fe colloid stabilization in natural waters because such high concentrations were required. One reason for this discrepancy may be that their Fe oxides were synthesized from the hydrolysis of Fe(III) salts, rather than the oxidation of Fe(II) followed by the hydrolysis of Fe(III).

Figure 4.3 is an SEM photograph of the Fe oxidation product from the reduced groundwater sample collected in the Tualatin River Basin and allowed to oxidize in the laboratory. The photograph shows Fe oxide particles very similar in size and structure to those synthesized from the solutions with high Si/Fe ratios. The initial Si/Fe molar ratio of the natural groundwater sample was 3.8. X-ray diffraction patterns of the material were similar to the patterns from 2-line ferrihydrite described by Schwertmann et al. (1984). The larger material in the background is believed to be suspended clay

minerals that were in the original sample at the time of collection. The striking similarity between the synthetic and natural Fe oxides suggests that our simple solutions and method of synthesis are simulating the natural formation of ferrihydrite through the oxidation of reduced groundwater.

One notable difference between the groundwater and synthetic solutions is the settling times (Table 4.1). Settling times in the groundwater sample were only slightly increased in the absence of NaCl, despite an Si/Fe molar ratio of 3.8. Settling times in the synthetic solutions with similar Si/Fe values were much longer. There are two possible explanations for this. First, the ferrihydrite in the groundwater sample may have been attached to larger clay particles that settled. Second, the presence of Ca in the groundwater may have caused the ferrihydrite to coagulate. The concentration of Ca in the groundwater sample was almost 2.0 mM, and a divalent cation such as Ca^{2+} is very effective at coagulating colloids (Hiemenz, 1986).

The effect of CaCl_2 concentrations on the settling times of the colloids synthesized at concentrations of 0.45 mM Si and 0.1 mM Fe, concentrations similar to the groundwater, was examined (Table 4.2). Calcium concentrations of 2.0 mM or higher were very effective in coagulating the model colloids; settling was only slightly affected at concentrations below this. Background concentrations of Ca range from 0.025 to 2.5 mM (Stumm and Morgan, 1981) so that higher background concentrations of Ca may coagulate ferrihydrite that might otherwise be stable.

Figure 4.4 is an SEM photo of the colloidal material ($<1.0 \mu\text{m}$) of a representative surface water sample from the Tualatin River Basin. A significant fraction of the total Fe in this system was stabilized in colloidal form (Chapter 3). Our chemical analysis of the material indicated that, in addition to Fe, the colloids contained Si as well as various concentrations of P, Ca, and Al. The size and structure of this colloidal material is very similar to the ferrihydrite formed in the other solutions. The appearance and chemical composition of these solids are evidence that this natural material is forming from the oxidation of Fe(II) in a manner similar to our laboratory procedure, and that the presence of Si plays an important role in stabilizing the colloids.

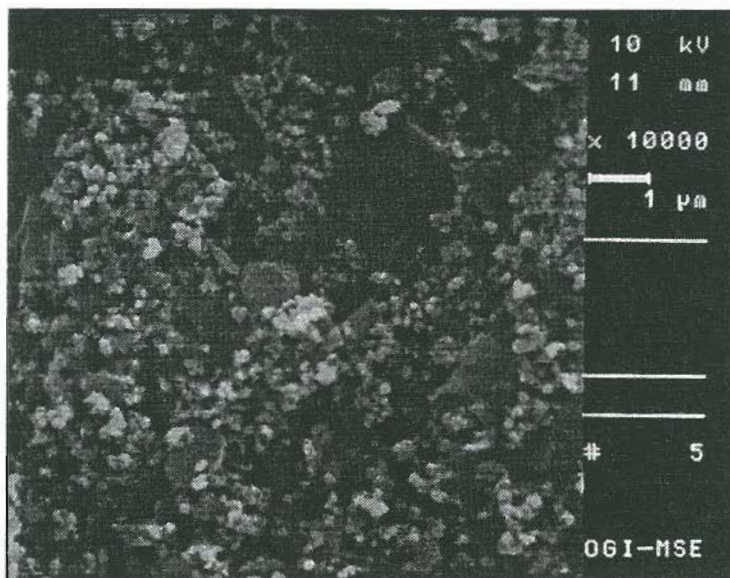


Figure 4.3 Iron oxides produced from the oxidation of a reduced groundwater sample of the Tualatin River Basin. The larger particles are believed to be clays.

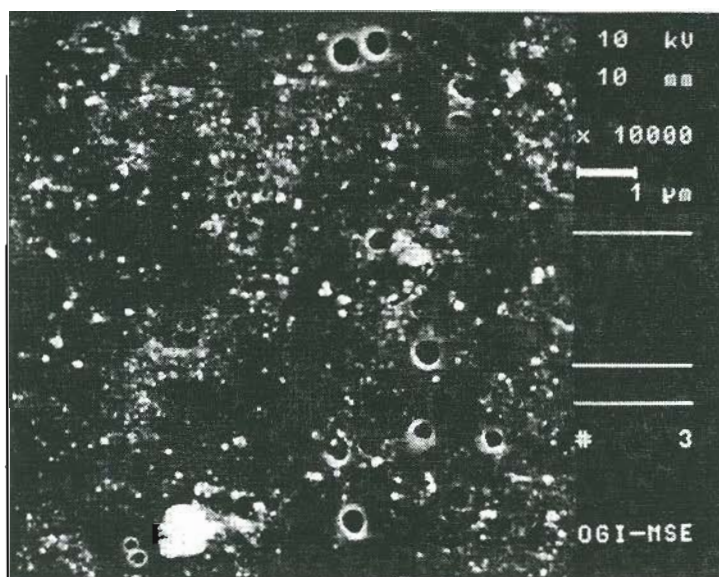


Figure 4.4 Iron oxide colloids retained by a polycarbonate filter from a surface water sample of the Tualatin River basin. The appearance and composition of these colloids are similar to ferrihydrite synthesized in the presence of silicate.

Table 4.2: Settling times for a ferrihydrite colloidal suspension in the presence of various calcium concentrations.

| (0.1 mM Fe and 0.45 mM Si) | |
|-------------------------------------|-------------------|
| CaCl ₂ concentrations | Settling times |
| mM | hours |
| 0.0 | >1000 |
| 0.5 | >1000 |
| 1.0 | 336 |
| 2.0 | 72 |
| 5.0 | 36 |
| 10.0 | 36 |

The Si stabilizes the ferrihydrite in two ways. First, as discussed above, ferrihydrite has a high solubility and should transform to more crystalline Fe oxides such as hematite or goethite (Schwertmann and Cornell, 1991). Adsorbed silicate inhibits the Ostwald ripening of ferrihydrite, either by blocking dissolution sites on the ferrihydrite or by hindering the nucleation of more stable Fe oxides (Schwertmann and Taylor, 1989). Second, the incorporation of Si into the solid will contribute to a negative surface charge and potential which will prevent coagulation. The addition of NaCl or CaCl₂ to the solutions promotes coagulation by decreasing the extent of the double layer at the particle surface.

The narrow particle size distribution of the ferrihydrite in the natural and synthetic samples is not surprising given their method of formation. To obtain a monodisperse population of particles, nucleation and crystal growth must be separated (Matijevic, 1981). During the oxidation of Fe(II), the appearance of the solid phase is preceded by the formation of dissolved Fe(III) complexes with hydroxide and silicate ligands. The concentration of these species builds up slowly until the critical supersaturation for

nucleation is reached and solid formation occurs. Thereafter, the rate of oxidation is slow enough that soluble Fe(III) is removed by crystal growth and the concentration never exceeds the level necessary for secondary nucleation to occur.

The spherical shape of the ferrihydrite particles may be related to the presence of hydrolyzing silicate (Matijevic, 1981). Hydrolysis products which consist of discrete, well-defined ionic complexes will most often yield particles of well-developed crystal habits. If hydrolysis results in the formation of polymeric metal complexes, spherical particles will be produced. It may be that the presence of silicate promotes the polymerization of hydrolyzed Fe(III), causing spherical particles to be formed.

4.4 Conclusions

At Si/Fe molar ratios of 0.1 or less, the oxidation of Fe(II) resulted in the formation of lepidocrocite, whereas, at Si/Fe molar ratios of 0.36 or higher, ferrihydrite was the oxidation product. The lepidocrocite was somewhat crystalline and settled out of solution within 24 hours. The ferrihydrite consisted of a monodisperse population of 0.1 μm spherical colloids that were stable with respect to Ostwald ripening and coagulation. At concentrations representative of natural systems ($[\text{Fe}]=0.1 \text{ mM}$, $[\text{Si}]=0.45 \text{ mM}$, $\text{Si/Fe}=4.5$), the colloidal ferrihydrite resulting from Fe(II) oxidation in the presence of Si remained in solution for more than 1000 hours. Concentrations of 2.0 mM CaCl_2 or 0.1 M NaCl caused them to settle. The ferrihydrite from synthetic solutions is very similar to natural Fe oxides obtained from two sources in the Tualatin River watershed: (1) a reduced groundwater sample that was allowed to oxidize in the laboratory and (2) the colloidal particles in the $<1.0 \mu\text{m}$ size class of surface water samples from the watershed. Evidence presented here suggests that colloidal Fe oxides in the Tualatin River system are forming from the oxidation of Fe(II) and that the presence of Si influences the mineralogy of the oxidation product and the stability of the colloids.

4.5 References

- American Public Health Association. 1989. Standard methods for the examination of water and wastewater. 17th ed. Amer. Publ. Health Assoc., New York, NY.
- Anderson, P. R., and M. M. Benjamin. 1985. Effects of silicon on the crystallization and adsorption properties of ferric oxides. *Environ. Sci. Technol.* 19:1048-1053.
- Boyle, E. A., J. M. Edmond, and E. R. Sholkovitz. 1977. The mechanism for iron removal in estuaries. *Geochim. Cosmochim. Acta* 41:1313-1324.
- Cameron A. J., and P. S. Liss. 1984. The stabilization of "dissolved" iron in freshwaters. *Water Res.* 18:179-185.
- Cornell, R. M., and U. Schwertmann. 1979. Influence of organic anions on the crystallization of ferrihydrite. *Clays Clay Miner.* 27:402-410.
- Crosby, S. E., D. R. Glasson, A. H. Cuttler, I. Butler, D. R. Turner, M. Whitfield, and G. E. Millward. 1983. Surface areas and porosities of Fe(III)- and Fe(II)-derived oxyhydroxides. *Environ. Sci. Technol.* 17:709-713.
- Dzombak, D. A., and F. M. Morel. 1990. Surface complex modeling: hydrous ferric oxide. John Wiley and Sons, New York, NY.
- Fox, L. E. 1984. The relationship between dissolved humic acids and soluble iron in estuaries. *Geochim. Cosmochim. Acta* 48:879-884.
- Hiemenz, P. C. 1986. Principles of colloid and surface chemistry. Marcel Dekker, Inc., New York, NY.
- Hiraide, M., M. Ishi, and A. Mizuike. 1988. Speciation of iron in river water. *Anal. Sci.* 4:605-609.
- Liang, L., and J. J. Morgan. 1990. Chemical aspects of iron oxide coagulation in water: Laboratory studies and implications for natural systems. *Aquat. Sci.* 52:32-55.
- Matijevic, E. 1981. Monodispersed metal (hydrous) oxides - A fascinating field of colloid science. *Acc. Chem. Res.* 14:22-29.
- McCarthy, J. F., and J. M. Zachara. 1989. Subsurface transport of contaminants. *Environ. Sci. Technol.* 14:537-541.
- O'Melia, C. 1980. Aquasols: The behavior of small particles in aquatic systems. *Environ. Sci. Technol.* 14:1052-1060.

- Schwertmann, U., and H. Thalmann. 1976. The influence of [Fe(II)], [Si], and pH on the formation of lepidocrocite and ferrihydrite during oxidation of FeCl₂ solutions. *Clay Minerals* 11:189-199.
- Schwertmann, U., L. Carlson, and H. Fechter. 1984. Iron oxide formation in artificial ground waters. *Schweiz. Z. Hydrol.* 46/2:185-191.
- Schwertmann, U., and R. M. Taylor. 1989. Iron oxides. p. 379-438. *In* J. B. Dixon and S. B. Weed (eds.) *Minerals in soil environments*. Soil Soc. Soc. Am., Madison, WI.
- Schwertmann, U., and R. M. Cornell. 1991. *Iron oxides in the laboratory: Preparation and characterization*. VCH, New York, NY.
- Sholkovitz E. R., E. A. Boyle, and N. B. Price. 1978. The removal of dissolved humic acids and iron during estuarine mixing. *Earth Planet Sci. Lett.* 40:1130-1136.
- Sigg, L., and W. Stumm. 1980. The interaction of anions and weak acids with the hydrous goethite (α -FeOOH) surface. *Colloids Surfaces*, 2:101-117.
- Stumm, W., and G. F. Lee. 1961. Oxygenation of ferrous iron. *Ind. Eng. Chem.* 53:143-146.
- Stumm, W., and J. J. Morgan. 1981. *Aquatic chemistry*. 2nd ed. John Wiley and Sons, New York, NY.
- Tamura, H., K. GoTo, T. Yotsuyanagi, and M. Nagayama. 1973. Spectrophotometric determination of iron (II) with 1,10-phenanthroline in the presence of large amounts of iron (III). *Talanta* 21:314-318.
- Tipping, E., and M. Ohnstad. 1984. Colloid stability of iron oxide from a freshwater lake. *Nature* 308:266-268.
- Tipping, E., D. W. Thompson, and C. Woof. 1989. Iron oxide particulates formed by the oxygenation of natural and model lakewaters containing Fe(II). *Arch. Hydrobiol.* 115/1:59-70.
- Waite, T. D., and F. M. M. Morel. 1984. Photoreductive dissolution of colloidal iron oxides in natural waters. *Environ. Sci. Technol.* 18:860-868.
- Waychunas, G. A., B. A. Rea, C. C. Fuller, and J. A. Davis. 1993. Surface chemistry of ferrihydrite: Part 1. EXAFS studies of the geometry of coprecipitated and adsorbed arsenate. *Geochim. Cosmochim. Acta* 57:2251-2269.

CHAPTER 5
PHOSPHORUS CHEMISTRY DURING IRON(II) OXIDATION
IN THE PRESENCE OF DISSOLVED SILICA

This study investigated phosphorus (P) sorption chemistry on iron (Fe) oxides under conditions similar to those of natural systems. Iron oxides were formed from the oxidation of Fe(II) at pH 7.0 under a CO₂/air mixture. Phosphate and silicate were added either before the oxidation (coprecipitation experiments) or 24 hours after the solid had formed (adsorption experiments). The coprecipitation of P and Fe resulted in very high initial concentrations of P in the solid phase; however, much of the coprecipitated P was rapidly released into solution as the Fe oxide recrystallized. The presence of Si favored the sorption of P by (1) inhibiting the dissolution and recrystallization of the Fe oxide and (2) promoting the formation of ferrihydrite, an Fe oxide with a high specific surface area and a high concentration of surface sites. Comparison of laboratory results and field data suggests that Fe-P colloids in surface waters of the Tualatin River formed through coprecipitation rather than adsorption and that Si is important in stabilizing the colloids.

5.1 Introduction

The chemistry of phosphorus (P) in aquatic systems is often controlled by interactions with iron (Fe) (Syers et al., 1973; Fox, 1989). Aqueous Fe occurs in one of two principal oxidation states, Fe(II) and Fe(III). The reduced form, Fe(II), is moderately soluble, but the oxidized form, Fe(III), is extremely insoluble and will hydrolyze and precipitate rapidly at the pH of most natural waters (Stumm and Lee, 1961).

The cycling between Fe(II) and Fe(III) occurs in a number of geochemical environments. The ready conversion between the two oxidation states leads to the production and dissolution of Fe oxide particles. Species such as phosphate, that interact with Fe, are associated with the solid phase under oxidizing conditions and solubilized under reducing conditions. The exact chemical mechanisms underlying the solid phase association are still open to interpretation. Adsorption, surface precipitation, solid state diffusion, and solid solution have all been postulated (Ryden et al., 1977; van Riemsdijk et al., 1984; Barrow, 1985; Dzombak and Morel, 1990; Fox, 1989). The general term "sorption" is used in this study to refer to the transfer of aqueous ion to an Fe oxide solid by any process (Sposito, 1986).

5.1.1 Iron/Phosphate Interactions

The interactions of Fe and P have been intensively studied (Ryden et al., 1977; Barrow, 1985; Fox 1989; Dzombak and Morel, 1990). Laboratory investigations of the sorption and surface chemistry of Fe oxides have usually been conducted with pre-formed, pure Fe(III)-derived precipitates that have been aged prior to experimental study. These investigations have yielded valuable information on Fe/P interactions. However, direct application of this research to natural systems may be problematic for several reasons.

In most natural environments, Fe oxides will likely form as a result of Fe(II) oxidation and subsequent precipitation rather than by rapid hydrolysis of Fe(III) salts. The physical and chemical properties of ferrous-derived precipitates differ from ferric-derived precipitates. Crosby et al. (1983) found that ferric-derived precipitates were amorphous, spherical aggregates (probably ferrihydrite) with higher surface areas and porosities. In contrast, ferrous-derived precipitates were more crystalline, with lower

surface areas and porosities.

Sorption of dissolved ions may be different depending on whether they are present during mineral formation or are added later, as is often the case in laboratory studies. In many environmental systems where Fe is cyclically reduced and oxidized, the solid forms in the presence of dissolved ions. Several studies have reported higher sorption of cations and anions, including phosphate, when they are present during the formation of Fe oxides rather than when added after precipitation (Einsele, 1938; Tessenow, 1974; Laxen, 1985). However, the concentration of sorbed ions often decreases with time as Ostwald ripening and particle aggregation reduce the number of surface sites on the oxide (Crosby et al., 1981; Anderson et al., 1985; Fuller et al., 1993).

Dissolved ions that are present in natural waters can affect the formation and the surface chemistry of the Fe oxide, which alters the sorption characteristics of the solid. Small quantities of organic acids and Si have been shown to inhibit the crystallization of amorphous Fe oxides, influence the nature of the Fe oxidation product, and affect the surface charge of the oxide (Schwertmann and Thalmann, 1976; Cornell and Schwertmann, 1979; Schwertmann et al., 1984).

5.1.2 Influence of Silicon

Silicon is of particular interest to Fe/P interactions. The concentration of dissolved Si in natural waters is high, ranging from 0.1 to 1.0 mM (Stumm and Morgan, 1981). Background concentrations of Si may influence P sorption processes by affecting the surface chemistry of the Fe oxides and by competing directly with phosphate for surface sites (Sigg and Stumm, 1980; Schwertmann et al., 1984; Anderson and Benjamin, 1985). It is instructive to examine how Si can affect two important surface properties of Fe oxides: the surface area per unit mass and the net charge of the surface.

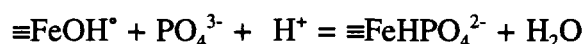
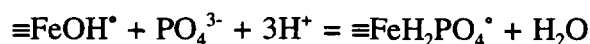
Adsorption of phosphate onto Fe oxide surfaces strongly depends on the surface area associated with a unit mass of solid. The exposed surface area contains the hydroxyl groups that interact with aqueous phosphate through reversible, ligand exchange reactions (Dzombak and Morel, 1990). The higher the specific surface area, the greater the number of surface hydroxyls available for reaction with phosphate.

The specific surface areas of naturally-occurring Fe oxides vary over an order of magnitude, from 30-50 m²/g for goethite and hematite (Schwertmann and Taylor, 1989) to 600 m²/g or more for ferrihydrite (Dzombak and Morel, 1990). Specific surface area is inversely correlated with the degree of crystallinity of the solid. Phosphorus sorption capacities of different Fe oxides are approximately equal when normalized to surface area (Borggaard, 1983).

The immediate products of Fe(II) oxidation in the pH range of natural systems are lepidocrocite and ferrihydrite (Schwertmann et al., 1984). Both of these phases are relatively soluble and, over time, they will convert to crystalline, less soluble forms, such as goethite (Schwertmann and Cornell, 1991). At low concentrations of Si, Fe(II) oxidation leads to lepidocrocite, a moderately crystalline phase with a characteristic X-ray diffraction pattern (Schwertmann et al., 1984). With higher concentrations of Si, Fe(II) oxidation produces ferrihydrite, an amorphous Fe oxide consisting of spherical or ellipsoidal particles with a specific surface area of 600 m²/g (Schwertmann et al., 1984; Dzombak and Morel, 1990). The higher specific surface area of ferrihydrite results in a higher concentration of surface sites for sorption of solutes. Therefore, Si may increase P sorption by promoting the formation of ferrihydrite rather than lepidocrocite.

While high sorption densities are theoretically possible with high specific surface areas, the degree of coordination on surface sites depends, to a large extent, on the surface charge of the solid. Any charged surface creates a potential gradient through which ions move. The net surface charge therefore affects the affinity of the solid for the solute.

Iron oxides generate surface charge through proton transfer reactions and the surface coordination of cations and anions. Specifically sorbed protons and cations increase the surface charge and potential of the solid, making the surface electrostatically more favorable for anion sorption. Specifically sorbed hydroxyls and anions decrease the surface charge and potential, having an unfavorable effect on anion sorption but promoting cation sorption (Dzombak and Morel, 1990). Reactions involving H⁺ and phosphate illustrate this change in surface charge:



Sorption of Si by Fe oxides makes the surface more negative and lowers the zero point of charge (ZPC) of the solid (Anderson and Benjamin, 1985). While the ZPC of pure ferrihydrite is about 8.1 (Dzombak and Morel, 1990), the ZPC of natural ferrihydrites has been reported to be as low as 6.0 due to the association of Si with the oxide (Schwertmann and Fechter, 1982). The lower ZPC due to the presence of Si should decrease P sorption.

Coprecipitated anions, such as phosphate and arsenate, may be released back into solution during the recrystallization of Fe oxides (Crosby et al., 1981; Fuller et al., 1993). However, Si inhibits Fe oxide recrystallization (Schwertmann and Thalmann, 1976). This may limit the release of coprecipitated anions, although this has not been reported in previous studies.

In addition, Si may reduce P sorption through competition with phosphate for anion surface sites on Fe oxides (Sigg and Stumm, 1980). Both phosphate and silicate are assumed to form inner-sphere complexes with goethite (Sigg and Stumm, 1980). Values of equilibrium sorption constants suggest that phosphate is sorbed much more strongly than silicate; however, the concentration of Si is usually at least an order of magnitude higher than P in natural waters (Syers et al., 1973; Stumm and Morgan, 1981).

5.1.3 Research Questions

The discussion above indicates that environmental conditions in natural systems differ from those in laboratory experiments and that those differences may affect Fe/P

interactions. Phosphorus sorption reactions on Fe oxides could be affected either favorably or unfavorably by the presence of Si. This requires further investigation. Evidence from a recent field study of the Tualatin River Basin of northwestern Oregon raised additional questions concerning Fe and P interactions in natural systems (Chapter 3). In that study, it was found that P was associated with colloidal Fe oxides in the surface waters of the Basin. The colloids appeared to be forming from the oxidation of Fe(II), in the presence of other dissolved ions, including phosphate and dissolved silica. The colloidal Fe oxides all contained significant amounts of Si, suggesting that Si may be an important factor in colloid stability.

This research pursues the study of Fe/P interactions in laboratory systems that simulated conditions in the natural environment. The central issues addressed in this study involve (1) the oxidation and hydrolysis of Fe(II) in the presence of phosphate and silica and (2) the influence of Si on surface properties and Fe/P interactions.

5.2 Materials and Methods

Experiments were designed to examine the P sorption properties of Fe oxides derived from the oxidation of Fe(II), with or without Si present. Solutions of 5.0 mM NaHCO₃ were buffered at pH 7.0 with a mixture of CO₂ and air. A pH of 7.0 was chosen because many natural waters, including those in the Tualatin Basin, are near neutral pH. The P_{CO_2} in the experiments was between 1.3 and 1.6. Total dissolved carbon was estimated to be 6.0 mM, which is near values observed in the field (Stumm and Morgan, 1981). Iron(II) as FeCl₂ was added to the solutions at initial concentrations of 0.1 or 0.5 mM. Air was the source of O₂ for Fe(II) oxidation. The solution pH dropped slightly (0.5-0.8 pH unit) upon addition of FeCl₂ but returned to pH 7.0 within 30 to 60 minutes.

The oxidation of Fe(II) was followed by measuring Fe(II) colorimetrically (Tamura et al., 1973) and was essentially complete in two hours or less. Phosphate (as K₂HPO₄) and silicate (as Na₂SiO₃) were added either before the oxidation, referred to as "coprecipitation" experiments, or 24 hours after solid formation, referred to as

"adsorption" experiments (Fuller et al., 1993). Sorption densities reported for the adsorption experiments are the values at 24 hours after addition of the solute, unless noted otherwise. Preliminary studies showed that sorption densities in the adsorption experiments varied little after 24 hours. In contrast, sorption densities in the coprecipitation experiments varied considerably with time.

Total concentrations of phosphate and silica were varied over realistic ranges; 0.002 to 0.050 mM P and 0.05 to 1.0 mM Si. Phosphate and silicate were measured with the ascorbic acid method and molybdo-silicate method, respectively, in both filtered (<0.05 μm) and unfiltered samples (APHA, 1989).

Light was excluded from all experiments with an aluminum foil wrap. Glass reaction vessels, which were used for all experiments, can leach Si into solution, but this process is only considered to be significant at high temperatures and high pH (Dzombak and Morel, 1990). Data from the experiments included the uptake/release of solutes over time, adsorption isotherms, and pH adsorption edges.

The structure and morphology of the Fe oxides were examined with a Zeiss DSM-960 scanning electron microscope (SEM). The crystalline structures of the Fe oxides were determined with X-ray diffraction. This information was used to evaluate the specific surface areas of the solids, based on the images and literature values for different Fe oxides.

Acid-base titrations can be used to determine the acidity constants and the ZPC for Fe oxide surfaces (Dzombak and Morel, 1990); however, the levels of CO_2 in these experiments made acid-base titrations very difficult to interpret. Attempts to decrease CO_2 concentrations and buffer the system with a strong base (unrealistic for natural systems) led to the formation of magnetite rather than lepidocrocite or ferrihydrite. Therefore, acidity constants and ZPC were not determined in these experiments.

The lowering of the ZPC of the Fe oxide by sorption of Si was evaluated indirectly through P adsorption edges. In these experiments, 0.5 mM Fe(II) was oxidized in the presence of various Si concentrations (0.0, 0.18, 0.45 mM Si), and 0.010 mM P was added 24 hours later. The pH was adjusted with 0.1 M HNO_3 or 0.1 M KOH and the percent P sorbed was measured after 24 hours.

The physical competition for anion sorption sites between silicate and phosphate was evaluated by simultaneously adding P and Si in a range of concentrations (0.002 to 0.030 mM P; 0.0, 0.18, and 0.45 mM Si) to pure Fe oxides aged 24 hours. Soluble phosphate and silicate were evaluated after 24 hours.

In another set of adsorption experiments, calcium as CaCl_2 was added to pure Fe oxides and mixed Fe-Si oxides, both aged 24 hours, to examine the effects of Si on cation sorption. Calcium concentrations ranged from 0.02 to 0.1 mM Ca.

In addition to the model solutions, a reduced groundwater sample was collected from the Tualatin River Basin, maintained anoxic until brought to the laboratory, and oxidized in the laboratory at pH 7.0 under a CO_2 /air mixture as described above. This sample had 0.26 mM Fe(II), 1.0 mM Si, and an alkalinity of 5.4 mM. Following the oxidation of Fe(II), the concentration of soluble P was measured over time. Phosphorus adsorption experiments were conducted with this sample to examine the capacity of the solid to sorb P in addition to that which was coprecipitated.

5.3 Results and Discussion

5.3.1 Adsorption vs. Coprecipitation without Silica

Much more P was initially associated with the Fe solid phase when the P was added before Fe(II) oxidation (coprecipitation) rather than after solid formation (adsorption) (Fig. 5.1). This is due to the increased availability of surface sites on the incipient oxide. Coprecipitation resulted in a near stoichiometric precipitate of P and Fe, regardless of the total P/Fe ratio. However, much of this initially sorbed P was released back into solution with time as the Fe oxide recrystallized (Fig. 5.1). The release of coprecipitated P was observed in all coprecipitation experiments involving pure Fe oxide. The release continued for approximately 200 hours (Fig. 5.1) before reaching a pseudo-equilibrium concentration very close to that found in the adsorption experiments. Equilibrium in the adsorption experiments was reached after 24 hours; there was little change in soluble P after this time (Fig. 5.1).

The release of coprecipitated P is related to the reduction in the surface area and concentration of surface sites caused by recrystallization of the Fe oxides. Other studies

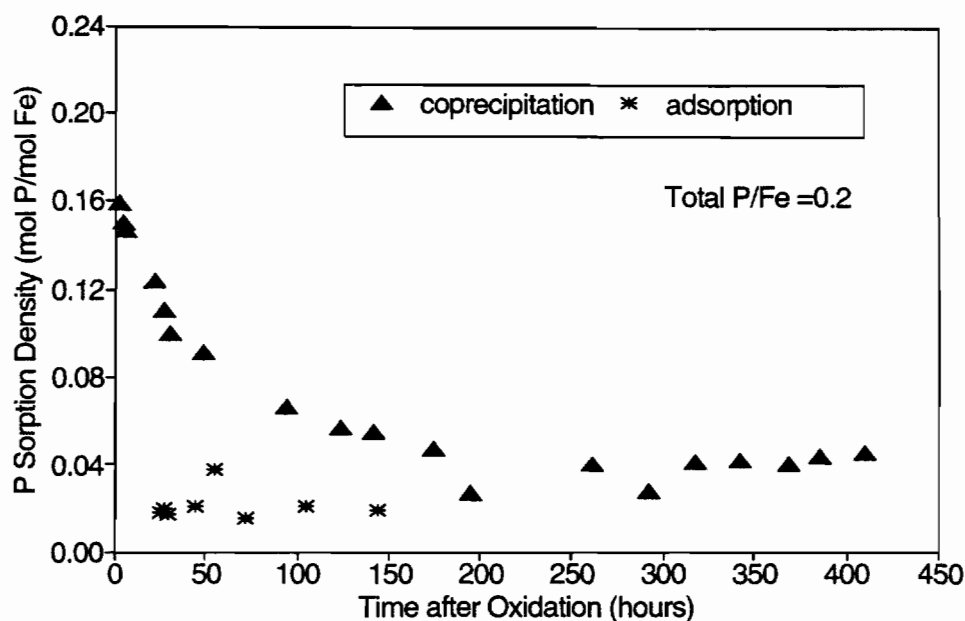


Figure 5.1 Phosphorus coprecipitation and adsorption experiments without Si (pH=7.0).

have described the release of initially sorbed species during recrystallization (Crosby et al., 1981; Anderson et al., 1985; Fuller et al., 1993).

There was very little difference in sorption densities observed between the coprecipitation and adsorption experiments at longer times. The fact that sorption densities in both experiments were approximately equal after 200 hours suggests that recrystallization occurred to the same extent in both experiments; it was simply much slower in the presence of phosphate. It may be that phosphate retards the recrystallization of the Fe(II)-derived oxide, which has been shown to recrystallize in just a few hours in the absence of other ions (Schwertmann and Cornell, 1991).

5.3.2 Adsorption vs. Coprecipitation with Silica

Like the coprecipitation experiments without Si, the coprecipitation of P, Si, and Fe resulted in a near stoichiometric precipitate of P and Fe, for the range of initial P/Fe

solution ratios examined (Table 5.1). In contrast to the Fe oxides without Si, very little of the coprecipitated P was released back into solution with time. The presence of Si during the coprecipitation of P and Fe slowed the release of coprecipitated P by inhibiting the Ostwald ripening and recrystallization of the oxide (Fig. 5.2). Sorption densities on the mixed Fe-Si oxides remained much higher in the coprecipitation experiments than in the adsorption experiments at all times.

Table 5.1: Initial Si and Fe Concentrations and Final Si Sorption Densities and Soluble Si for adsorption and coprecipitation with dissolved silica.

| Total [Fe] | Total [Si] | Initial | Solid | Soluble Si |
|------------|------------|---------|-------|------------|
| mM | mM | Si/Fe | Si/Fe | mM |
| 0.5 | 0.05 | 0.10 | 0.01 | 0.05 |
| 0.5 | 0.18 | 0.36 | 0.09 | 0.14 |
| 0.5 | 0.50 | 1.0 | 0.16 | 0.42 |
| 0.1 | 0.45 | 4.5 | 0.28 | 0.42 |

In the coprecipitation experiments, the sorption densities of Si and P were in the same range; however, compared to soluble Si, a much lower value of soluble P was prescribed at a given sorption density, reflecting the stronger affinity of P for the solid. The amount of solid phase Si in the coprecipitation experiments depended on the initial Si and Fe concentrations but was always a small fraction of the total Si. The coprecipitation experiments with or without Si are compared in Figure 5.3.

Similar results were observed for the reduced groundwater sample that was allowed to oxidize in the laboratory. Iron and P coprecipitated stoichiometrically and there was very little release of the coprecipitated P back into solution (soluble P=0.002 mM after 350 hours). Concentrations of Si were high enough in this sample (1.0 mM) to inhibit recrystallization.

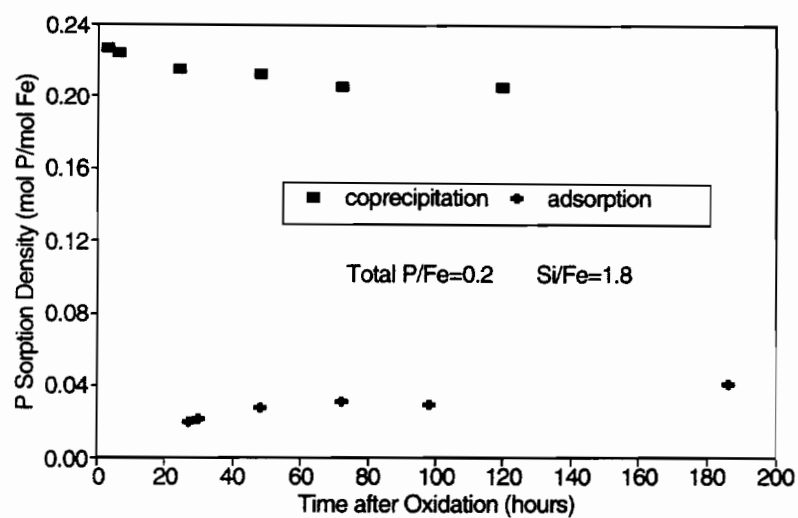


Figure 5.2 Phosphorus coprecipitation and adsorption experiments with Si (pH=7.0).

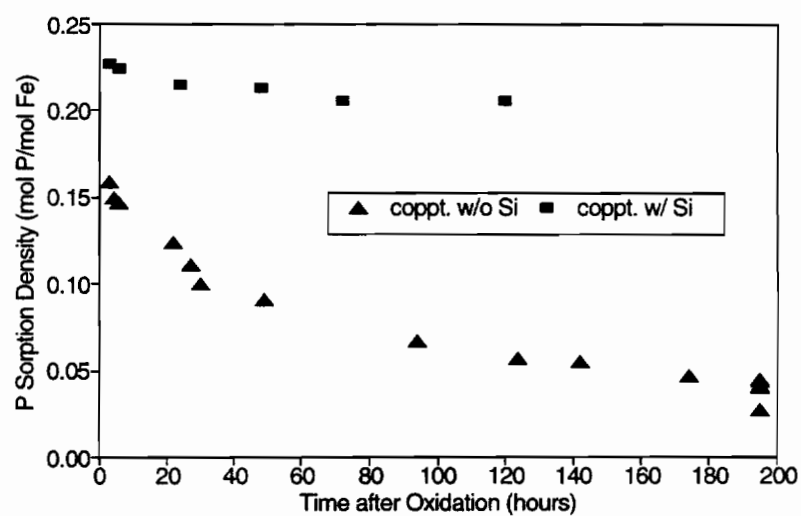


Figure 5.3 Coprecipitation of Fe and P in the presence or absence of Si. This data was previously presented in Figs. 1 and 2.

Lepidocrocite was identified as the Fe(II) oxidation product at initial Si/Fe solution ratios of 0.10 or less. At initial Si/Fe ratios of 0.36 or higher, ferrihydrite was formed. This is similar to the Si/Fe ratio reported by Schwertmann et al. (1984) for ferrihydrite formation from Fe(II) oxidation. The oxidation product in the groundwater sample was determined to be ferrihydrite as well. As discussed above, ferrihydrite is an amorphous Fe oxide with a high specific surface area and concentration of surface sites and sorption is expected to be greater on this solid. Scanning electron microscopy revealed that the ferrihydrite consisted of a number of spherical aggregates with diameters of 0.1 μm or less, whereas, the lepidocrocite had a much coarser, blocky structure. A gradual transition from the blocky structure to the spherical aggregates was observed as the solid phase Si increased, reflecting the development of ferrihydrite rather than lepidocrocite. The Si must be present during Fe(II) oxidation for ferrihydrite to form; adding it 24 hours after the oxidation did not alter the Fe oxidation product. This is similar to the findings of Anderson and Benjamin (1985).

5.3.3 Adsorption Experiments on Pure Fe Oxides and Mixed Fe-Si Solids

Adsorption experiments were conducted to compare the maximum P sorption capacity of the pure Fe oxides and the mixed Fe-Si oxides. As expected, based on the higher specific surface area, the sorption density on the mixed Fe-Si oxides was much greater (Fig. 5.4). Values were nearly three times as great as on pure Fe oxides and the trend in the data suggests that this is not the maximum value. The data in Fig. 5.4 imply that, under these experimental conditions (initial Si/Fe=0.36 to 0.5), the increase in specific surface area resulting from the presence of Si during Fe(II) oxidation is more important than the decrease in ZPC of the solid or competition for anion sorption sites. It may be that at higher Si/Fe ratios, these other factors become more important.

Calcium sorption on pure Fe oxides and mixed Fe-Si oxides was compared as well (Fig. 5.5). The influence of Si on Fe oxide mineralogy and the ZPC of the solid should be favorable for cation sorption, as discussed above, and there will be no competition for surface sites between silica and cations. Calcium sorption was much greater on the mixed Fe-Si oxide as compared to the pure Fe oxide. This has important implications for the

role of Si in trace metal sorption on Fe oxides.

Competition of silicate and phosphate for anion sorption sites was evaluated by adding both anions simultaneously to the pure Fe oxide aged 24 hours (Fig. 5.6). Phosphate sorption was reduced by an average of 11% in the presence of 0.18 mM Si and 34% in the presence of 0.5 mM Si. These experimental results are similar to the modeled competition of Si and P on goethite (Sigg and Stumm, 1980).

The effect of Si on pH adsorption edges can be seen in Figure 5.7. In the absence of Si, a maximum of 50% of the P is sorbed on the pure Fe oxides (lepidocrocite) at low pH because of the lower specific surface area of the solid. However, the percent P sorbed decreases more slowly at higher pH compared to the mixed Fe-Si oxides (ferrihydrite), due to the higher ZPC of the lepidocrocite and the lack of competition from silicate for surface sites. The mixed Fe-Si oxide systems have a higher concentration of surface sites, a lower ZPC, and silicate and phosphate compete for anion sorption sites. Because silicate adsorption is maximized near pH 9.0 while phosphate adsorption is highest under acidic conditions (Sigg and Stumm, 1980), silicate competition is greater at higher pH. The P adsorption edges for the mixed Fe-Si oxides show very high sorption percentages at low pH but rapid decreases in the percent P sorbed at higher pH. As the solid Si concentration increases from 0.09 to 0.16 Si/Fe, the P adsorption edge is displaced to the left.

5.3.4 Comparison of Field Data and Laboratory Results

The maximum P sorption densities for the coprecipitation experiments, with Si, and the adsorption experiments on the mixed Fe-Si solids, are compared in Figure 5.8. Because of the change in sorption density with time, each coprecipitation experiment is represented by two values joined by a line; the value at 24 hours (the left point) and the final value anywhere from 75 to 160 hours (the right point), depending on the experiment. Silicon must be present in the coprecipitation experiments to inhibit the recrystallization of the oxide and slow the release of coprecipitated P. Compared to the adsorption experiments, coprecipitation was much more effective in retaining P in solid form. The amount of P sorbed in the adsorption experiment is not exceptionally low; values of

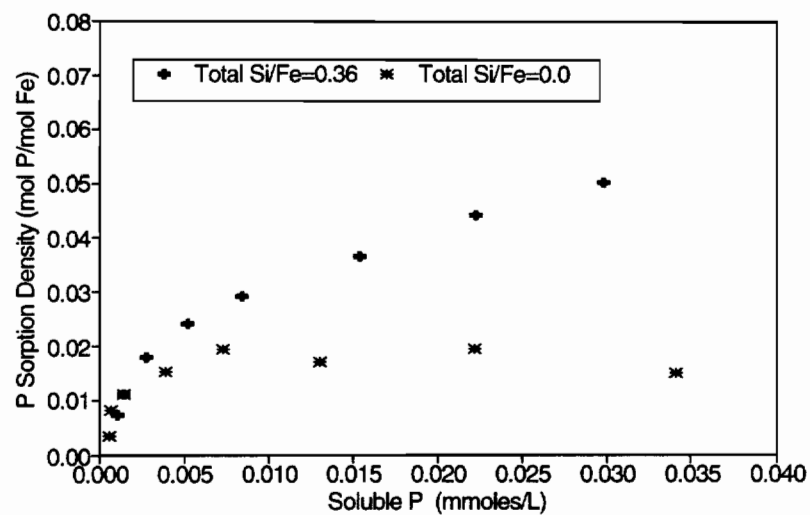


Figure 5.4 Phosphorus adsorption on pure Fe oxides and mixed Fe-Si oxides (pH=7.0).

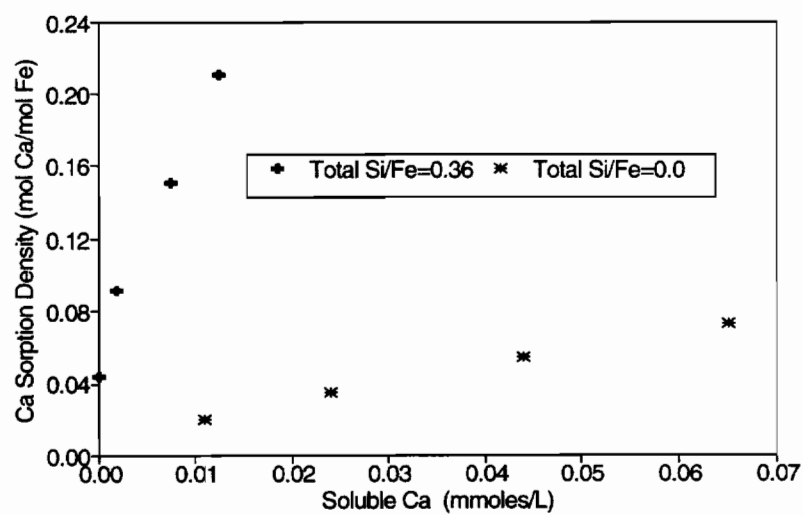


Figure 5.5 Calcium adsorption on pure Fe oxides and mixed Fe-Si oxides (pH=7.0).

sorption densities for the range of soluble P in these adsorption experiments are very similar to others reported in the literature (Ryden et al., 1977; McLaughlin et al., 1981; Lijklema, 1981).

The P/Fe sorption densities of the colloids from the Tualatin River waters are plotted as a function of soluble P and compared with the laboratory results (Fig. 5.8). It is apparent that the adsorption experiment prescribes far too low of a sorption density, given the range of soluble P found in the field. Sorption densities and soluble P values in the coprecipitation experiments match very closely with the field data. This is evidence that the colloids in the Tualatin Basin waters have formed through a coprecipitation process rather than an adsorption process and that the influence of Si is important in the retention of coprecipitated P.

One observation with the suspended material of the Tualatin River was that, while there was a significant fraction of P associated with the solid phase under natural conditions, preliminary laboratory experiments with the material indicated that there was very little capacity to sorb additional P (USGS, unpublished data). Adsorption experiments with synthesized coprecipitates of P, Si, and Fe and the coprecipitates from the groundwater sample revealed that very little additional P was removed from solution by these solids as well, relative to the amount already associated with the solid phase.

These observations may be a result of the separate processes of coprecipitation and adsorption. In the Tualatin samples, much of the solid phase P associated with suspended sediment was associated with Fe oxides. Iron-bound P may have formed through a process similar to the laboratory coprecipitation experiments, as Fe(II) oxidized and coprecipitated with P and Si. The data from the coprecipitation experiments suggest that P, Fe, and Si precipitate stoichiometrically at total P/Fe ratios up to 0.4. Additional uptake of P from solution after coprecipitation and mineral formation is through an adsorption process and is much less effective at retaining P.

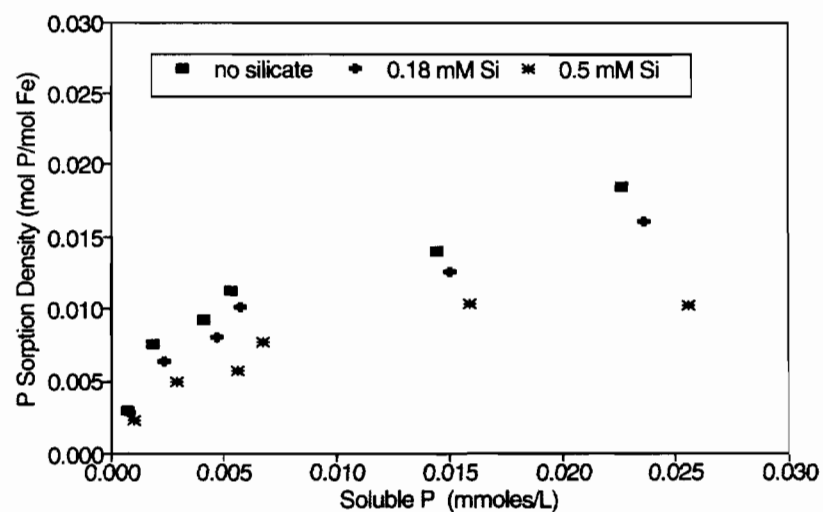


Figure 5.6 Simultaneous adsorption of P and Si added 24 hours after Fe oxide formation (pH=7.0).

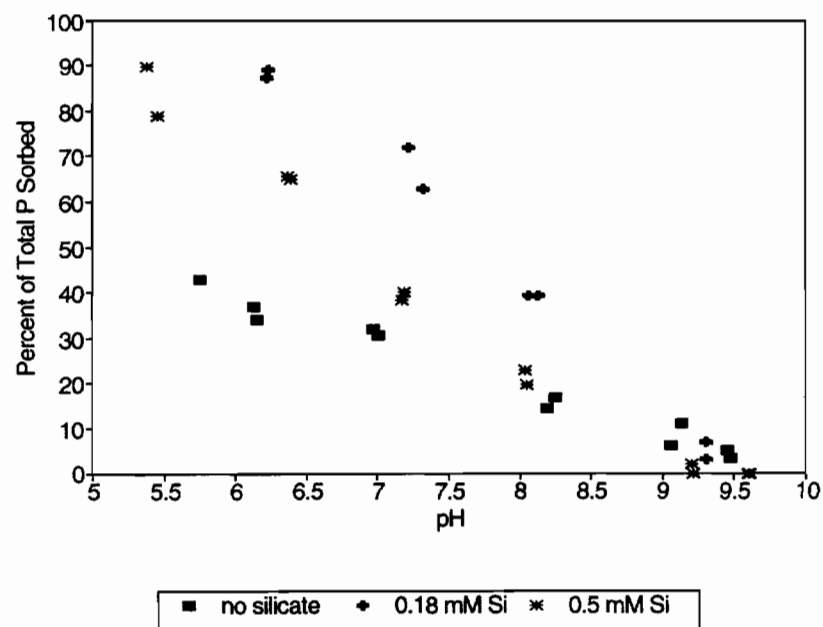


Figure 5.7 Phosphorus adsorption edges on pure Fe oxides and mixed Fe-Si oxides.

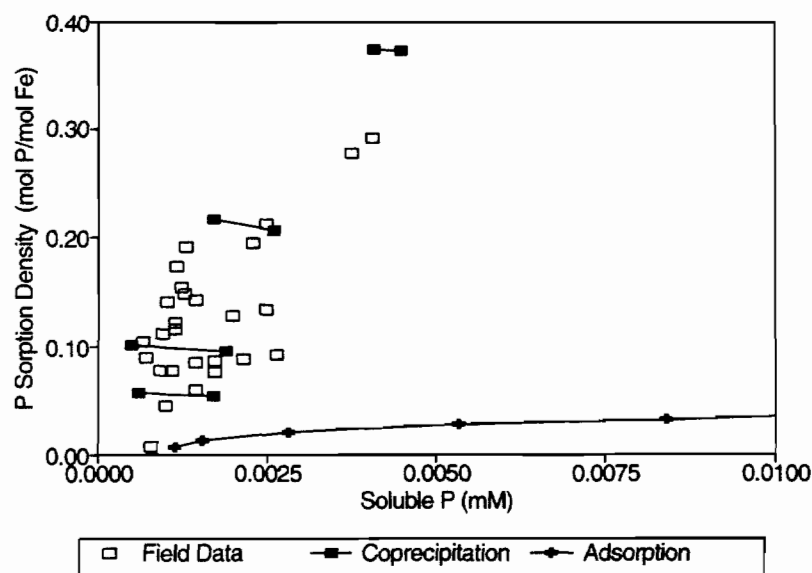


Figure 5.8 Sorption densities as a function of soluble P in four coprecipitation experiments and one adsorption experiment, all with Si present, and the natural colloidal material from the Tualatin River waters. (see text for symbol explanation).

5.3.4 Experimental Interpretation

Earlier investigations have studied coprecipitation, Fe(II)- and Fe(III)-derived Fe oxides, and the effects of Si on sorption processes (Crosby et al., 1981; Anderson and Benjamin, 1985; Fuller et al., 1993). None of these studies reported sorption behavior similar to that observed in this work. We examine the differences between these studies and our own work to emphasize the importance of simulating natural processes in the experimental procedures.

Anderson and Benjamin (1985) found that oxyanion sorption decreased as the Si content of the Fe oxide increased, due to the lower ZPC of the solid. However, the solids in their study were all derived from the rapid hydrolysis of Fe(III), which results in the formation of ferrihydrite, irrespective of the solution chemistry. Ferrihydrite has a characteristically high specific surface area which does not vary significantly (Dzombak and Morel, 1990). The solids in our study were derived from Fe(II) oxidation. Crystal growth of Fe(II)-derived Fe oxides is more likely to be slower because of the dependence

on oxidation rates as well as hydrolysis rates. This slower rate of crystal growth results in a more crystalline product provided that other solutes, like dissolved Si, do not inhibit crystallization. Our results indicate that the increase in surface area and the inhibition of recrystallization due to the presence of Si during Fe(II) oxidation have a much greater effect on P sorption than the decrease in the ZPC of the solid. This effect may not be observed unless Fe(II)-derived solids are used for study.

Crosby et al. (1981) reported that P sorbed on freshly prepared Fe(II)-derived oxides was slowly released back into solution over a 20 hour period, in contrast to Fe(III)-derived oxides which retained sorbed P for the entire period. The desorption was assumed to be due to recrystallization and caused the authors to question the role of Fe(II)-derived oxyhydroxides in controlling P and other trace components in natural waters. However, they did not consider that other dissolved constituents present in natural waters, like organic acids and Si, would inhibit recrystallization. This study shows that natural concentrations of Si can stabilize the Fe oxide and limit the release of coprecipitated P. Organic acids may have a similar effect.

Fuller et al. (1993) reported much greater sorption of arsenate initially on ferrihydrite in coprecipitation experiments compared to adsorption experiments. They described the slow release of coprecipitated arsenate from Fe(III)-derived ferrihydrite over an 800 hour period. Sorption densities of arsenate in the coprecipitation experiments appeared to be converging with analogous adsorption experiments at longer time periods. The sorption chemistry of arsenate, another oxyanion, is expected to be similar to phosphate. The authors did not study the effects of Si, although they did speculate that long-term release of coprecipitated species may be limited by the presence of organic acids and dissolved silica.

The large difference in sorption behavior between the coprecipitation process and the adsorption process has important implications for interpreting experimental results. In many systems, such as groundwater contamination sites, contaminants might be added to stable, existing Fe oxides. Adsorption experiments would realistically simulate this process in these systems. In other systems, the ready cycling between Fe(II) and Fe(III) implies that phosphate, silicate, and other ions are very likely to be present during the

oxidation and precipitation of Fe. For these systems, the coprecipitation experiments would simulate this process much more realistically. Undoubtedly, the lability and bioavailability of coprecipitated ions will differ as well. Modeling efforts should consider the formation process as well. Modeling parameters based on data from adsorption experiments would greatly underestimate the amount of solid phase sorbate at a given soluble concentration in the coprecipitation process.

5.4 Conclusions

The results presented here imply that sorption processes in the natural environment may be very different from those commonly studied in the laboratory. In most systems, Fe oxides form as a result of Fe(II) oxidation in the presence of phosphate and other dissolved ions like silicate. The sorption of phosphate is much more effective when present during Fe oxide formation (coprecipitation experiments) rather than added after the solid has formed (adsorption experiments). The presence of Si influences the surface and sorption properties of Fe oxides as well. The most important effect of Si in this study is inhibition of Fe oxide recrystallization, thereby favoring the formation of amorphous ferrihydrite. Comparison of these laboratory results and field data from the Tualatin River system suggest that Fe-P colloids in the river have formed in manner similar to the coprecipitation experiments in this study.

5.5 References

- American Public Health Association. 1989. Standard methods for the examination of water and wastewater. Amer. Public Health Assoc., New York, NY.
- Anderson, M. A., M. I. Tejedor-Tejedor, and R. R. Stanforth. 1985. Influence of aggregation on the uptake kinetics of phosphate by goethite. *Environ. Sci. Technol.* 19:632-637.
- Anderson, P. R., and M. M. Benjamin. 1985. Effects of silicon on the crystallization and adsorption properties of ferric oxides. *Environ. Sci. Technol.* 19:1048-1053.
- Barrow, N. J. 1985. Reaction of plant nutrients and of pollutants with variable-charge soils. *Adv. Agron.* 38:282-288.

- Borggaard, O. K. 1983. Effect of surface charge and mineralogy of iron oxides on their surface areas and anion-adsorption properties. *Clays Clay Minerals* 31:230-232.
- Cornell, R. M., and U. Schwertmann. 1979. Influence of organic anions on the crystallization of ferrihydrite. *Clays Clay Miner.* 27:402-410.
- Crosby, S. E., E. I. Butler, D. R. Turner, M. Whitfield, D. R. Glasson, and G. E. Millward. 1981. Phosphate adsorption onto iron hydroxides at natural concentrations. *Environ. Technol. Lett.* 2:371-378.
- Crosby, S. E., D. R. Glasson, A. H. Cuttler, I. Butler, D. R. Turner, M. Whitfield, and G. E. Millward. 1983. Surface areas and porosities of Fe(III)- and Fe(II)-derived oxyhydroxides. *Environ. Sci. Technol.* 17:709-713.
- Dzombak, D. A., and F. M. Morel. 1990. Surface complex modeling: hydrous ferric oxide. John Wiley and Sons, New York, NY.
- Einsele, W. 1938. Über chemische und kolloidchemische Vorgänge in Eisenphosphat-systemen unter limnolchemischen und limnogeologischen Gesichtspunkten. *Arch. Hydrobiol.* 33:361-387.
- Fox, L. E. 1989. A model for inorganic control of phosphate concentrations in river waters. *Geochim. Cosmochim. Acta* 53:417-428.
- Fuller, C. C., J. A. Davis, and G. A. Waychunas. 1993. Surface chemistry of ferrihydrite: Part 2. Kinetics of arsenate adsorption and coprecipitation. *Geochim. Cosmochim. Acta* 57:2271-2282.
- Laxen, D. P. H. 1985. Trace metal adsorption/coprecipitation on hydrous ferric oxide under realistic conditions. *Water Res.* 19:1229-1236.
- Lijklema, L. 1980. Interaction of orthophosphate with iron(III) and aluminum hydroxides. *Environ. Sci. Technol.* 14:537-541.
- McLaughlin, J. R., J. C. Ryden, and J. K. Syers. 1981. Sorption of inorganic phosphate by iron- and aluminum-containing components. *J. Soil Sci.*, 32:365-377.
- Ryden, J. C., J. R. McLaughlin, and J. K. Syers. 1977. Mechanisms of phosphate sorption by soils and hydrous ferric oxide gel. *J. Soil Sci.* 28:72-92.
- Schwertmann, U., and H. Thalmann. 1976. The influence of [Fe(II)], [Si], and pH on the formation of lepidocrocite and ferrihydrite during oxidation of FeCl₂ solutions. *Clay Minerals* 11:189-199.
- Schwertmann, U., and H. Fechter. 1982. The point of zero charge of natural and

- synthetic ferrihydrites and its relation to adsorbed silicate. *Clay Minerals* 17:471-476.
- Schwertmann, U., L. Carlson, and H. Fechter. 1984. Iron oxide formation in artificial ground waters. *Schweiz. Z. Hydrol.* 46/2:185-191.
- Schwertmann, U., and R. M. Taylor. 1989. Iron oxides. p. 379-438. *In* J. B. Dixon and S. B. Weed (eds.) *Minerals in soil environments*. Soil Sci. Soc. Am., Madison, WI.
- Schwertmann, U., and R. M. Cornell. 1991. *Iron oxides in the laboratory: Preparation and characterization*. VCH, New York, NY.
- Sigg, L., and W. Stumm. 1980. The interaction of anions and weak acids with the hydrous goethite (α -FeOOH) surface. *Colloids Surfaces*, 2:101-117.
- Sposito, G. 1986. Distinguishing adsorption from surface precipitation. p. 217-228. *In* J.A. Davis and K.F. Hayes (ed.) *Geochemical processes at mineral surfaces*. ACS Symposium Series 323, Chicago, IL Sept. 8-13, 1985. ACS, Washington, DC.
- Stumm, W., and G. F. Lee. 1961. Oxygenation of ferrous iron. *Ind. Eng. Chem.* 53:143-146.
- Stumm, W., and J. J. Morgan. 1981. *Aquatic chemistry*. 2nd ed. John Wiley and Sons, New York, NY.
- Syers, J. F., R. F. Harris, and D. E. Armstrong. 1973. Phosphate chemistry in lake sediments. *J. Environ. Qual.* 2:1-14.
- Tamura, H., K. GoTo, T. Yotsuyanagi, and M. Nagayama. 1973. Spectrophotometric determination of iron (II) with 1,10-phenanthroline in the presence of large amounts of iron (III). *Talanta* 21:314-318.
- Tessenow, U. 1974. Solution, diffusion, and sorption in the upper layer lake sediments. IV. Reaction mechanisms and equilibria in the system iron-manganese-phosphate with regard to the accumulation of vivianite in Lake Ursee. *Arch. Hydrobiol. Suppl.* 47:1-79.
- van Riemsdijk, W. H., L. J. M. Boumans, and F. A. M. de Haan. 1984. Phosphate sorption by soils: I. A diffusion-precipitation model for reaction of phosphate with metal oxides in soil. *Soil Sci. Soc. Am. J.* 48:537-541.

CHAPTER 6

SUMMARY AND CONCLUSIONS

The extent, variability, and origin of colloidal phosphorus (P) and iron (Fe) was investigated in the Tualatin River Basin of northwest Oregon. In an iterative and systematic manner, this research combined field studies and laboratory experiments to address questions and observations concerning Fe/P chemistry. Great effort was given to designing model systems in the laboratory that simulated field conditions and processes in the Tualatin Basin and elsewhere. The priority and detail given to simulating natural systems produced results which are unique to this research, despite the fact that Fe/P interactions have been studied intensively for a number of years. The general results of this research are summarized below.

Phosphorus and iron were associated in colloid-sized particles in surface waters of the Tualatin River basin. Correlations were strong between colloidal concentrations of P and Fe but not between total or particulate concentrations. This implies that P and Fe were most directly associated in the smaller size fractions of suspended sediments. Concentrations of suspended sediment and P were not correlated either. Studies of other systems have interpreted such a correlation as evidence that eroded particles are a significant source of P.

The fraction of the total P and total Fe in colloidal form varied considerably, depending on location and time of year. Results from the Bronson Creek study indicated that colloidal P and Fe were more prevalent during periods of low flow and low dissolved oxygen. This led to the hypothesis that the colloids form as groundwater- or sediment-released Fe(II) and P diffuse to oxygen-containing surface waters, causing Fe(II) to

oxidize and coprecipitate with P. In addition to P and Fe, Si was a major component of the colloids.

Laboratory experiments were conducted to examine the formation process of the colloids under controlled conditions. Colloidal Fe oxides were formed through the oxidation of Fe(II) in model solutions under conditions that simulated the natural environment. At low concentrations of Si, Fe(II) oxidation resulted in lepidocrocite formation and colloidal suspensions were not stable. At background concentrations of Si typical of the Tualatin and other systems, Fe(II) oxidation resulted in the formation of stable ferrihydrite colloids. The association of Si with the Fe oxides stabilizes the colloids in two ways: (1) through the contribution to the surface charge and potential and (2) through the inhibition of Ostwald ripening and recrystallization of the Fe oxide. The synthesized ferrihydrite colloids were very similar in appearance, composition, and structure to Fe oxide colloids from surface waters of the Tualatin River.

The sorption chemistry of P and Fe oxides was evaluated under conditions simulating natural systems. The presence of P during Fe(II) oxidation (coprecipitation of P and Fe) resulted in a much higher P/Fe solid ratio than when P was added after the Fe oxide mineral had formed. However, this solid phase was only metastable and most of the coprecipitated P was subsequently released to solution during recrystallization of the Fe oxide. The presence of Si during coprecipitation of P and Fe inhibited the recrystallization of the Fe oxide and maintained the high P/Fe solid ratios. The soluble P values and sorption densities prescribed by the coprecipitation of P, Si, and Fe were very similar to the field values observed in surface waters of the Tualatin Basin. This is evidence that the P- and Fe-containing colloids in the surface waters formed through coprecipitation rather than adsorption. The study results are significant in noting: (1) the exceptional differences in sorption chemistry between coprecipitation and adsorption of P and (2) the important role of Si in maintaining Fe oxide-associated P in colloidal form.

Colloidal Fe-P has several implications for the chemical and physical behavior, the bioavailability, and the management of P in aquatic systems. Colloidal P will be transported along with the dissolved phase but will retain the physico-chemical properties of the solid phase. This unique dichotomy of properties implies that colloidal P will

behave differently from either dissolved or larger particulate forms of P and may have to be considered explicitly in our conceptual and numerical models of aquatic systems.

The longer residence time of colloidal Fe-P in suspension may affect the bioavailability of P in aquatic systems. Colloidal Fe-P will remain in the photic zone, accessible to algae, longer than other larger P-containing particles. Iron-associated P has been shown to be bioavailable in several studies. This is expected if the P is reversibly sorbed on Fe oxide particle surfaces. However, the bioavailability and lability of P coprecipitated with Fe remains to be evaluated.

The efficacy of management strategies to control P may be affected by colloidal Fe-P. Settling basins designed to remove particulate P or constructed wetlands designed to remove soluble P may not remove colloidal Fe-P. Management strategies that affect the hydrology of the system may affect the formation and fraction of colloidal Fe-P as well. In the Tualatin, low surface water flows will increase the relative importance of groundwater contributions, which may increase the fraction of colloidal Fe-P. Enhanced surface flows will dilute the groundwater component and increase the dissolved O_2 concentration in the water column and sediments, both of which may result in a decrease in the fraction of colloidal Fe-P.

Colloids can be important in the transport, chemistry, bioavailability, and management of environmental pollutants such as phosphate. A complete understanding of the behavior of these pollutants may not be possible until questions concerning colloidal forms are addressed and resolved. This research has expanded the knowledge of Fe-P colloid chemistry and begun to address some of these questions.

APPENDIX A

FILTRATION ARTIFACTS IN DETERMINING SIZE FRACTIONATION

Concentrations of dissolved constituents in natural waters are frequently determined with filtration (Laxen and Chandler, 1982). However, the presence of material in colloidal form renders the method problematic (Buffle et al., 1992). Colloids may be small enough to pass through the filter pores and inflate "dissolved" concentrations if detected analytically.

One objective of this work was to evaluate the effectiveness of various filter sizes in removing colloidal P and colloidal Fe oxides. The concentrations of "dissolved" P and Fe in filtrates from filters of two pore sizes, 0.4 and 0.05 μm , were measured in a number of river samples from the Tualatin Basin. The 0.4 μm pore size was used because a 0.4 or 0.45 μm pore size filter is commonly used to distinguish between soluble and solid phases (APHA, 1989). The 0.05 μm pore size was chosen because this is approximately the lower diameter limit of most Fe oxide colloids observed in the field (see Chapter 2).

Figure A.1 plots the P concentrations of the 0.4 μm filtrate versus the 0.05 μm filtrate. The solid line is the 1:1 relation: the points should plot on this line if both filtrates contained only dissolved phases. The fact that most points are above the solid line indicates that the 0.4 μm filtrate overestimates dissolved P concentrations, sometimes by more than 100%. The data also show that the ascorbic acid method for orthophosphate measurement is quite capable of hydrolyzing and measuring other forms of P in filtrates, as has been noted previously (APHA, 1989).

For Fe concentrations, the differences between the filtrates are even more outstanding (Fig. A.2). The 0.4 μm filtrate seriously overestimates dissolved Fe concentrations by as much as 1000% or more. Because of the insolubility of Fe(III),

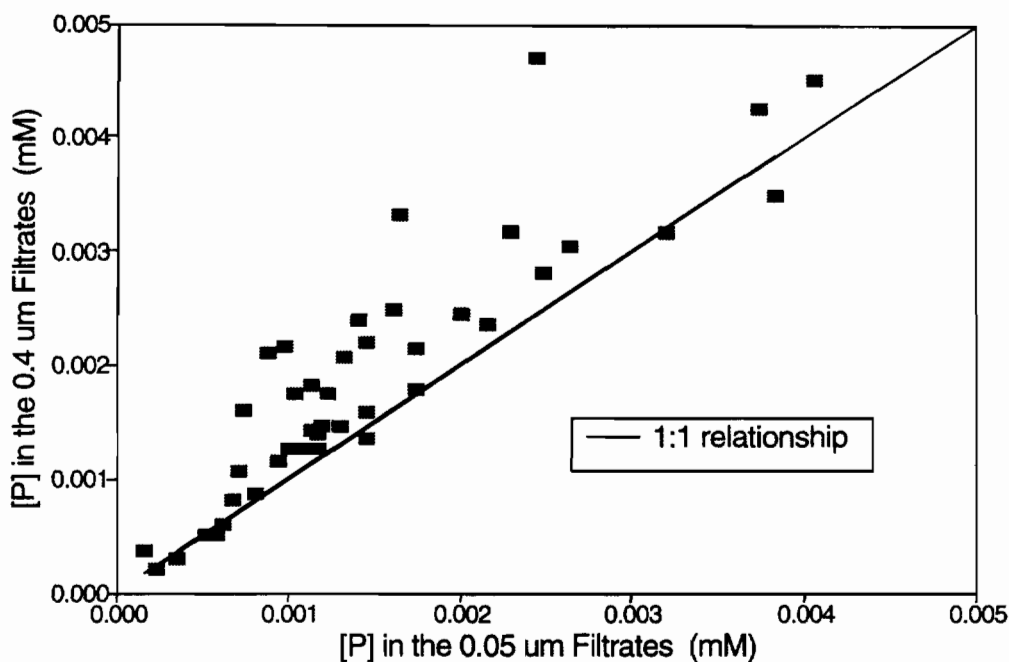


Figure A.1 Phosphorus concentrations in river sample filtrates from 0.4 μm and 0.05 μm pore size filters.

dissolved Fe is often assumed to be Fe(II). Obviously, estimates of Fe(II) concentrations based on the 0.4 μm filtrate would be erroneous. The data sets for both elements show that colloids are capable of passing through the pores of filters and inflating estimates of dissolved concentrations.

Filtration is one of the most convenient methods for size fractionation of suspended particles (Buffle et al., 1992). As discussed in Chapter 2, filters can retain colloids that are smaller than the filter pores. Since this colloidal material is inadvertently segregated out with larger particles, the colloidal phase is underestimated. Scanning electron microscopy (SEM) photos of the suspended sediment retained on filter surfaces were used to evaluate the extent of this error qualitatively. Figure A.3 is an SEM photo of the surface of a 1.0 μm pore size polycarbonate membrane filter used to filter a river sample. The lighter particles are suspended material that was retained on the filter and the dark circles are the 1.0 μm pores. It is obvious that while some of the material

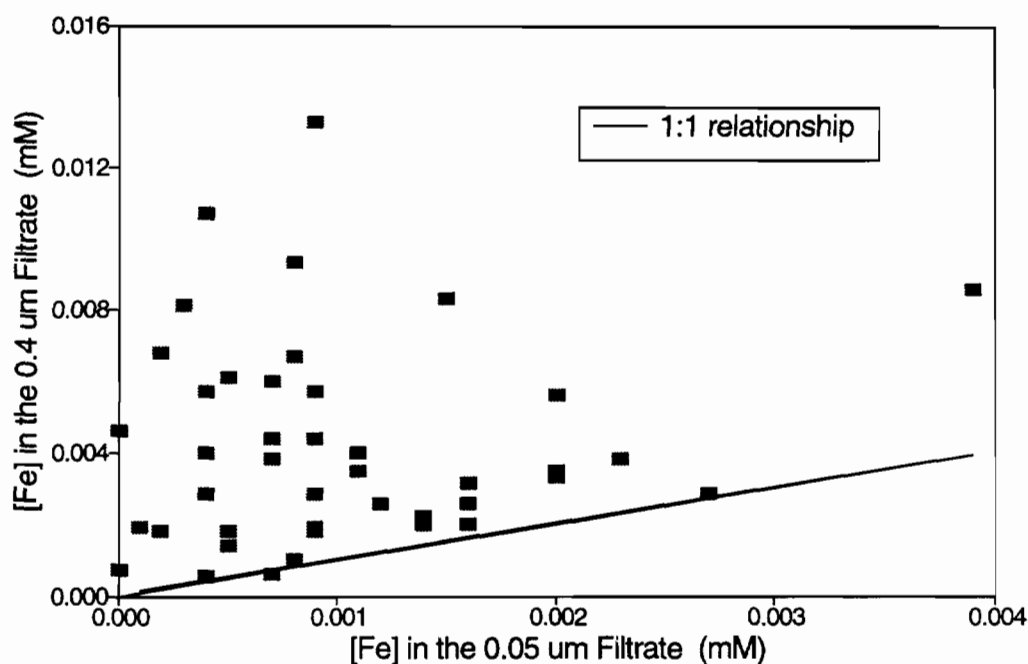


Figure A.2 Iron concentrations in river sample filtrates from 0.4 µm and 0.05 µm pore size filters.

retained by the filter is greater than 1.0 µm in size, much of it smaller than this. Note that some of the larger particles that appear on the filter could actually be aggregates of smaller particles that can't be distinguished because of the low resolution of SEM.

Figure A.4 is an SEM photo of suspended sediment retained by a 0.4 µm pore size filter. Almost all of the material retained by this filter appears to be smaller than the pores. Much of this colloidal material contains Fe and P.

In the field, both of these artifacts may occur during filtration. The use of 0.05 µm pore size filters in this study probably limited the inclusion of colloids in the filtrates. But the erroneous retention of colloids on larger filters most certainly occurred, despite efforts to minimize this artifact (Chapter 3). Since both of these artifacts will tend to underestimate the extent of colloidal phases, the assessment of colloidal concentrations in this study is conservative.

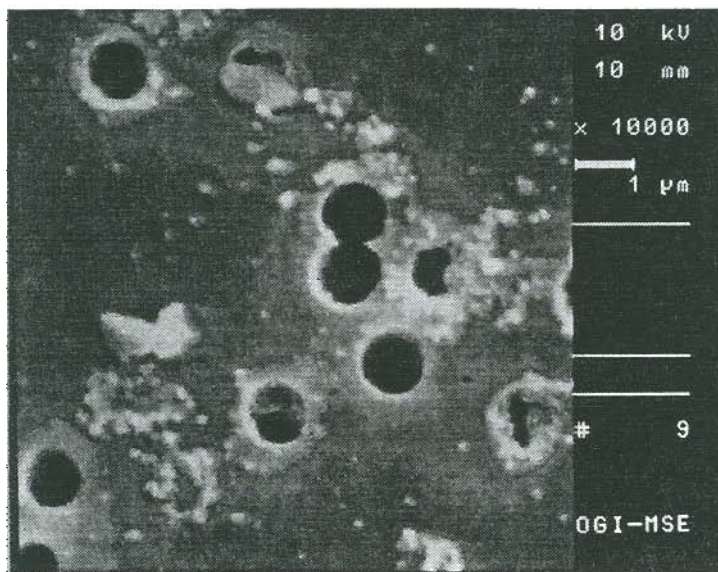


Figure A.3 Scanning electron micrograph of the suspended sediment from a river sample retained on a 1.0 μm filter.

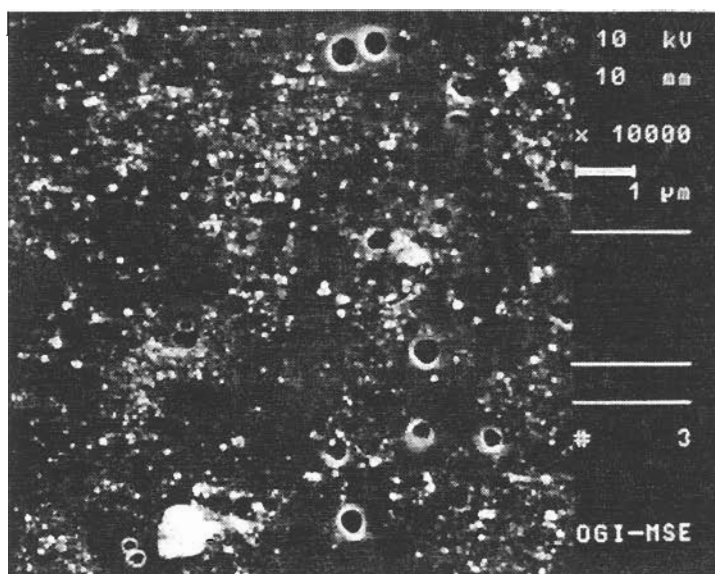


Figure A.4 Scanning electron micrograph of the suspended sediment from a river sample retained on a 0.4 μm filter.

References

American Public Health Association. 1989. Standard methods for the examination of water and wastewater. 17th ed. Amer. Publ. Health Assoc., New York, NY.

Buffle, J., D. Perret, and M. Newman. 1992. The use of filtration and ultrafiltration for size fractionation of aquatic particles, colloids, and macromolecules. p. 171-230. *In*: J. Buffle and H. van Leeuwen (eds.) Environmental particles. Lewis Publ., Boca Raton, FL.

Laxen, D. P. H. and I. M. Chandler. 1982. Comparison of filtration techniques for size distribution in freshwaters. *Anal. Chem.* 54:1350-1355.

APPENDIX B

ENERGY DISPERSIVE SPECTROSCOPY AS A TOOL FOR ELEMENTAL ANALYSIS OF SUSPENDED SEDIMENTS

Electron dispersive spectroscopy (EDS) is a analytical technique for performing elemental analysis on microvolumes. The technique is used in conjunction with scanning electron microscopy (SEM), which provides a source of electromagnetic radiation. When electromagnetic radiation strikes an atom, inner shell electrons may be emitted. Outer shell electrons of greater potential energy will fill the inner shell vacancy and, in the process, emit characteristic energies in the form of X-rays. The energy spectrum is collected and used to identify the composition of the sample.

Individual particles and colloids on filter surfaces were analyzed with EDS. The ZAF-4 method was used for quantitative analysis. The filters were dried in a desiccator under a vacuum and then coated with carbon. Better image results were obtained with gold coatings on the filters; however, carbon was used to coat the filters for elemental analysis. This was because the gold peak is in the same region as the phosphorus peak and gold coatings may have interfered with the detection of phosphorus.

One complication with EDS is that X-ray spatial resolution is considerably worse than image spatial resolution. It depends on the critical excitation energy of the element, the accelerating voltage of the SEM and the density of the sample, and is usually on the order of microns. Decreasing the accelerating voltage can improve X-ray spatial resolution. An accelerating voltage of 15 keV was used in this study. This was the minimum accelerating voltage that would detect Fe. X-ray spatial resolution was estimated to be 1 to 3 μm , which is still larger than many of the individual particles on the filter.

X-ray volumes are characteristically teardrop-shaped, spreading laterally with depth. Because of this geometry, most of the elemental information in each spectrum originates from either a small area on the filter surface or the filter itself. During collection of spectra from individual particles, interference from adjacent particles was not as much a concern as interference from the filter material. Spectra from blank polycarbonate filters consisted of C and O only. Quantitative analysis of these two elemental ratios in the sample was problematic since it was impossible to separate C and O associated with the particles from filter C and O. Also, because elemental information originated from both the particle and the filter, the exact X-ray volume was unknown. This meant that the atomic percentages, as calculated by the ZAF-4 method, did not represent the composition of the solid alone. For this reason, only atomic ratios and not atomic percentages were used in the data analysis. Atomic ratios should be independent of the X-ray volume, with the exception of C and O as noted above.

Examples of EDS spectra and quantitative analyses from two representative colloids are presented (Fig. B.1-B.2). Elemental peaks in the spectra are identified. Atomic ratios for each spectra were calculated from the atomic percentages by hand.

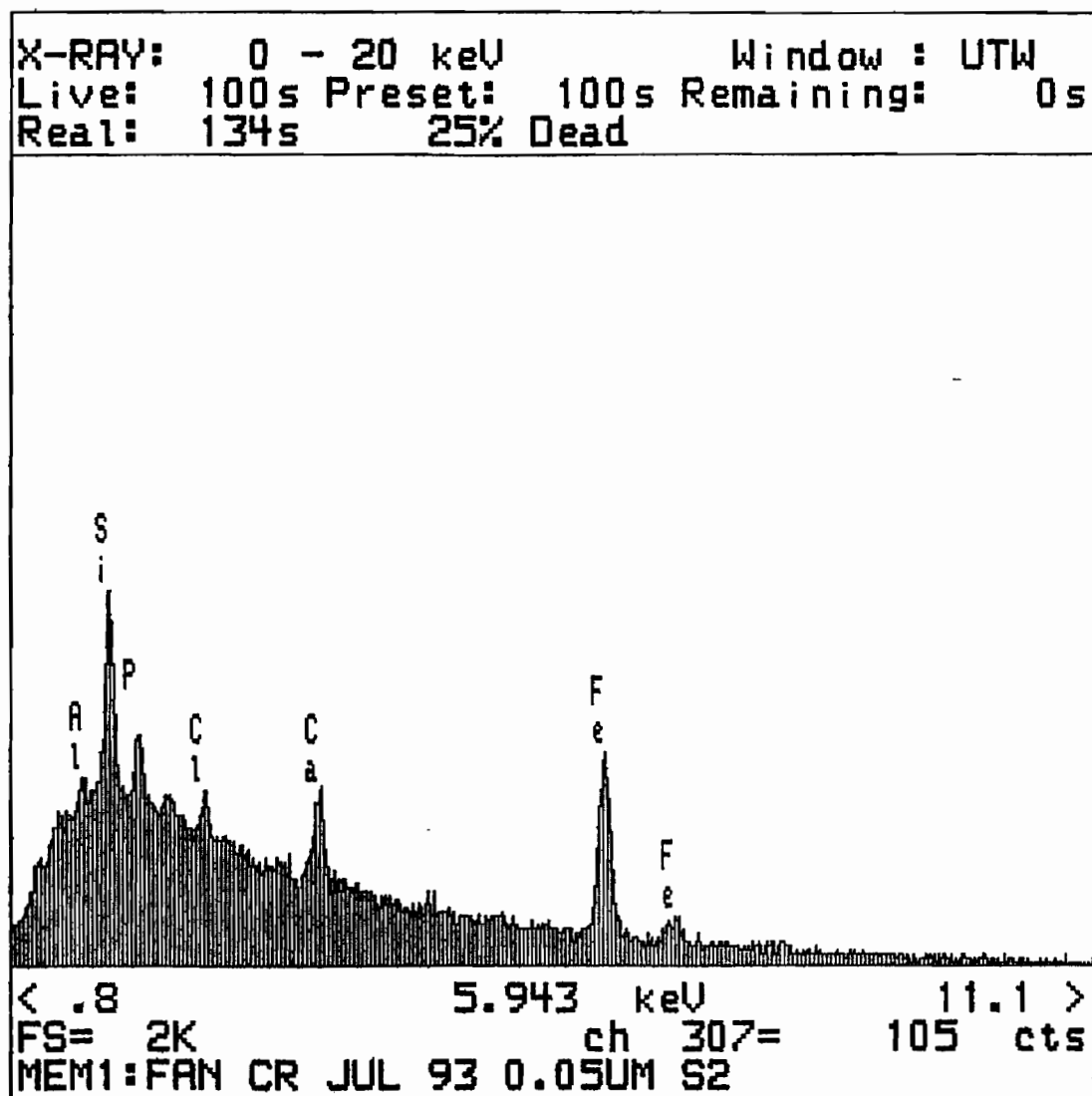


Figure B.1 Example of the energy spectra from a colloid collected in Fanno Creek, July 1993.

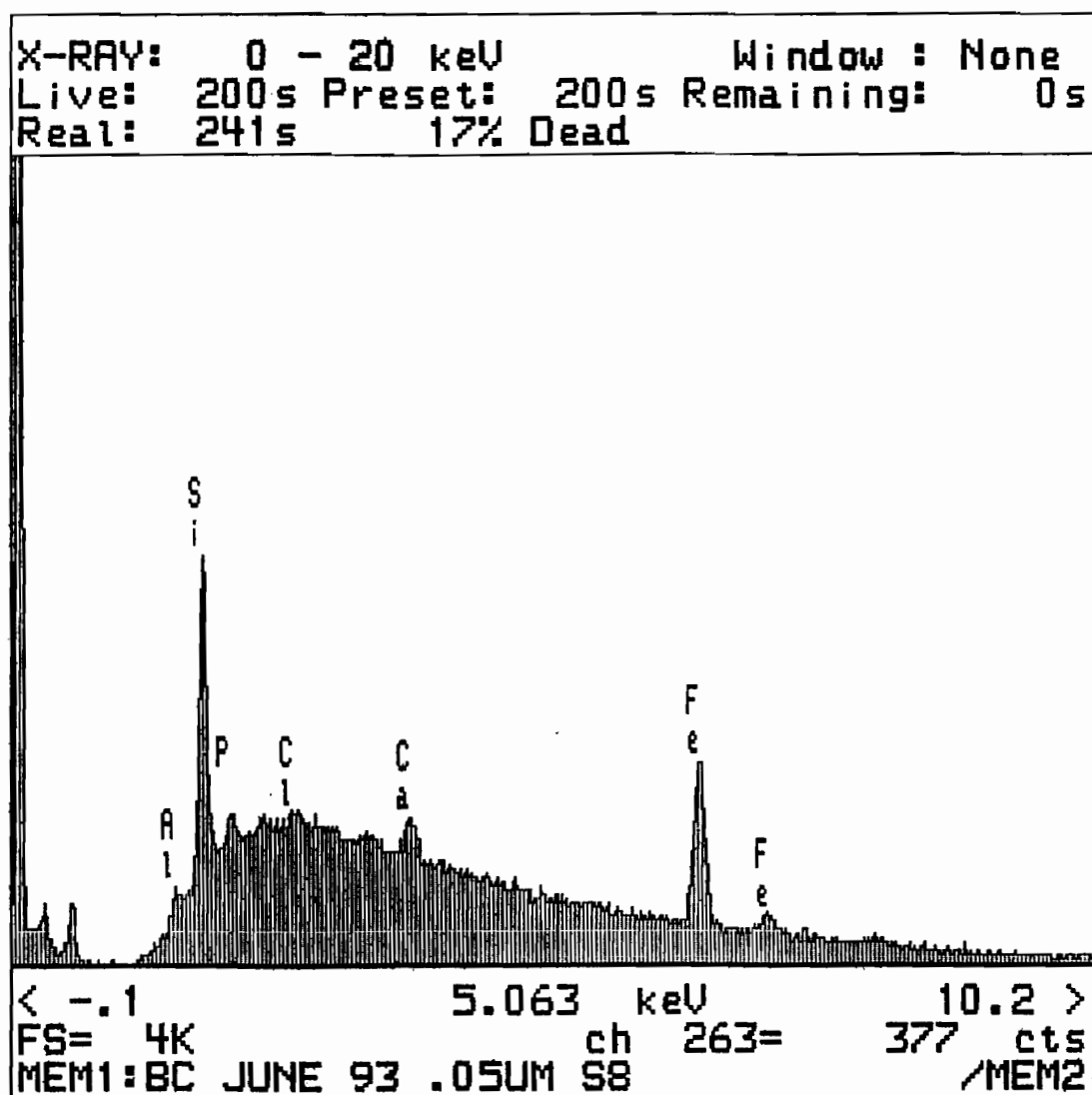


Figure B.2 Example of the energy spectra from a colloid collected in Bronson Creek, June 1993.

APPENDIX C
COMPLETE DATA SETS FOR THE TWO FIELD STUDIES

Bronson Creek Study

| Sampling Date | Flow cfs | Turbidity NTU | pH | Electrical Conductivity µmhos/cm | Temperature C° | Dissolved O ₂ mM | Alkalinity mM | [Si] mM |
|---------------|-----------------|------------------|------|--|-------------------|-----------------------------------|------------------|------------|
| 8/4/92 | nm ^a | nm | 7.26 | 246 | 19.0 | 0.13 | nm | nm |
| 8/6/92 | nm | nm | 7.26 | 295 | 20.0 | 0.28 | nm | nm |
| 8/8/92 | <0.5 | 11.9 | 7.11 | 249 | 18.2 | 0.08 | nm | nm |
| 8/10/92 | <0.5 | 8.7 | 7.13 | 372 | 19.5 | 0.07 | nm | nm |
| 8/12/92 | <0.5 | 7.0 | 7.27 | 276 | 20.5 | 0.06 | nm | nm |
| 8/14/92 | <0.5 | 9.0 | 7.12 | 293 | 19.2 | 0.06 | nm | nm |
| | | | | | | | | |
| 9/21/92 | <0.5 | 3.6 | 7.08 | 246 | 15.9 | 0.09 | nm | nm |
| 9/23/92 | <0.5 | 4.0 | 7.11 | 254 | nm | 0.07 | nm | nm |
| 9/24/92 | 1.3 | 11.9 | 7.25 | 180 | 17.0 | 0.14 | nm | nm |
| 9/25/92 | 0.7 | 9.7 | 7.22 | 201 | 16.6 | 0.12 | nm | nm |
| 9/28/92 | <.5 | 7.5 | 7.11 | 209 | 14.5 | 0.1 | nm | nm |
| 9/30/92 | <.5 | 4.9 | 7.13 | 210 | 15.0 | 0.09 | nm | nm |

^a not measured

Bronson Creek Study (cont.)

| Sampling Date | Flow cfs | Turbidity NTU | pH | Electrical Conductivity µmhos/cm | Temperature C° | Dissolved O ₂ mM | Alkalinity mM | [Si] mM |
|---------------|-------------|------------------|------|--|-------------------|-----------------------------------|------------------|------------|
| 11/16/92 | 0.8 | 5.1 | 6.99 | 212 | 9.0 | 0.17 | nm | 0.320 |
| 11/18/92 | nm | 4.4 | 6.95 | 215 | 9.1 | 0.18 | 0.85 | 0.332 |
| 11/20/92 | 2.4 | 9.0 | 7.06 | 207 | 8.9 | 0.21 | 1.04 | 0.375 |
| 11/23/92 | 5.6 | 41.6 | 6.86 | 148 | 8.4 | 0.26 | 0.7 | 0.400 |
| 11/25/92 | 1.9 | 31.6 | 7.10 | 172 | 5.3 | 0.28 | 0.89 | 0.431 |
| | | | | | | | | |
| 2/8/93 | <0.5 | 13.3 | 7.12 | 202 | 6.9 | 0.29 | 1.04 | 0.423 |
| 2/22/93 | <0.5 | 11.0 | 7.24 | 210 | 4.1 | 0.35 | 0.96 | 0.393 |

Bronson Creek Study (cont.)

| Sampling Date | Reactive [P] <0.05 µm mM | Reactive [P] <1.0 µm mM | Total [P] unfiltered mM | [Fe] <0.05 µm mM | [Fe] <1.0 µm mM | [Fe] unfiltered mM |
|---------------|--------------------------------|-------------------------------|-------------------------------|------------------------|-----------------------|--------------------------|
| 8/4/92 | 0.0017 | 0.0059 | 0.0087 | 0.0004 | 0.0291 | 0.0298 |
| 8/6/92 | 0.0025 | 0.0068 | 0.0106 | 0.0008 | 0.0232 | 0.0360 |
| 8/8/92 | 0.0009 | 0.0028 | 0.0042 | 0.0008 | 0.0123 | 0.0190 |
| 8/10/92 | 0.0014 | 0.0036 | 0.0063 | 0.0002 | 0.0139 | 0.0188 |
| 8/12/92 | 0.0007 | 0.0025 | 0.0067 | 0.0007 | 0.0125 | 0.0254 |
| 8/14/92 | 0.0006 | 0.0030 | 0.0113 | 0.0007 | 0.0116 | 0.0397 |
| | | | | | | |
| 9/21/92 | 0.0005 | 0.0027 | 0.00520 | 0.0008 | 0.0077 | 0.0150 |
| 9/23/92 | 0.0010 | 0.0032 | 0.00536 | 0.0008 | 0.0102 | 0.0172 |
| 9/24/92 | 0.0010 | 0.0014 | 0.00560 | 0.0004 | 0.0061 | 0.0169 |
| 9/25/92 | 0.0009 | 0.0013 | 0.00672 | 0.0005 | 0.0035 | 0.0191 |
| 9/28/92 | 0.0005 | 0.0015 | 0.00536 | 0.0005 | 0.0077 | 0.0197 |
| 9/30/92 | 0.0009 | 0.0018 | 0.00399 | 0.0013 | 0.0079 | 0.0156 |

Bronson Creek Study (cont.)

| Sampling Date | Reactive [P] <0.05 µm mM | Reactive [P] <1.0 µm mM | Total [P] unfiltered mM | [Fe] <0.05 µm mM | [Fe] <1.0 µm mM | [Fe] unfiltered mM |
|---------------|--------------------------------|-------------------------------|-------------------------------|------------------------|-----------------------|--------------------------|
| 11/16/92 | 0.0005 | 0.0009 | 0.0019 | 0.0004 | 0.0027 | 0.0070 |
| 11/18/92 | 0.0007 | 0.0010 | 0.0021 | 0.0005 | 0.0032 | 0.0058 |
| 11/20/92 | 0.0006 | 0.0007 | 0.0022 | 0.0006 | 0.0024 | 0.0075 |
| 11/23/92 | 0.0015 | 0.0021 | 0.0055 | 0.0014 | 0.0027 | 0.0218 |
| 11/25/92 | 0.0008 | 0.0014 | 0.0049 | 0.0021 | 0.0024 | 0.0191 |
| | | | | | | |
| 2/8/93 | 0.0009 | 0.0016 | 0.0024 | 0.0004 | 0.0017 | 0.0090 |
| 2/22/93 | 0.0011 | 0.0016 | 0.0024 | 0.0004 | 0.0029 | 0.0089 |

Tualatin Basin Study

| Sampling Site | Sampling Date | Flow cfs | Turbidity NTU | pH | Electrical Conductivity µmhos/cm | Temperature C° | Total Suspended Solids mg/L | Dissolved O ₂ mM | Alkalinity mM |
|------------------------------|---------------|-------------|------------------|------|--|-------------------|--------------------------------------|-----------------------------------|------------------|
| Scoggins Cr at Old Hwy 47 | 4/19/93 | nm | 7.6 | 6.97 | 74 | 5.4 | nm | 0.33 | 0.52 |
| | 6/3/93 | nm | 4.6 | 6.13 | 75 | 6.6 | nm | 0.28 | 0.52 |
| | 7/12/93 | nm | 2.9 | 6.95 | 88 | 7.8 | 1.6 | 0.34 | 0.48 |
| | 8/26/93 | nm | 3.6 | 6.99 | 61 | 9.0 | 4.8 | 0.33 | 0.48 |
| | 10/4/93 | nm | 6.7 | 7.22 | 70 | 11.3 | 6.6 | 0.22 | 0.56 |
| | 11/15/93 | nm | 4.4 | 6.52 | 80 | 10.9 | 3.2 | 0.26 | 0.60 |
| Dairy Cr at Hwy 8 | 4/19/93 | 695.0 | 12.3 | 6.63 | 90 | 12.3 | nm | 0.25 | 0.54 |
| | 6/3/93 | 501.0 | 16.6 | 6.56 | 88 | 13.6 | 8.0 | 0.23 | 0.59 |
| | 7/12/93 | 53.0 | 9.0 | 7.07 | 92 | 14.8 | 6.0 | 0.25 | 0.76 |
| | 8/26/93 | 26.7 | 8.5 | 7.19 | 108 | 15.0 | 7.4 | 0.28 | 0.96 |
| | 10/4/93 | 22.9 | 6.9 | 7.29 | 136 | 13.3 | 5.0 | 0.17 | 0.88 |
| | 11/15/93 | 30.8 | 4.4 | 6.54 | 128 | 3.6 | 2.2 | 0.28 | 1.04 |

Tualatin Basin Study (cont.)

| Sampling Site | Sampling Date | Flow cfs | Turbidity NTU | pH | Electrical Conductivity µmhos/cm | Temperature C° | Total Suspended Solids mg/L | Dissolved O ₂ mM | Alkalinity mM |
|----------------------------|---------------|-------------|------------------|------|--|-------------------|--------------------------------------|-----------------------------------|------------------|
| Rock Cr at River Rd | 4/19/93 | 395.0 | 20.5 | 6.78 | 164 | 13.2 | nm | 0.26 | 1.10 |
| | 6/3/93 | 199.0 | 29.4 | 6.60 | 170 | 15.6 | 18.0 | 0.24 | 1.15 |
| | 7/12/93 | 18.7 | 6.1 | 7.42 | 295 | 15.9 | 4.2 | 0.21 | 2.00 |
| | 8/26/93 | 17.6 | 5.2 | 7.64 | 332 | 14.5 | 5.6 | 0.26 | 1.92 |
| | 10/4/93 | 24.2 | 7.9 | 7.53 | 398 | 13.2 | 4.6 | 0.22 | 2.08 |
| | 11/15/93 | 30.2 | 5.2 | 7.23 | 310 | 3.7 | 2.6 | 0.26 | 2.96 |
| Bronson Cr at Walker Rd | 4/20/93 | 7.2 | 18.6 | 7.14 | 168 | 13.7 | nm | 0.32 | 1.20 |
| | 6/4/93 | 4.5 | 7.5 | 6.69 | 196 | 18.5 | 2.5 | 0.23 | 1.20 |
| | 7/13/93 | <0.5 | 5.2 | 7.01 | 30 | 18.1 | 8.4 | 0.18 | 1.84 |
| | 8/27/93 | <0.5 | 4.8 | 6.98 | 251 | 17.5 | 5.4 | 0.16 | 2.03 |
| | 10/5/93 | <0.5 | 3.8 | 7.02 | 288 | 14.3 | 4.8 | 0.09 | 2.08 |
| | 11/16/93 | <0.5 | 9.6 | 6.96 | 295 | 5.7 | 8.2 | 0.25 | 1.68 |

Tualatin Basin Study (cont.)

| Sampling Site | Sampling Date | Flow cfs | Turbidity NTU | pH | Electrical Conductivity µmhos/cm | Temperature C° | Total Suspended Solids mg/L | Dissolved O ₂ mM | Alkalinity mM |
|----------------------------|---------------|-------------|------------------|------|--|-------------------|--------------------------------------|-----------------------------------|------------------|
| Fanno Cr at Durham Rd | 4/20/93 | 50.0 | 12.2 | 7.02 | 206 | 13.1 | nm | 0.27 | 1.32 |
| | 6/4/93 | 42.0 | 16.3 | 6.85 | 193 | 15.7 | 11.0 | 0.25 | 1.32 |
| | 7/13/93 | 6.5 | 5.4 | 7.29 | 243 | 15.5 | 1.2 | 0.24 | 1.84 |
| | 8/27/93 | 27.2 | 6.5 | 7.10 | 255 | 15.2 | 5.6 | 0.23 | 1.96 |
| | 10/5/93 | nm | 6.5 | 7.18 | 311 | 14.3 | 2.6 | 0.21 | 2.24 |
| | 11/16/93 | 6.5 | 10.5 | 6.82 | 244 | 5.7 | 7.8 | 0.24 | 1.84 |
| Tualatin at Stafford Rd | 4/20/93 | 2770 | 15.4 | 6.88 | 115 | 11.7 | nm | 0.27 | 0.68 |
| | 6/4/93 | 1270 | 21.6 | 6.73 | 144 | 15.4 | 4.0 | 0.24 | 0.88 |
| | 7/13/93 | 235 | 12.6 | 7.17 | 190 | 18.3 | 13.2 | 0.29 | 1.16 |
| | 8/27/93 | 112 | 6.0 | 7.08 | 217 | 18.2 | 9.8 | 0.32 | 1.20 |
| | 10/5/93 | 123 | 7.9 | 6.75 | 241 | 15.6 | 6.0 | 0.27 | 0.96 |
| | 11/16/93 | 161 | 4.1 | 6.89 | 242 | 7.8 | 3.2 | 0.21 | 2.06 |

Tualatin Basin Study (cont.)

| Sampling Site | Sampling Date | Reactive [P] <0.05 μm mM | Reactive [P] <1.0 μm mM | Total [P] <1.0 μm mM | Total [P] unfiltered mM | [Fe] <0.05 μm mM | [Fe] <1.0 μm mM | [Fe] unfiltered mM | [Si] unfiltered mM |
|------------------------------|---------------|---|--|---------------------------------------|-------------------------------|-----------------------------------|----------------------------------|--------------------------|--------------------------|
| Scoggins Cr at Old Hwy 47 | 4/19/93 | 0.0006 | 0.0006 | 0.0007 | 0.0016 | 0.0012 | 0.0024 | 0.0120 | 0.218 |
| | 6/3/93 | 0.0005 | 0.0005 | 0.0004 | 0.0007 | 0.0004 | 0.0024 | 0.0057 | 0.240 |
| | 7/12/93 | 0.0002 | 0.0002 | 0.0005 | 0.0006 | 0.0014 | 0.0019 | 0.0030 | 0.224 |
| | 8/26/93 | 0.0002 | 0.0002 | 0.0004 | 0.0005 | 0.0008 | 0.0016 | 0.0046 | 0.235 |
| | 10/4/93 | 0.0004 | 0.0002 | 0.0005 | 0.0006 | 0.0007 | 0.0003 | 0.0042 | 0.239 |
| | 11/15/93 | 0.0012 | 0.0014 | 0.0015 | 0.0019 | 0.0005 | 0.0018 | 0.0035 | 0.216 |
| Dairy Cr | 4/19/93 | 0.0008 | 0.0008 | 0.0010 | 0.0020 | 0.0007 | 0.0049 | 0.0251 | 0.255 |
| | 6/3/93 | 0.0009 | 0.0017 | 0.0016 | 0.0031 | 0.0004 | 0.0100 | 0.0417 | 0.329 |
| | 7/12/93 | 0.0007 | 0.0012 | 0.0015 | 0.0025 | 0.0020 | 0.0070 | 0.0200 | 0.392 |
| | 8/26/93 | 0.0011 | 0.0018 | 0.0018 | 0.0031 | 0.0039 | 0.0097 | 0.0190 | 0.425 |
| | 10/4/93 | 0.0015 | 0.0023 | 0.0026 | 0.0032 | 0.0016 | 0.0098 | 0.0142 | 0.439 |
| | 11/15/93 | 0.0010 | 0.0014 | 0.0016 | 0.0022 | 0.0015 | 0.0100 | 0.0136 | 0.381 |

Tualatin Basin Study (cont.)

| Sampling Site | Sampling Date | Reactive [P] <0.05 μ m mM | Reactive [P] <1.0 μ m mM | Total [P] <1.0 μ m mM | Total [P] unfiltered mM | [Fe] <0.05 μ m mM | [Fe] <1.0 μ m mM | [Fe] unfiltered mM | [Si] unfiltered mM |
|-------------------------|---------------|-------------------------------|------------------------------|---------------------------|-------------------------|-----------------------|----------------------|--------------------|--------------------|
| Rock Cr at River Rd | 4/19/93 | 0.0015 | 0.0017 | 0.0020 | 0.0039 | 0.0016 | 0.0064 | 0.0289 | 0.303 |
| | 6/3/93 | 0.0023 | 0.0038 | 0.0042 | 0.0058 | 0.0002 | 0.0080 | 0.0452 | 0.395 |
| | 7/12/93 | 0.0026 | 0.0029 | 0.0038 | 0.0050 | 0.0016 | 0.0047 | 0.0122 | 0.508 |
| | 8/26/93 | 0.0037 | 0.0047 | 0.0044 | 0.0057 | 0.0020 | 0.0055 | 0.0112 | 0.526 |
| | 10/4/93 | 0.0041 | 0.0050 | 0.0053 | 0.0068 | 0.0020 | 0.0051 | 0.0114 | 0.544 |
| | 11/15/93 | 0.0025 | 0.0032 | 0.0033 | 0.0042 | 0.0001 | 0.0036 | 0.0073 | 0.492 |
| Bronson Cr at Walker Rd | 4/20/93 | 0.0007 | 0.0012 | 0.0015 | 0.0031 | 0.0016 | 0.0062 | 0.0262 | 0.261 |
| | 6/4/93 | 0.0010 | 0.0029 | 0.0032 | 0.0041 | 0.0009 | 0.0186 | 0.0232 | 0.415 |
| | 7/13/93 | 0.0012 | 0.0012 | 0.0018 | 0.0021 | 0.0009 | 0.0098 | 0.0124 | 0.338 |
| | 8/27/93 | 0.0011 | 0.0017 | 0.0021 | 0.0027 | 0.0011 | 0.0061 | 0.0118 | 0.409 |
| | 10/5/93 | 0.0013 | 0.0015 | 0.0015 | 0.0033 | 0.0009 | 0.0022 | 0.0106 | 0.374 |
| | 11/16/93 | 0.0017 | 0.0019 | 0.0025 | 0.0053 | 0.0005 | 0.0026 | 0.0057 | 0.166 |

Tualatin Basin Study (cont.)

| Sampling Site | Sampling Date | Reactive [P] <0.05 μm mM | Reactive [P] <1.0 μm mM | Total [P] <1.0 μm mM | Total [P] unfiltered mM | [Fe] <0.05 μm mM | [Fe] <1.0 μm mM | [Fe] unfiltered mM | [Si] unfiltered mM |
|----------------------------|---------------|---|--|---------------------------------------|-------------------------------|-----------------------------------|----------------------------------|--------------------------|--------------------------|
| Fanno Cr at Durham Rd | 4/20/93 | 0.0011 | 0.0015 | 0.0017 | 0.0026 | 0.0009 | 0.0055 | 0.0213 | 0.324 |
| | 6/4/93 | 0.0013 | 0.0028 | 0.0029 | 0.0047 | 0.0005 | 0.0081 | 0.0317 | 0.428 |
| | 7/13/93 | 0.0017 | 0.0022 | 0.0028 | 0.0037 | 0.0023 | 0.0079 | 0.0124 | 0.547 |
| | 8/27/93 | 0.0025 | 0.0030 | 0.0033 | 0.0045 | 0.0011 | 0.0047 | 0.0126 | 0.513 |
| | 10/5/93 | 0.0022 | 0.0026 | 0.0031 | 0.0044 | 0.0009 | 0.0064 | 0.0162 | 0.619 |
| | 11/16/93 | 0.0010 | 0.0019 | 0.0021 | 0.0050 | 0.0004 | 0.0068 | 0.0159 | 0.495 |
| Tualatin at Stafford Rd | 4/20/93 | 0.0015 | 0.0017 | 0.0025 | 0.0033 | 0.0027 | 0.0045 | 0.0211 | 0.250 |
| | 6/4/93 | 0.0020 | 0.0030 | 0.0032 | 0.0044 | 0.0000 | 0.0078 | 0.0251 | 0.365 |
| | 7/13/93 | 0.0038 | 0.0035 | 0.0048 | 0.0065 | 0.0014 | 0.0015 | 0.0094 | 0.364 |
| | 8/27/93 | 0.0012 | 0.0012 | 0.0020 | 0.0036 | 0.0009 | 0.0016 | 0.0048 | 0.381 |
| | 10/5/93 | 0.0032 | 0.0032 | 0.0041 | 0.0104 | 0.0000 | 0.0007 | 0.0046 | 0.374 |
| | 11/16/93 | 0.0012 | 0.0019 | 0.0025 | 0.0032 | 0.0007 | 0.0053 | 0.0078 | 0.331 |

Colloidal P and colloidal Fe concentrations in both studies are correlated in Fig. 3.6, Chapter 3. Three samples that had negative values of colloidal P, as estimated from the difference between the [P] in the 1.0 μm filtrates and the 0.05 μm filtrates, were not included in the regression analysis. The negative values were probably attributable to analytical error or to filtration artifacts, as discussed in Chapter 3. Seven other samples had very low values of colloidal P ($<0.04 \mu\text{M}$), as estimated by difference. These low values were averaged and only the average was included in correlations. This was done for clarity. Including all seven values individually or excluding them completely made no difference in the value of the correlation coefficient.

BIOGRAPHY

The author was born and raised in St. Louis, Missouri in 1958. After spending far too many of his formative years in the Midwest, he moved to Montana. He received a B.S. degree in forestry with an emphasis in soil science from the University of Montana in 1981. His career in forestry was deferred for the prospect of playing jazz piano professionally. In 1985, he moved to Portland, Oregon to pursue this occupation. After several years of tolerating late hours, noisy audiences, and indoor air pollution, graduate school was a welcome option. He was admitted to Oregon Graduate Institute in 1989 and received his Ph.D. in 1995.

Tim was married to Susan Powers in 1985. Tim and Susan are currently living in Portland with the newest member of the family, Miles. Tim's immediate plans after completion of this thesis include a few days in the Columbia Gorge, in pursuit of the perfect jibe. He will then continue his search for interesting work in or around Portland.